

2016

Hybrid Inorganic Core- Conjugated Polymer Shell Nanoparticles Prepared by Surface-Initiated Polymerization

Sourav Chatterjee

Louisiana State University and Agricultural and Mechanical College, sourav.dce@gmail.com

Follow this and additional works at: https://digitalcommons.lsu.edu/gradschool_dissertations

 Part of the [Chemistry Commons](#)

Recommended Citation

Chatterjee, Sourav, "Hybrid Inorganic Core- Conjugated Polymer Shell Nanoparticles Prepared by Surface-Initiated Polymerization" (2016). *LSU Doctoral Dissertations*. 3141.

https://digitalcommons.lsu.edu/gradschool_dissertations/3141

This Dissertation is brought to you for free and open access by the Graduate School at LSU Digital Commons. It has been accepted for inclusion in LSU Doctoral Dissertations by an authorized graduate school editor of LSU Digital Commons. For more information, please contact gradetd@lsu.edu.

HYBRID INORGANIC CORE- CONJUGATED POLYMER SHELL
NANOPARTICLES PREPARED BY SURFACE-INITIATED
POLYMERIZATION

A Dissertation

Submitted to the Graduate Faculty of the
Louisiana State University and
Agricultural and Mechanical College
in partial fulfillment of the
requirements for the degree of
Doctor of Philosophy

in
The Department of Chemistry

by
Sourav Chatterjee
B.Sc., Delhi University, 2002
M.Sc., Delhi University, 2005
M.S., University of Massachusetts Lowell, 2009
August 2016

Dedicated to my late father Tapash Kumar Chatterjee and my mother Banhi Sikha Chatterjee and my well-wishers.

ACKNOWLEDGEMENTS

First, I am really thankful to my family for their unconditional support and love; without them, I would not be able to come along. For my mother Banhi Sikha Chatterjee, and my late father Tapash Kumar Chatterjee and my brother Sawayambhu Chatterjee and my close friends whom I can always trust and get support I need in times of adversity.

I would like to thank my advisor Professor Evgueni E. Nesterov for his continuous guidance and support to work efficiently to become a good scientist. I would also like to thank my co-advisor Professor Paul Russo for his constant guidance. Both of them have given me valuable suggestions in academics and personal life. I have learned a lot from them and truly respect and admire them for their passion and dedication to science.

A special thanks to my committee member and collaborator Prof. Louis Haber for his willingness to educate me. I would also like to thank my other committee members Prof. David Spivak and Prof. David Young for their constant support.

To all my group members, past and present: Sang Gil Youm, Rajib Mondal, Chien-Hung Chiang, Chun-Han Wang, Peter Kei, Gerard Ducharme, Fatemeh Khamespanah, Xujun Zhang, Drs. Cornelia Rosu, Carlos Chavez, Xin Li, Wayne Huberty, Mellisa Collins, Jinwoo Choi, Deepa Pangen, Brian Imsick. I am indebted to all my group members (past and present) for making our laboratory an enjoyable place to work and learn each day.

Special acknowledgment to Drs. Ying Xiao, Thomas Weldeghiorghis, Frank Fronczek, Rafael Cueto, Yaroslav Losovyj, Jibao He and late Dale Treleaven for their expertise; Prof. Louis Haber and Dr. Tony Karam for their help in transient absorption studies and Britney Herbert for proof reading my thesis.

TABLE OF CONTENTS

ACKNOWLEDGEMENTS.....	iii
LIST OF TABLES.....	vii
LIST OF FIGURES.....	viii
LIST OF SCHEMES.....	xi
LIST OF ABBREVIATIONS.....	xii
ABSTRACT.....	xiv
CHAPTER 1. SYNTHESIS OF CONJUGATED POLYMERS VIA SURFACE-INITIATED POLYMERIZATION.....	1
1.1 Introduction.....	1
1.2 Polymer brushes.....	3
1.3 Synthesis of conjugated polymers via controlled chain-growth polymerization.....	6
1.3.1 <i>In-situ</i> catalytic initiator for Kumada-catalyst transfer polymerization.....	6
1.3.2 <i>Ex-situ</i> generated initiators for Kumada-catalyst transfer polymerization.....	9
1.3.3 Pd-catalyzed, Suzuki-Miyaura, and Stille-controlled catalyst transfer polymerization.....	10
1.3.4 N-Heterocyclic Carbene ligands stabilized catalysts.....	12
1.3.5 Chain-growth catalyst transfer polymerization of electron-deficient aromatic monomers.....	12
1.4 Surface-initiated polymerization of conjugated polymers.....	14
1.5 <i>Grafting through</i> approach.....	24
1.6 Research focus.....	26
1.7 References.....	27

CHAPTER 2. SYNTHESIS OF HYBRID CORE-SHELL PARTICLES CONSISTING OF SILICA CORE AND CONJUGATED BLOCK COPOLYMER SHELL PREPARED BY SURFACE-INITIATED POLYMERIZATION.....	36
2.1 Introduction.....	36
2.2 Results and Discussion.....	40
2.2.1 Synthesis of conjugated polymer grafted silica particles.....	40
2.2.2 Photophysical properties of hybrid nanoparticles.....	47
2.2.3 Photophysical properties of thin films prepared from hybrid nanoparticles.....	53
2.2.4 Transient absorption studies of hybrid materials.....	54
2.3 Conclusions.....	62
2.4 References.....	63
CHAPTER 3. SYNTHESIS OF HYBRID CORE-SHELL PARTICLES CONSISTING OF SILICA CORE AND TRIBLOCK COPOLYMER SHELL PREPARED BY SURFACE-INITIATED POLYMERIZATION.....	68
3.1 Introduction.....	68
3.2 Results and Discussion.....	71
3.2.1 Synthesis and characterization.....	71
3.2.2 Photophysical properties of hybrid silica-conjugated polymers.....	75
3.2.3 Solvatochromism	83
3.3 Conclusions.....	85
3.4 References.....	86
CHAPTER 4. RELATIONS BETWEEN STRUCTURE AND PHOTOPHYSICAL PROPERTIES IN HYBRID GOLD@SILICA NANOPARTICLES WITH CONJUGATED POLYMER SHELLS.....	92
4.1 Introduction.....	92
4.2 Results and Discussion.....	95
4.2.1 Synthesis of Au@SiO ₂ -homo and block copolymers.....	95

4.2.2 Photophysical properties of hybrid Gold@Silica-conjugated polymer nanoparticles.....	97
4.2.3 Transient absorption studies of Gold@Silica-conjugated polymer nanoparticles...	99
4.3 Conclusion.....	105
4.4 References.....	106
CHAPTER 5. EXPERIMENTAL SECTION.....	111
5.1 General information.....	111
5.2 Transient absorption optical setup.....	111
5.3 Synthetic details	112
5.3.1 Synthesis of Silica nanoparticles.....	112
5.3.2 Preparation of gold nanoparticles.....	113
5.3.3 Preparation of gold@silica nanoparticles.....	113
5.3.4 Synthesis of Triethoxy(5-iodothiophen-2-yl)silane (P1).....	114
5.3.5 Synthesis of Bis[1,3-bis(diphenylphosphino)propane]nickel(0).....	114
5.3.6 Immobilization of precursor P1 on gold@silica or silica nanoparticles and conversion to Ni(II)- modified nanoparticles	115
5.3.7 General preparation of gold@silica or silica nanoparticles core with conjugated polymer shell.....	115
5.3.8 General preparation of block copolymer coated gold@silica or silica nanoparticles.....	116
5.4 References.....	116
Appendix A: Permissions.....	118
Appendix B: Nuclear Magnetic Resonance Data.....	128
Vita.....	130

LIST OF TABLES

Table 2.1: Molecular weight and DP of conjugated polymer shell hybrid particles from TGA . 45

Table 4.1: Comparison of transient times of Silica@conjugated polymers with Au@Silica-conjugated polymers.....104

LIST OF FIGURES

Figure 1.1 Mechanism of Kumada chain-growth catalyst-transfer quasi-“living” polymerization to form P3ATs	8
Figure 1.2 Various routes to prepare external initiator in the catalyst-transfer polymerization.....	10
Figure 1.3 Externally initiated chain growth Suzuki-Miyayura polymerization to form P3HTs..	11
Figure 1.4 Stille chain-growth polymerization to form PPE.....	11
Figure 1.5 Synthesis of electron-deficient PBTz using diamine Ni(II) catalyst.....	13
Figure 1.6 Preparation of the Br-TNDIT-Br/Zn radical-anion monomer and its catalyst-transfer polymerization.....	14
Figure 1.7 P3HT film prepared by <i>grafted from</i> approach using photo-cross-linked PS-Br.....	16
Figure 1.8 Synthesis of SiO ₂ -grafted P3HT nanoparticles by surface-confined polymerization..	17
Figure 1.9 Proposed surface disproportionation mechanism.....	18
Figure 1.10 Grafting of PFO from microparticles <i>via</i> SI-KCTP.....	19
Figure 1.11 Surface-initiated polymerization of microparticles having microporous conjugated polymer shell.....	20
Figure 1.12 Synthesis of surface-grafted thiophene bromide initiator.....	22
Figure 1.13 Sonagashira surface polymerization on silica particles to form PPE shell.....	25
Figure 1.14 Synthesis of alkyne-functionalized SiO ₂ substrates and formation of surface-confined polyacetylene film using tungsten catalyzed polymerization.....	26
Figure 2.1 (A) TEM image of as synthesized silica nanoparticles; (B) Size distribution histogram of the nanoparticles; (C) SANS analysis of silica nanoparticles in D ₂ O solution (10 mg/mL).....	42
Figure 2.2 TGA of %weight loss with temperature change of hybrid particles.....	44
Figure 2.3 Core-shell model.....	46
Figure 2.4 SANS analysis of grafted conjugated homopolymer and diblock copolymers on SiO ₂ hybrid nanoparticles in DCB (10 mg/ml). Fitting curves were obtained using models described in the text.....	46

Figure 2.5 Absorption (A), excitation (B), emission (C) spectra of SiO ₂ @PT-b-PPP and SiO ₂ @PPh-b-PTh in 1,2-dichlorobenzene (DCB). Fluorescence quantum yield (%) SiO ₂ @PT (0.1); SiO ₂ @PPP (26.32); SiO ₂ @PT-b-PP (1.55); SiO ₂ @PPP-b-PT (0.13).....	50
Figure 2.6 Excitation (A), emission (B) spectra of SiO ₂ @PT-b-PPP and SiO ₂ @PPP-b-PT drop casted on a glass slide.....	54
Figure 2.7 (a) Representative transient absorption spectra of colloidal SiO ₂ -polyphenylene nanoparticles using 380 nm excitation pulses (conc. 0.5 mg/ml). (b) Transient absorption time-profiles of the SiO ₂ -polyphenylene nanoparticles measured at 470 nm. (c) Decay spectra obtained using global analysis of the time-dependent transient absorption spectra.....	56
Figure 2.8 (a) Representative transient absorption spectra of colloidal SiO ₂ -polythiophene nanoparticles using 380 nm pump pulses (conc. 0.5 mg/ml). (b) Transient absorption time profiles of the SiO ₂ -polythiophene nanoparticles measured at 700 nm. (c) Decay spectra obtained using global analysis of the time-dependent transient absorption spectra.....	57
Figure 2.9 (a) Representative transient absorption spectra of colloidal SiO ₂ -polyphenylene-b-polythiophene nanoparticles using 380 nm excitation pulses (conc. 0.5 mg/ml). (b) Transient absorption time-profiles of the SiO ₂ -polyphenylene-b-polythiophene nanoparticles measured at 425 nm and 650 nm. (c) Decay spectra obtained from global analysis of the time-dependent transient absorption spectra.....	58
Figure 2.10 (a) Representative transient absorption spectra of SiO ₂ -polythiophene-b-polyphenylene nanoparticles using 380 nm excitation pulses (conc. 0.5 mg/ml). (b) Transient absorption time-profiles of the SiO ₂ -polythiophene-b-polyphenylene nanoparticles measured at 450 nm and 650 nm. (c) Decay spectra obtained from global analysis the time-dependent transient absorption spectra.....	61
Figure 3.1 TEM spectra of silica particles with size distribution.....	72
Figure 3.2 SANS analysis of grafted homopolymer, diblock copolymer and triblock copolymers grafted on SiO ₂ particles dispersed in 1,2-dichlorobenzene.....	74
Figure 3.3 Absorbance spectra of homopolymer, diblock copolymer and triblock copolymers grafted on SiO ₂ particles dispersed in 1,2-dichlorobenzene and THF (0.3 mg/ml)....	78
Figure 3.4 Excitation spectra of homopolymer, diblock copolymer and triblock copolymers grafted on SiO ₂ particles dispersed in 1,2-dichlorobenzene and THF (emission at 650 nm) (0.3 mg/ml).....	79
Figure 3.5 Emission spectra of homopolymer, diblock copolymer and triblock copolymers grafted on SiO ₂ particles dispersed in 1,2-dichlorobenzene and THF (0.3 mg/ml).....	82

Figure 3.6 Emission spectra of hybrid silica-triblock copolymer particles in chloroform, 1,2-dichlorobenzene, and THF showing effect of solvent on spectroscopic properties of these hybrid silica polymer nanoparticles (0.3 mg/ml).....	83
Figure 3.7 Emission spectra of hybrid silica-diblock copolymer nanoparticles in chloroform, 1,2-dichlorobenzene, and THF showing effect of solvent on spectroscopic properties of these nanoparticles (0.3 mg/ml).....	84
Figure 4.1 TEM images of nanoparticles: (a) Au; (b) Au@SiO ₂ ; (c) Au@SiO ₂ -PT; (d) Au@SiO ₂ -PPP; (e) Au@SiO ₂ -PT-b-PPP; (f) Au@SiO ₂ -PPP-b-PT.....	96
Figure 4.2 Normalized absorption spectra of Au@SiO ₂ -Conjugated polymer nanoparticles in 1,2-dichlorobenzene.....	97
Figure 4.3 Normalized emission spectra of Au@SiO ₂ -Conjugated polymer nanoparticles in 1,2-dichlorobenzene solution (0.3 mg/mL).....	98
Figure 4.4 (a) Transient absorption spectra of Au@SiO ₂ -PPP after excitation with 380 nm excitation pulses. (b) Transient absorption time-profiles of Au@SiO ₂ -PPP. (c) Decay spectra of Au@SiO ₂ -PPP obtained by global analysis of the time profiles.....	100
Figure 4.5 (a) Transient absorption spectra of Au@SiO ₂ -PT after excitation with 380 nm excitation pulses. (b) Transient absorption time-profiles of Au@SiO ₂ -PT. (c) Decay spectra of Au@SiO ₂ -PT obtained by global analysis of the time profiles.....	101
Figure 4.6 (a) Transient absorption spectra of Au@SiO ₂ -PPP-b-PT after excitation with 380 nm excitation pulses. (b) Transient absorption time-profiles of Au@SiO ₂ -PPP-b-PT. (c) Decay spectra of Au@SiO ₂ -PPP-b-PT obtained by global analysis of the time profiles.....	102
Figure 4.7 (a) Transient absorption spectra of Au@SiO ₂ -PT-b-PPP after excitation with 380 nm excitation pulses. (b) Transient absorption time-profiles of Au@SiO ₂ -PT-b-PPP. (c) Decay spectra of Au@SiO ₂ -PT-b-PPP obtained by global analysis of the time profiles.....	103
Figure 5.1 Schematic diagram of the ultrafast transient absorption setup.....	112

LIST OF SCHEMES

Scheme 2.1 Synthesis of regioregular poly(3-hexyl thiophene).....	39
Scheme 2.2 Preparation of silica nanoparticles grafted with shell composed of conjugated polymer or block copolymer	43
Scheme 3.1 Synthesis of homopolymer, diblock copolymer and triblock copolymer shells grafted on silica particles	73
Scheme 4.1 Synthesis of Au and Au@SiO ₂ nanoparticles.....	95
Scheme 4.2 Synthesis of multilayer shells of block copolymers on Au@SiO ₂ nanoparticles by surface-initiated living Kumada polymerization technique.....	96
Scheme 5.1 Synthesis of Triethoxy(5-iodothiophen-2-yl)silane (P1).....	114

LIST OF ABBREVIATIONS

Acac	Acetylacetonate
ATRP	Atom-Transfer Radical Polymerization
Bipy	2,2'-bipyridyl
biTh	Bithiophene
BHJ	Bulk-heterojunction
CP	Conjugated Polymer
CV	Cyclic Voltammogram
DCM	Dichloromethane
DMF	<i>N,N</i> -dimethylformamide
dppp	1,3-bis(diphenylphosphino)propane
dppe	1,2-bis(diphenylphosphino)ethane
DSC	Differential Scanning Calorimetry
GRIM	Grignard Metathesis
GPC	Gel-permeation Chromatography
ET	Energy Transfer
HOMO	Highest Occupied Molecular Orbital
HT	Head-to-Tail
IPr	1,3-bis(2,6-diisopropylphenyl)imidazol-2-ylidene
KCTP	Kumada Catalyst-Transfer Polycondensation
LDA	Lithium Diisopropylamide
LUMO	Lowest Unoccupied Molecular Orbital
MALDI-ToF	Matrix-assisted Laser Desorption/Ionization-Time of Flight
MeOH	Methanol
MS	Mass Spectroscopy
NHC	N-heterocyclic carbene
NIR	Near-infrared
NMR	Nuclear Magnetic Resonance
NP	Nanoparticle
OLED	Organic Light-emitting Diode
P3AT	Poly(3-alkylthiophene)
P3HT	Poly(3-hexylthiophene)
PT	Polythiophene
PBTz	Polybenzotriazole
PCBM	Phenyl-C61-butyric acid methyl ester
PDI	Polydispersity Index
PEDOT	Poly(3,4-ethylenedioxythiophene)
PF	Polyfluorene
Ph	Phenyl
PAA	Polyallene
PPE	Poly(<i>p</i> -phenylene ethynylene)
PPP	Poly- <i>p</i> -phenylene
PPV	Poly(<i>p</i> -phenylene vinylene)
PS	Polystyrene
Qdot	Quantum Dot

rr	Regioregular
SANS	Small-angle Neutron Scattering
TEM	Transmission Electron Microscopy
TGA	Thermogravimetric Analysis
THF	Tetrahydrofuran
UV-vis	Ultraviolet-visible
DCB	Dichlorobenzene
COD	1,5-cyclooctadiene

ABSTRACT

Hybrid core-shell nanoparticles have attracted attention due to their unique characteristics which combine properties of the inorganic core and organic shell in a way that generates new properties which do not exist for the two individual parts. This makes them promising candidates for the design of stimuli-responsive materials, chemo- and biosensors, and various biomedical applications. In this dissertation research, we designed and prepared a series of hybrid environmentally responsive nanoparticles where fluorescent block copolymers, including various combinations of polythiophene (PT), poly(*p*-phenylene) (PPP), poly(3-hexylthiophene) (P3HT) and polyallene (PA), were grafted on the surface of inorganic nanoparticles using surface-confined Kumada catalyst-transfer polymerization. The studied inorganic core included silica and silica on gold nanoparticles. We found that the photophysical properties of the hybrid nanoparticles were strongly dependent on the proximity of the organic polymer shells to the inorganic surface (Au), polymer block sequence in the organic shell, and external stimuli such as solvent or pH.

This dissertation primarily focuses on the development and preparation of well-defined hybrid inorganic core – organic polymer materials. This preparation stems from the well-defined and highly efficient surface-confined Ni(II) catalytic initiator which provided controlled chain-growth polymerization to form conjugated polymer shells. The role of inorganic core and other structural effects on the properties of the conjugated polymer shells were studied using both steady-state and time resolved transient spectroscopies. Better knowledge and understanding of these fundamental properties will enable rational control of these properties at the molecular level and will create the fundamental basis for the design of future optoelectronic and sensing materials.

CHAPTER 1. SYNTHESIS OF CONJUGATED POLYMERS VIA SURFACE-INITIATED POLYMERIZATION

1.1 Introduction

The initial studies on conjugated polymers by Heeger, Shirakawa, and MacDiarmid¹ opened a new research field of major interest and significance.¹ In the past few decades, an enormous body of work has been done in design, synthesis, characterization, and application of different types of conjugated polymers, and now these materials are steadily moving towards commercialization, especially as optoelectronic and sensing materials.²⁻¹¹

The technological possibilities offered by these optoelectronic materials are immense due to the opportunity to make light-weight, large-area mechanically flexible devices using solution-casting or printing techniques.¹² Due to relatively low production and device fabrication cost, and ability to the tailor-make materials with desired characteristics, flexibility, and low density, organic electronic materials are used in organic light-emitting diodes, field-effect transistors, photodetectors, organic photovoltaics, and sensor devices.¹³⁻¹⁶ The performance of these materials strongly depends on the pre-organization of the polymer molecules in solution from which they are cast into films. Unfunctionalized conjugated polymers tend to have strong π - π interactions between the chains and are practically insoluble in common solvents. Thus, substantial work has been done to synthesize polymers with long-chain alkyl solubilizing groups. Though such functionalization does help to confer processibility, it comes at a cost of polymer charge transport properties, mesoscale organization, etc. Thus, a small change in polymer structure may modify the chain conformations which will affect the intermolecular interactions and thus will alter the overall electronic and optoelectronic characteristics of the thin films. The spun-cast films are also prone to oxidation, thermal expansion/contraction, delamination, abrasion, etc.¹⁷

Another factor which affects the performance of conjugated polymer based devices is the interface of polymer with traditional electronic components such as metal or metal oxide. For example, in light emitting diodes, charges are generated from anode and cathode electrodes; charge transfer and recombination of charges take place only at donor-acceptor interfaces.¹⁸⁻¹⁹ Thus, for the practical efficiency of these devices, anode and cathode work functions should be matched with the highest occupied molecular orbitals (HOMO) of the hole transporting layer and with the lowest unoccupied molecular orbital (LUMO) of the light emitting layer. Also, wetting and adhesion of polymer layer with electrodes drastically affect the performance and lifetime of the device. Thus, modification of interface can significantly help to passivate surface charge traps, improve energy level alignment and enhance material compatibilities. All of these can be achieved by coating of an interlayer or by covalent functionalization of the electrode surface. Surface grafting is more useful than coating process as it prevents delamination of the film, controls the orientation of the polymer molecules with respect to the substrate which is not achieved in traditional solution-based deposition processes (printing, spin coating, drop-casting, doctor-blading).²⁰

Another important issue is the poor electron mobility of n-type organic semiconductors compared to p-type semiconductors that lead to unbalanced electron and hole transport in active layers. This unbalanced charge will accumulate at donor-acceptor interface that gives rise to inefficient charge transport and charge recombination. Thus, the hybrid organic-inorganic materials can prove to be useful as n-type inorganic materials have electron mobilities of several orders of magnitudes higher than n-type organic materials, and thus their presence will help to overcome this imbalance. Also, inorganic materials have better stability towards oxygen and moisture, which is a key factor to overall device stability.²¹

More recently, many research groups have turned their attention to designing hybrid organic – inorganic materials in order to improve performance characteristics of the resulting materials. Most of the typically used inorganic counterparts are nanocrystals such as CdSe, CdTe, etc.,²²⁻²⁴ or metal oxides such as ZnO, TiO₂²⁵⁻²⁶, which have an advantage as they can absorb visible light and contribute to the photocurrent. One key factor in designing hybrid materials is to modify these nanostructures carefully, for example, with proper control of their aggregation behavior, as excessive aggregation can alter electronic characteristics and thus limit the material performance. Also, functionalizing the surface of inorganic nanoparticles can increase stability of their colloidal solutions which in turn will increase the surface area and improve the exciton dissociation.²⁷⁻²⁹

In addition, hybrid nanoparticles show better sensitivity in chemosensor detection as compared to conjugated polymers alone.³⁰⁻³¹ This introductory chapter presents fundamental information on polymer brushes and outline major routes to controlled synthesis of conjugated polymers, mainly paying attention to nickel and palladium catalyzed processes. Second, we will discuss current state of the art of surface-initiated (also often called surface-confined) polymerization to form conjugated polymer brushes, mainly paying attention to the *grafting-from* technique.

1.2 Polymer Brushes

Surface-grafted polymer thin films are more viable than spin-casted thin films as the polymer chains in the former are covalently bonded to the surface which gives extra stability required in thin-film device fabrication and applications.³¹ Surface thickness can be tuned by varying polymerization time, and the resulting film will show some preferential molecular organization and alignment in the bulk of the film. In some cases, the polymer chains may be aligned uniformly in the direction normal to the film surface and this would be a preferred orientation for charge transport across the film as intramolecular hole/electron transport is faster

than intermolecular hopping between the chains. This will also help in better charge transport and charge injection due to the tight, at the covalent bond level, attachment of the polymer to the inorganic substrate.^{18, 32-33}

Polymer brushes (also known as tethered polymers) first gained attention in the 1980s when De Gennes used computational and theoretical analysis to predict brush conformation of coil polymers.³⁴ To attain good selectivity and reliable control of polymer thickness and chain alignment, “living polymerization”, such as anionic, cationic or radical polymerization was used. With recent advances in controlled radical polymerization, synthesis of these polymers becomes viable with low polydispersity and high selectivity. Surface-confined conjugated polymers are prepared by different grafting techniques.

Synthesis of dense polymer films can be achieved via either *grafting to* or *grafting from* approach. *Grafting to* technique is the one in which end-functionalized polymer reacts with complementary functionalized substrates. Hawker group showed that by manipulating end-grafting statistical random copolymers, interfacial energies of polymers at a solid surface can be changed and can be controlled by synthesis.³⁵ Their method gave low grafting density because surface immobilization of the first fraction of polymer chains would prevent diffusion of more incoming chains by forming a barrier to the surface. This limitation is due to thermodynamics as well kinetics. As the end-functionalized polymer chains start reacting with the surface, surface coverage with polymer chain increases and quickly the polymer concentration near the surface becomes larger than the solution concentration. Thus, the further chains have to cross this concentration gradient to get attached to the surface.³⁶ Thus, such diffusion will slow down the process and hence grafting density will be lower.

As a result of this intrinsic drawback of the *grafting to* approach, *grafting from* technique has become a preferred choice for the synthesis of different conjugated polymers on the surface. This method uses a monolayer of initiator which is first attached covalently to the surface.³⁷ After activation, i.e. formation of polymerization catalyst on the surface, polymer chains start growing from the surface, and the chain growth is only limited by the diffusion of monomer to the growing chain end. Thus, this potentially can give thick film with a high grafting density which is not possible to obtain using *grafting to* approach.

A third approach was loosely defined in literature is *grafting through* approach. It involves polymer chain initiation step taking place in solution or in bulk followed by attaching one end of the polymer chains to the surface followed by further polymerization from the surface-confined polymer molecules.³⁸ This process gives random chain length and uncontrolled surface density.

A crucial point is the availability of reliable anchoring group for the surface attachment. Self-assembled monolayers are a well-established method, and this method is robust, ordered and technologically attractive for surface engineering. Depending upon nature of the substrates, different chemical groups can be used as anchoring, such as diazonium,³⁹ thiols and sulfides,⁴⁰ silanes, and phosphorus-based⁴¹ functional groups. These approaches have been commonly used to graft conjugated polymers to insulating or electroactive surfaces.

Polymer brushes have been studied extensively due to the prospective technological applications. Polymer brushes are considered as an array of coiled macromolecular chains attached to a surface. In their unperturbed state, the polymer brushes may coil and also can overlap with adjacent coils, which will significantly alter the polymer conformation. This state is called mushroom state. In a “good” solvent, polymer chains will be extended as far as possible and will extend toward solvent along the direction normal to the surface. This will give concentrated coil

polymer brushes. *Grafting from* approach is capable of providing such surface-initiated polymer brushes. For high grafting density value, i.e. close to 1 coil chain nm⁻², the concentrated brush can be highly anisotropic. Theoretically, it has been predicted that closely packed polymer chains adopt extended and stretched conformations.⁴² When polymer grafting density is high, grafted polymers stretch out away from the surface to minimize interactions with the neighboring polymer chains and thus resulting in high surface coverage. Very few studies have been done to explain or predict the conformation or evolution of thickness of surface-confined rigid rod-like polymer chain upon interaction with solvent.

1.3 Synthesis of conjugated polymers via controlled chain-growth polymerization

1.3.1 *In-situ* catalytic initiator for Kumada catalyst transfer polymerization

Controlled/living polymerization has become an attractive technique to grow polymer brushes following *grafting from* strategy as this offers good control of polymer brush thickness, chemical composition, and mesostructural architecture. Examples include atom transfer radical polymerization (ATRP), reversible addition-fragmentation chain transfer (RAFT), nitroxide-mediated radical polymerization (NMP), ring opening metathesis polymerization (ROMP), Suzuki and Yamamoto polycondensation and Kumada catalyst-transfer polymerization method (KCTP).⁴³⁻⁵⁰

The early work on polymerization using Kumada coupling based Grignard Metathesis (GRIM) with nickel(1,3-diphenylphosphinopropane) dichloride (Ni(dppp)Cl₂) was carried out by McCullough's group⁵¹⁻⁵² and became widely popular for synthesizing regioregular poly(3-alkylthiophene)s (P3ATs). Soon after the initial report on McCullough's GRIM method, Rieke reported an alternative route to the synthesis of P3ATs.⁵³ Rieke's route is based on Negishi coupling, and uses highly active "Rieke zinc" first reacting with 2,5-dibromo-3-alkylthiophenes to

yield an intermediate organozinc compounds which, upon subsequent treatment with Ni(dppp)Cl₂ produce regioregular P3ATs. The major drawback of both McCullough's GRIM and Rieke polymerization methods was that they provided broad molecular weight distribution due to the step-growth polymerization mechanism involved.

More recently, Yokozawa demonstrated that, upon carrying out reaction at lower temperature, the number averaged molecular weight M_n of P3AT polymers increased in proportion with monomer conversion, along with narrow polydispersities and molecular weight linearly dependent on the amount of Nickel catalysts used.⁵⁴⁻⁵⁵ Polymerization was carried out at room temperature, and M_n was proportional to the feed ratio of [Grignard]₀/[Ni catalyst]₀ resulting in PDI as low as 1.1 and M_n of 29,000 Da. McCullough later confirmed the Yokozawa results with zinc and Grignard monomers. He postulated that, at lower temperature, the polymerization occurred by quasi-“living” chain growth Kumada catalyst transfer polymerization (KCTP) mechanism.

The mechanism of Kumada catalyst transfer polymerization can be summed as in figure 1. It involves three steps: (1) oxidative addition, (2) transmetalation and (3) reductive elimination. Until the early 2000s, such nickel catalyzed polymerization was carried out at higher temperatures and was assumed to occur as a polycondensation reaction via stepwise process (step-growth mechanism). In 2005, Yokozawa showed that, when carried out at ambient temperature, GRIM method proceeds through chain-growth fashion. Consequently, McCullough explained in a separate article that polymerization process happens in the controlled/living manner, but the mechanism depends on reaction time, the amount of monomer to nickel catalyst loading which will control polydispersity, molecular weight and regioregularity of the resulting polymers.

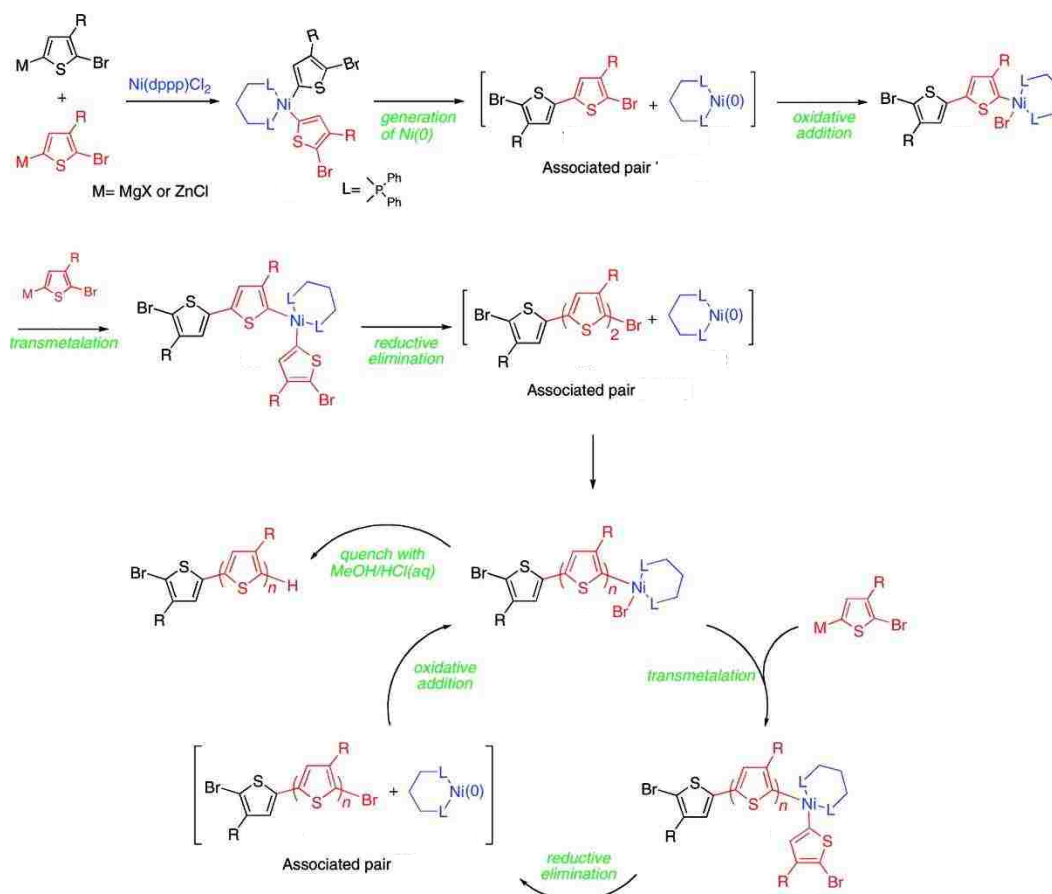


Figure 1.1 Mechanism of Kumada chain-growth catalyst-transfer quasi-“living” polymerization to form P3ATs. Reproduced with permission from ref. 52 Copyright © 2008 American Chemical Society.

McNeil’s group showed that electron-donating ability (electron rich character) of π -complexed ligand controls the chain-growth nature of the polymerization process.⁵⁶⁻⁵⁷ Kiriy provided more details on the polymerization mechanism. They found that Ni active catalytic center could randomly walk in both directions along the growing polymer chain.⁵⁸ McCullough and Yokozawa asserted that KCTP was indeed quasi-“living” chain growth polymerization process which allows controlling the degree of polymerization through the amount of catalyst loading, and allows to increase the degree of polymerization with an increase in monomer content.

The rate-determining step in polymerization is the transmetalation as Ni(dppp)Cl_2 acts as both catalyst and initiator. After reductive elimination of two thienyl monomers, the Ni center ends

up as an intermediate termed as *associative pair*. This pair will always end up giving Tail-Tail (T-T) coupling, thus giving less than 100% regioregular polymers. *In-situ* polymerization can result in increased polydispersities due to the slow reactivity of initiating species.

1.3.2 *Ex-situ* generated initiators for Kumada catalyst transfer polymerization

To enhance the control in synthesis of polymer chains by KCTP process, *ex-situ*³² generated external catalytic initiators were developed by Luscombe⁵⁹ (Route A) and Kiriy (routes B, C) as shown in figure 1.2. This involves generation of *ex-situ* initiators by reacting Ni(0) complex with aryl halides to form Ni(II) catalytic complexes. Though Ni(PPh₃)₄ can initiate polymerization, it results in low molecular weight oligomers and high polydispersity. To avoid disproportionation reaction, the monodentate ligand was exchanged with bidentate phosphine ligand after oxidative addition to the square-planar complex to enforce phosphines in *cis* rather than *trans* (as with monodentate ligands) position to each other. This gives extra stability, thus minimizing disproportionation and chain transfer processes and allows random-walking of π -complex via the formation of Ni(0) π -complex. Although the critical role of such a complex in KCTP has been postulated for a long time, only recently did McNeil deliver substantial experimental evidence for the formation of π -complex and its role in the polymerization.⁵⁷ Molecular weight of the polymers obtained by this externally initiated KCTP process is typically high, with moderate polydispersities and good regioregularity. A disadvantage of this *ex-situ* polymerization following earlier Luscombe and Kiriy methods (routes A-C in Figure 1.2) is that due to ligand exchange monodentate PPh₃ remains in the reaction mixture. Also, due to the reactivity of *ex-situ* generated Ni(II) catalytic initiators, the polymerization is highly sensitive to moisture and oxygen and the catalysts are very difficult to purify. Furthermore, presence of

monodentate ligands can enhance disproportionation side reactions and also can facilitate aryl-aryl homocoupling.

The simplest direct approach to preparing uncontaminated Ni(II) external catalytic initiators would be the direct oxidative addition of Ni(0) complexes with bidentate ligands to aryl halides. This will produce polymers with no contamination of monodentate ligands and other undesirable impurities. In 2014, Nesterov's group⁶⁰ reported that the external catalytic initiator produced by oxidative addition between Ni(dppp)₂ and aryl halides can actually initiate Kumada "living" polymerization producing defect-free PT polymers and block copolymers with high molecular weight and 100% regioregularity (route D in Figure 1.2).

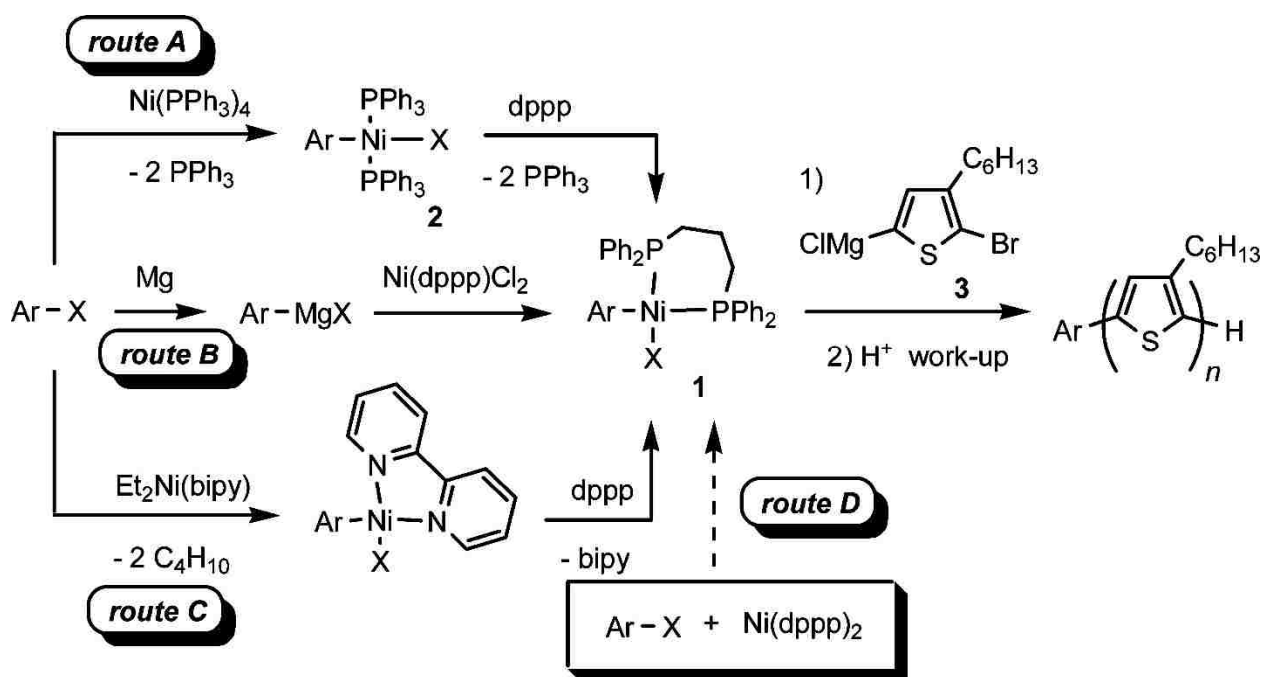


Figure 1.2 Various routes to prepare external initiator in the catalyst-transfer polymerization. Reproduced with permission from ref. 60. Copyright © 2014 American Chemical Society.

1.3.3 Pd-catalyzed Suzuki-Miyaura and Stille controlled catalyst transfer polymerization

External initiation using Pd-based aryl-Pd complexes leads to chain transfer polycondensation reaction using boronic ester functionalized monomer. Traditionally, Suzuki-Miyaura polycondensation is a step-growth polymerization involving two different bifunctional

monomers: diboronic esters (AA monomer) and aryl dihalides (BB monomer). However, Yokozawa showed that when using AB-type single monomer with boronic acid and halide functionality within the same molecule, the polymerization follows chain transfer mechanism producing polymers with high molecular weight and low polydispersities.⁶¹ Huck demonstrated Suzuki-Miyaura chain growth polymerization using various types of Pd-catalysts to synthesize conjugated polymers (figure 1.3).⁶² The reaction between Pd(*t*-Bu₃P)₂ with different aryl halides gives various kinds of initiators that could provide numerous well-defined conjugated polymers.

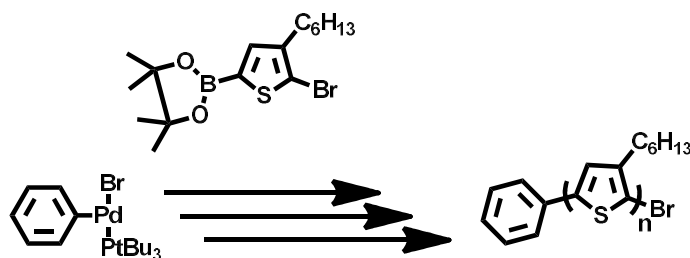


Figure 1.3 Externally initiated chain growth Suzuki-Miyaura polymerization to form P3HTs.

While the Suzuki-Miyaura chain growth method was used with boronic ester/halide bifunctional monomers to give well-defined conjugated polymers, stannyl/halide bifunctional monomers can also be used in a similar way for polymerization by Stille cross-coupling.

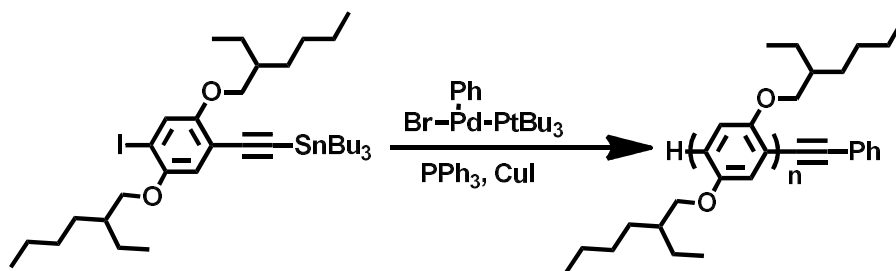


Figure 1.4: Stille chain-growth polymerization to form PPE.

Bielawski and coworkers showed the synthesis of poly(*p*-phenylene ethynylene) (PPE) by chain growth catalyst transfer polymerization using *t*-Bu₃PPd(Ph)Br catalyst with various

phosphine ligands and CuI (figure 1.4).⁶³ This method gives well-defined block copolymers with high molecular weight and low polydispersities.

1.3.4 N-Heterocyclic Carbene ligand stabilized catalysts

To facilitate the catalyst transfer step, various groups make use of N-heterocyclic carbenes (NHCs) due to their electron-rich nature and strong σ donation. McNeil previously showed that electronic stabilization of the Ni(0) π complex is attributed to the electron donating ability of the phosphine ligands in Ni(dppe)₂ as determined via multiple polymerization experiments with various phosphine ligands.⁶⁴⁻⁶⁵ Steric effects caused by 2,6-diisopropylphenyl substituents and electron-donating capability of NHC provide the sufficient stabilization energy required for adequate catalyst transfer rate. Though P3HT and PPP can be prepared using NHC-based catalysts, polyfluorene cannot be synthesized.

Mori synthesized P3HT in a chain growth fashion by using NHC-ligated Ni catalyst. It acts similar to its Pd analog, but in this case, 2-chloro-2-alkylthiophenes was used to generate thienyl magnesium monomer using magnesium amide TMP-MgCl. 3LiCl.⁶⁶ The NHC-ligated Ni catalysts initiated reaction to form P3HT in a chain growth fashion resulting in the polymer with high molecular weight and low polydispersity. This reaction is unique as it opens up the possibility to use more readily available chloro-substituted monomers instead of commonly used bromo or iodo substituted counterparts. This is essential for the future discovery of various aromatic monomers having chlorine substituents.

1.3.5 Chain-growth catalyst-transfer polymerization of electron-deficient aromatic monomers

Much of the research progress has involved electron-rich monomers, with much less emphasis on electron-deficient monomers, because of the much higher efficiency of KCTP with electron-rich monomers as compared to the electron-deficient monomers. The much weaker

association of nickel catalyst with the growing electron-deficient polymer chain typically results in premature dissociation of the catalyst from growing polymer chains producing chains with low molecular weight, high polydispersities, and broad molecular weight distribution. Seferos recently devised new and well-defined Ni catalysts based on diimine ligands (Figure 1.5).⁶⁷ This led to the preparation of a series of diimine ligands with substituents ranging from electron-donating to electron-withdrawing which demonstrated that increase in stabilization energy will favor chain growth process. Thus, electron donating –OMe substituents showed the best results producing electrodeficient polybenzotriazole polymers with high molecular weight and low polydispersities (figure 1.5).

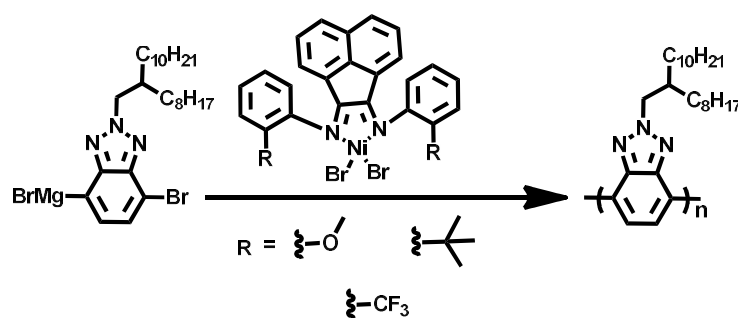


Figure 1.5 Synthesis of electron-deficient PBTz using diimine Ni(II) catalyst.

Senkovskyy⁶⁸ and Kiriyy⁶⁹ tried polymerizing an electron-deficient monomer by making use of the naphthalenediimide radical anion. It revealed a novel pathway for the polymerization of electron deficient monomer radical treated with Ni(II) catalysts. It was demonstrated that this polymerization did not go through KCTP type of mechanism but rather followed reductive coupling. Radical anion monomer generated by *in situ* treatment of reactive Zn with naphthalenediimide underwent initiation with Ni(dppe)Br₂ or PhNi(dppe)Br catalysts. Polymerization proceeded in the chain growth fashion resulting in polymer with controlled molecular weight and low polydispersity (figure 1.6).

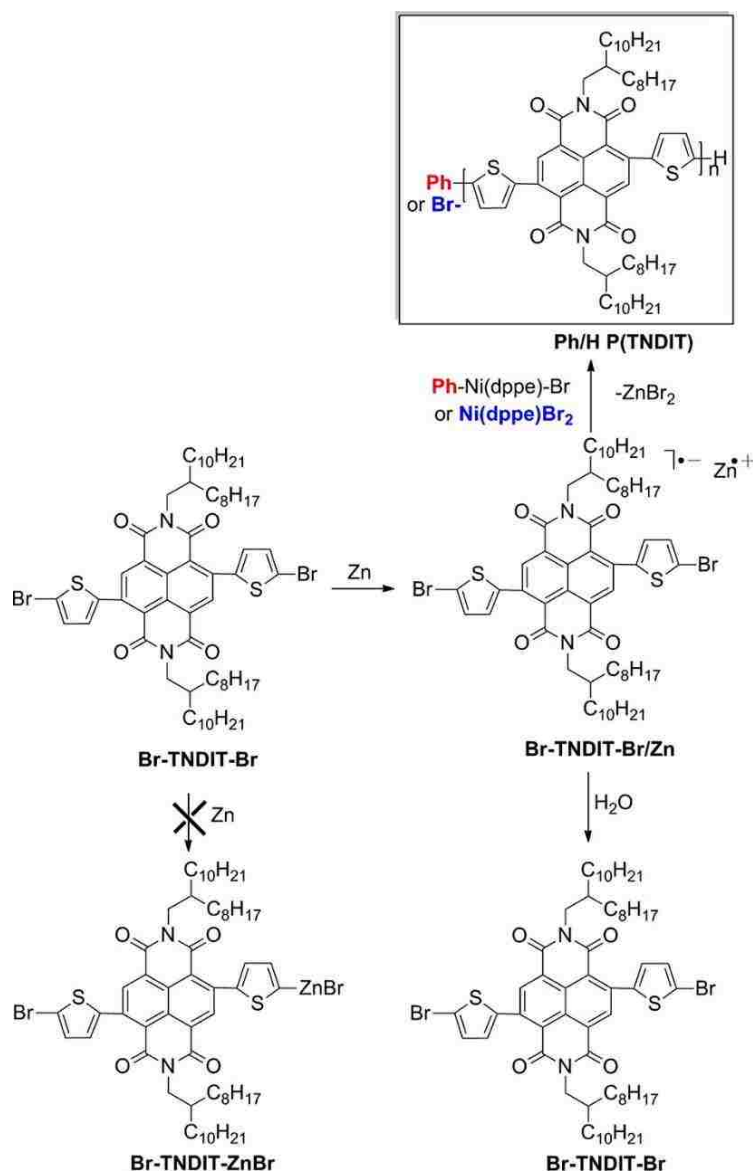


Figure 1.6 Preparation of the Br-TNDIT-Br/Zn radical-anion monomer and its catalyst-transfer polymerization. Reproduced with permission from ref. 69. Copyright © 2011 American Chemical Society.

1.4 Surface-initiated polymerization of conjugated polymers

With a groundbreaking discovery by McCullough⁵¹⁻⁵² and Yokozawa⁵⁴⁻⁵⁵ that step growth polymerization could be converted to chain growth polymerization, it became possible to prepare polymers in controlled/living chain growth fashion. This opened up the possibility to use KCTP to prepare various types of conjugated polymers attached to surfaces.

Kiriy and coworkers first reported that surface-initiated Kumada polymerization of 2-bromo-5-chloromagnesio-3-alkylthiophene occurred in the chain growth fashion to form regioregular head-to-tail P3HT. They initially used Ni(dppp)Cl₂ catalyst for surface-initiated polymerization which would initiate the polymerization from the surface, but got low molecular weight and low yield. At that point, they decided to use Ni(dppp)₂ for preparing an external catalytic initiator from poly(4-bromostyrene) (PS-Br). It was found that Ni(dppp)₂ was too unreactive in oxidative addition with non-activated aryl halides. Therefore, they ended up using more reactive Ni(PPh₃)₄ for the oxidative addition. They observed a facile reaction at room temperature between Ni(PPh₃)₄ and bromobenzene to give (PPh₃)₂Ni(Ph)Br. NMR, GPC, and MALDI-TOF characterization confirmed that this catalyst could be used for chain growth polymerization, in which P3HT of 5000 g mol⁻¹ with PDI of 1.2 and almost 100% regioregularity was obtained. Poly(4-bromostyrene) was then spun-cast on silicon wafer, crosslinked using UV light and converted to a surface-immobilized Ni catalyst by treatment of the film with Ni(PPh₃)₄, and subsequent polymerization was carried out at 0 °C. The polymerization took place only from the surface-immobilized initiator and there was no polymerization observed in solution. Furthermore, it was observed that polymerization occurred not only on the surface of cross-linked PS-Br but also in its bulk, due to the formation of solvent-swollen interpenetrating network (figure 1.7).⁷⁰⁻⁷¹

Kiriy further extended their approach by grafting P3HT on poly(4-vinylpyridine)-*block*-poly(4-iodostyrene), P4VP-*b*-PS.⁷² Using this block copolymer enabled preparation of nanopatterned catalytic surfaces, and hence nanopatterned conjugated polymer films. The ability to prepare nanopatterned thin films of conjugated polymers can have significant impact on prospective optoelectronic applications of conjugated polymers. P4VP is a polymer which, due to

its polar nature, can adhere and bind to the surface of the polar substrates such as silicon wafers, quartz or glass slides. The surface-confined thin films were formed by first spin-casting P4VP₇₅-*b*-PS(I)₃₁₃ solution on silicon wafer followed by treatment of the monolayer with Ni(PPh₃)₄ catalyst. The reaction of the activated layer with Grignard monomer gave P4VP₇₅-*b*-PS(I)₃₁₃-*g*-P3HT, with the film thickness between 30 and 50 nm. They also fabricated bulk heterojunction solar cells using this film with FF=25%, and V_{oc} = 0.2 V. Poor photovoltaic performance was attributed to inefficient charge separation due to the presence of 1.5 nm insulating P4VP layer.

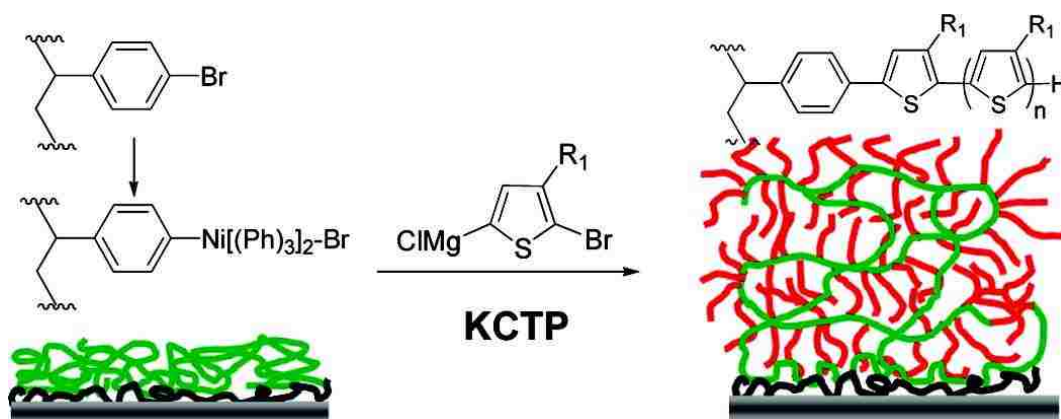


Figure 1.7 P3HT film prepared by *grafting from* approach using photo-crosslinked PS-Br. Reproduced with permission from ref. 71. Copyright © 2008 American Chemical Society.

To increase the efficiency of surface-confined polymerization, Kiriya and coworkers used ligand exchange method to initiate polymerization from silica particles.⁷³ A bromobenzene compound possessing a silyl anchor was covalently attached to the surface of two kinds of monodisperse silica particles – mesoparticles of 460 nm diameter and nanoparticles of 4 nm diameter. The monolayer-modified silica particles were then treated with Et₂Ni(Bipy) followed by ligand exchange with dppp or dpppe to form surface modified Ni(II) initiator which was then treated with 2-bromo-5-chloromagnesio-3-hexylthiophene monomer to give hybrid polymer-

functionalized mesoparticles and “hairy” nanoparticles. It was observed that only 10% of unbound P3HT was formed in solution indicating good surface selectivity. For the mesoparticles, degree of polymerization was about 250 with PDI of 1.1-1.2. Absorption and fluorescence spectra of the polymer grafted to mesoparticles were red-shifted by 170 nm (relative to P3HT in dilute solution), with the absorption spectra being more structured than the fluorescence spectra. This was attributed to planarization of conjugated backbone and interchain aggregation between surface-confined P3HT chains causing efficient delocalization of π -electrons (figure 1.8).

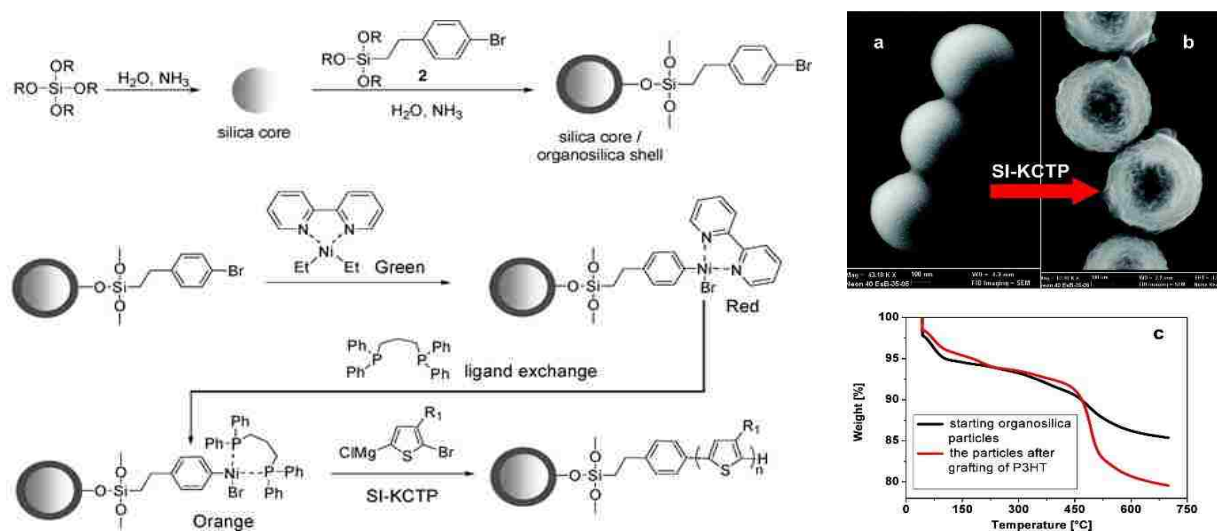


Figure 1.8 Synthesis of SiO₂-grafted P3HT nanoparticles by surface-confined polymerization. Reproduced with permission from ref. 73. Copyright © 2009 American Chemical Society.

The effect of surface curvature was studied by comparing between P3HT-grafted silica meso- and nanoparticles. The nanoparticles showed excellent solubility and resulting P3HT grafted polymer had M_n of only 4000 g mol⁻¹. Optical properties of the hybrid P3HT-functionalized nanoparticles were similar to that of linear P3HT polymers in solution. Finally, solar cells made using these particles showed the efficiency of 1.8-2.3%.

Locklin's group⁷⁴ used Grignard reagent bearing ferrocene as an electrochemical probe to study the efficiency of surface-confined polymerization and surface density of various surface-

immobilized catalytic initiators. They found that $\text{Ni}(\text{COD})_2$ with Bipy taken in 1:1 ratio was more efficient for surface-confined polymerization than $\text{Ni}(\text{COD})_2$ with dppp or dppe (1:1 ratio). They also showed that ligand exchange approach was not efficient for the polymerization on atomically flat gold surface due to disproportionation between adjacent surface-immobilized nickel complexes as shown in figure 1.9. In the case of indium tin oxide and SiO_2 wafer, no disproportionation reaction happened as grafting density of monolayer for these substrates was lower. Films with thickness of 30-60 nm were obtained, and some free unbound polymer was always found in solution indicating possible chain transfer side reactions as a sign of less controlled nature of the polymerization.

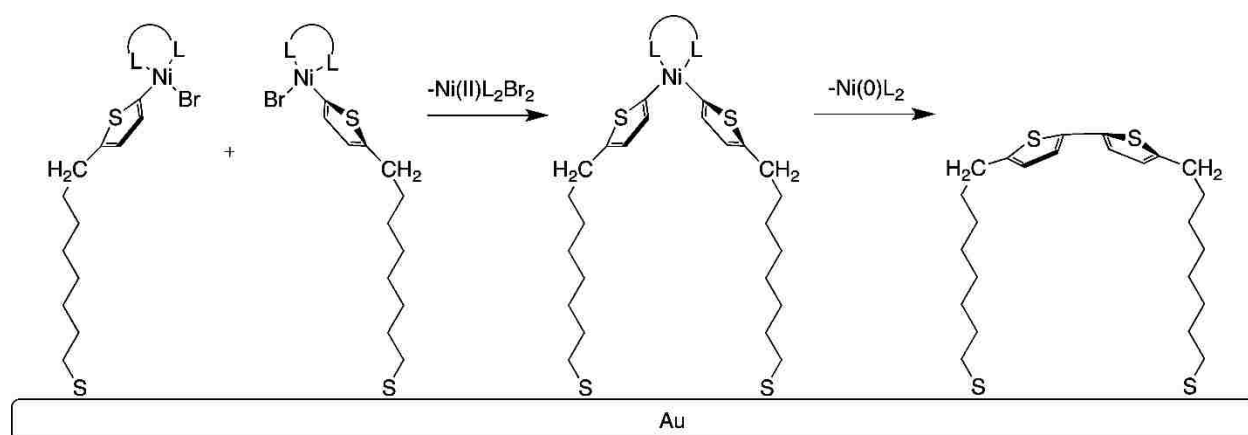


Figure 1.9: Proposed surface disproportionation mechanism. Reproduced with permission from ref. 74. Copyright © 2011 American Chemical Society.

More recently, Kiriya studied surface-initiated polymerization of poly(9,9-dioctylfluorene) (PFO) on functionalized silica mesoparticles.⁷⁵⁻⁷⁶ In particular, 880 nm monodisperse silica particles surface-functionalized with iodophenyl group were treated with $\text{Et}_2\text{Ni}(\text{bipy})$ and followed by ligand exchange with dppe. The bidentate ligand dppe (1,2-bis(diphenylphosphino)ethane) was chosen due to its better solubility that prevents aggregation of the particles during the immobilization step. Upon generating surface-immobilized $\text{Ni}(\text{II})$ catalytic initiator, the fluorenyl

Grignard monomer was added at room temperature to form particles with surface-attached PFO shell. Degrafting of the polymer using HF treatment showed M_n of 48000 g mol⁻¹ and PDI of 3.7, and indicated grafting density of 0.89 chain nm⁻² which corresponded to relatively dense surface film. TGA showed loss of 10% of weight which corresponded to approximately 25 nm thick shell. The same size silica particles (880 nm) was used to form water soluble conjugated polymers. 3-Bromohexylthiophene was polymerized from bromophenyl surface-functionalized silica particles. This was followed by converting bromo side group to an amino group by reacting first with potassium phthalimide followed by reduction by hydrazine hydrate to an amino group. This amine functionalized polyelectrolyte was sensitive to pH and soluble in water. UV-VIS and fluorescence spectroscopy data showed dependence of optical properties on change in pH of the surrounding environment, illustrating that this material can be useful for future sensory applications (figure 1.10).



Figure 1.10: Grafting of PFO from microparticles *via* SI-KCTP. Reproduced with permission from ref. 76. Copyright © 2010 Royal Chemical Society.

Kiry also first reported surface-initiated KCTP of tetrafunctional AB 2 monomers grown on silica mesoparticles.⁷⁷ An important feature of this monomer design was that it comprised of two π -conjugated subunits, and each unit was acting independently as AB monomer. Thus, in KCTP conditions, each subunit would polymerize separately in a chain growth fashion. The presence of spiro-orthocarbonate group ensured formation of the microporous structure. Surface-

initiated polymerization of AB monomer followed the same protocol as used for poly(3-[6-aminohexyl]thiophene) brushes (*vide supra*). The thickness of the film as determined by SEM was 30 nm. The porosity of the polymer was measured by BET, and the specific surface area was found to be $158 \text{ m}^2 \text{ g}^{-1}$ which was lower than that of bulk polymer ($463 \text{ m}^2 \text{ g}^{-1}$) (figure 1.11).

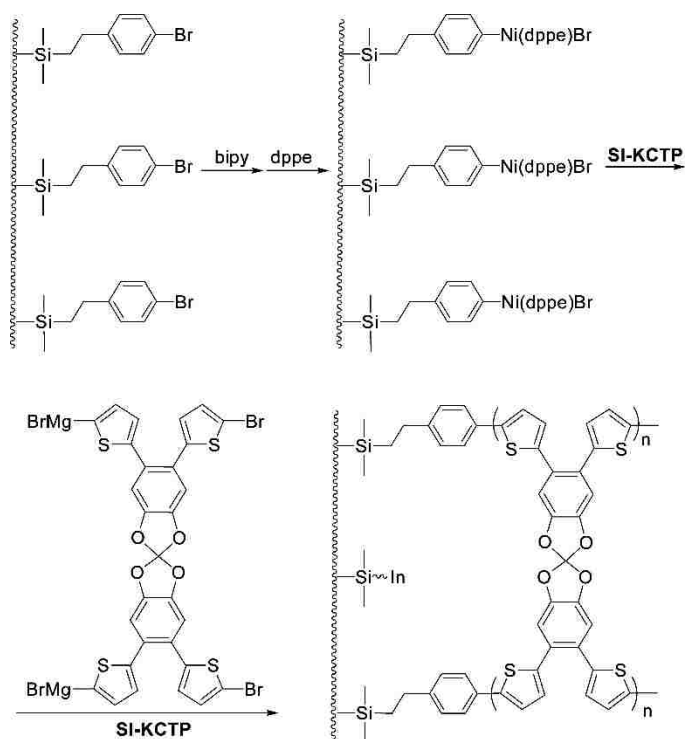


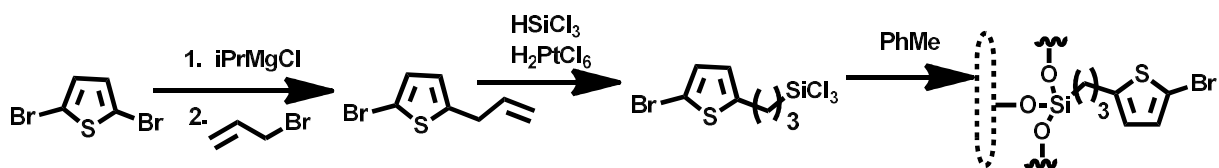
Figure 1.11: Surface-initiated polymerization of microparticles having microporous conjugated polymer shell. Reproduced with permission from ref. 77. Copyright © 2012 American Chemical Society

Locklin's group demonstrated preparation of surface-confined polythiophene and poly-*p*-phenylene films on gold wafers.⁷⁸ First, the substrate was functionalized with aryl bromide by reduction of thiol anchoring group on the gold surface. Then the monolayers were treated with $\text{Ni}(\text{COD})(\text{PPh}_3)_2$ ($\text{COD} = 1,5\text{-cyclooctadiene}$) to give the surface-immobilized catalytic initiating units. Then, the treated wafer was immersed in a solution of Grignard monomer, ClMg-Ar-I , to provide 14 nm PT and 42 nm PPP. In that work, they also observed formation of polymer precipitate in solution which was due to the chain transfer of nickel species from surfaces to

monomer in solution, thus indicating less robust character of the chain-growth mechanism of surface-confined polymerization.

As a continuation of the above study, Locklin extended the idea by looking into the effect of sterics in surface-initiated Kumada polymerization by polymerizing a series of 1-iodo-4-chloromagnesio monomers with alkoxy side chains with varying length ranging from H to hexyl.⁷⁹ Aryl bromide monolayer was prepared as shown in figure 1.12. First, dibromothiophene was treated with isopropyl magnesium chloride to form Grignard reagent which was subsequently reacted with allyl bromide to give allyl terminated thiophene compound. Hydrosilylation of the alkene using H_2PtCl_6 as a catalyst gave chlorosilane having alkyl chain terminated with reactive thienyl bromide. Chlorosilane was immobilized onto activated silicon oxide surfaces by immersion of slides into a solution of chlorosilane in toluene. This monolayer then was treated sequentially with $\text{Ni}(\text{COD})_2$ and dppe to form nickel complex which was then used to polymerize different *p*-phenylene Grignard reagents to form poly-*p*-phenylene thin films. It was found that the thickness of the film varied depending on the size of side groups. Ellipsometry and AFM studies showed that unsubstituted aryl monomer produced a thicker layer in comparison to the monomer with hexyl substituents. Thickness of the film was: H= 30 nm, methyl = 17 nm, ethyl = 12 nm and hexyl = 4.8 nm. Also, the authors observed that no polymerization took place if brominated monomers were used instead of iodo-substituted monomers.

Figure 1.12 Synthesis of surface-grafted thiophene bromide initiator



In the same study, they also showed that addition of LiCl salt to the reaction mixture led to

smoother films. This was due to the ability of LiCl to break the aggregate formation in Grignard solution and to increase the nucleophilicity.

To show the feasibility of KCTP process, Locklin and coworkers have tried different initiating systems Ar-Ni(II)-Br on different planar substrates such as silica and indium tin oxide (ITO) surface. Poly(3-methylthiophene) films of uniform thickness of 40-65 nm were prepared using 2-bromo-5-chloromagnesio-3-methylthiophene as a monomer.⁷⁴

Luscombe and coworkers used SI-KCTP to grow poly(3-methylthiophene) on ITO substrates.⁸⁰ They used 4-chloro-3-methyl-benzylphosphonic acid solution to get initiator monolayer which was further treated with Ni(COD)(PPh₃)₂ solution and dppe to give final Ni catalytic complex. One important observation found in this study was that thickness of the film can be tuned with a change in the Grignard monomer concentration (from 0.03 M to 0.18 M). The film thickness increased linearly with monomer concentration varying from 30 nm at 0.03 M to 50 nm at 0.05 M to 80 nm at 0.09 M and 265 nm at 0.18 M. The author showed that varying thickness with concentration can be attributed to steric effects of growing chain on the diffusion of reaction components. Thus, when surface grafted chain has reached a critical point, monomer diffusion to reaction site may be reduced. Using a higher concentration of monomer can overcome this and provide a thicker film. Thicker and tunable films are important for some optoelectronic applications.⁸¹

Palladium catalyst complexes were also investigated recently in preparation of π -conjugated polymer brushes. Kiriy's group demonstrated the first surface-initiated palladium catalyzed Suzuki catalyst transfer polycondensation to graft polyfluorene films to polystyrene surface.⁸² They attached [2-(4-bromo-phenyl)ethyl]chlorodimethylsilane to a PS-Br surface layer followed by reacting with Pd(*Pt*-Bu₃)₂ in toluene at 70 °C to give an active catalytic Pd-complex.

This surface bound initiator was then treated with THF solution containing 7-bromo-9,9-bis(2-ethylhexyl)-9H-fluoren-2-ylboronic acid ester in the presence of aqueous sodium carbonate solution for 2-3 h. Polymerization processes gave a thicker and smoother film of 100 nm thickness with rms of 1.1 nm as determined by AFM data. It was also pointed out that polymerization only took place at the surface of PS-Br, in contrast to what the same group claimed previously for SI-KCTP for a similar nickel(II)-catalyzed reaction. They also used this technique for nanopatterning to form a quasi-periodic hexagonal array of round shaped discs.

Following the same idea, Locklin and coworkers synthesized poly(3-methylthiophene) on ITO-coated glass substrates. ITO-glass substrate was first functionalized with (4-bromobenzyl)phosphonic acid followed by reaction with $\text{Pd}(P\text{-}t\text{-Bu}_3)_2$ to give surface-immobilized Pd-catalyst complex which was then treated with a solution of 2-bromo-3-methyl-5-chloromagnesiothiophene to give poly(3-methylthiophene) brushes on the surface, with the film thickness >100 nm.⁸³ They also demonstrated that P3MT films were anisotropic by using polarized UV-VIS spectroscopy. The films showed higher absorbance for p-polarized light than for the s-polarized light at an angle of 45° , thus indicating that orientation of surface-confined polymer chains in the film was somewhat perpendicular to the substrate.

Recently, Bielawski synthesized well-defined poly(*p*-phenylene ethynylene) (PPE) brushes via controlled Stille catalyst transfer polymerization.⁶³ They used stannylated monomer, (2,5-bis(2-ethylhexyloxy)-(4-iodophenyl)ethynyl)tributyl stannate which, upon treatment with copper iodide, PPh_3 and $\text{PhPd}(t\text{-Bu}_3\text{P})\text{Br}$ initiator in THF solution, gave PPE in 94% yield with PDI of 1.67. The addition of more monomer did not change the PDI. Thus, the polymerization seemingly occurred in a chain-growth fashion. They then used this protocol to graft PPE on silica particles. Silica particles of 200 nm were functionalized with [2-(4-bromophenyl)-ethyl]

triethoxysilane to give SiO₂-PhBr (3.6 mmol m⁻² grafting density), which was then reacted with a palladium catalyst, Pd(*Pt*-Bu₃)₂ to afford SiO₂-Ph-Pd(*Pt*-Bu₃)-Br macroinitiator. This macroinitiator was further treated with copper iodide, PPh₃, and the stannyl monomer in THF at 50 °C to give SiO₂-PPE particles with M_n of 24.5 kDa and 62% yield. To prove that polymerization occurred via chain growth mechanism, they added fresh aliquots of the stannyl monomer to the unquenched SiO₂-PPE solution and measured the M_n using size exclusion chromatography (SEC) after degrafting the polymer by treating the nanoparticles with HF solution. M_n of the resulting brushes was doubled upon this treatment which indicated that the polymerization indeed occurred by the chain-growth mechanism.

1.5 Grafting through approach

For surface grafted polymerization on inorganic nanomaterials such as CdSe quantum dots, Heck surface polymerization was employed. CdSe quantum dots (QDs) are a particular class of inorganic semiconductors which gain attraction due to their applications in photovoltaic cells,⁸⁴ light emitting diodes,⁸⁵ and bio-sensors.⁸⁶ QDs are synthesized in the presence of ligands such as phosphine oxide that stabilize the particles during the growth process and also prevent them from aggregation and oxidation in air.⁸⁷ Emrick and coworkers reported the synthesis of QD-based PPV copolymers.⁸⁸⁻⁸⁹ They synthesized QDs in the presence of phosphine oxide ligand having phenyl bromide functionality. This bromine terminated QDs were then further modified in the conditions of palladium-catalyzed Heck polymerization with 1,4-di-*n*-octyl-2,5-divinylbenzene and 1,4-dibromo-2,5-di-*n*-octylbenzene to form QDs-PPV copolymer. Grafted polymer was characterized by NMR and MALDI-TOF to confirm the formation of surface-attached oligomeric units about 3-6 repeating units long. Photoluminescence studies showed quenching of fluorescence indicating efficient charge transfer from PPV shell to CdSe QDs.

Schanze's group were first to report Sonogashira coupling to graft conjugated polymers (PPE) on silica surfaces.⁹⁰ Silica particles were first treated with aryl iodide to give SiO₂-ArI units which were further reacted with CuI, Pd(Ph₃)₄ and monomer to form SiO₂-PPE grafted polymer shell. TGA showed a loss of weight due to polymer content clearly proving grafting of the polymer on silica surface. Polymer layer thickness was calculated to be 12 nm which corresponded to 10 repeating units, assuming normal to the surface orientation of CP chains.

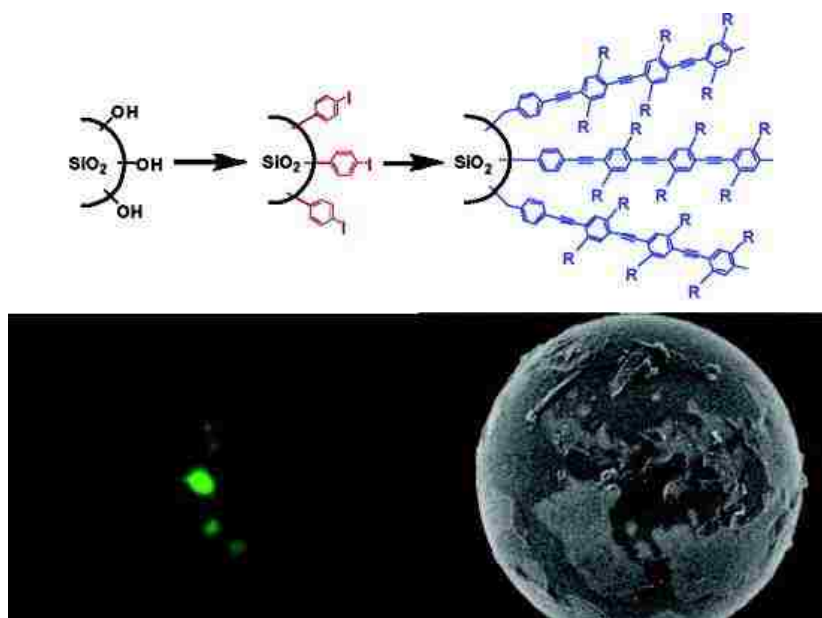


Figure 1.13 Sonogashira surface polymerization on silica particles to form PPE shell. Reproduced with permission from ref. 90. Copyright © 2007 American Chemical Society.

Another important point noticed was formation of a lot of polymer aggregates in solution, with some aggregates being as large as 50 nm. This might be attributed to improper washing, and some polymer which was formed in solution was actually physisorbed onto the surface. The authors also showed that electron transfer and energy transfer quencher ions could efficiently quench or suppress the fluorescence and thus these materials could be used in biological fluorescent sensors (figure 1.13).

Carter's group also tried to graft polyacetylene brushes onto a silicon wafer using metathesis reaction. They first modified the silicon surface via silane bearing alkyne group followed by microwave irradiation of 5-decyne with catalytic amount of WCl_6/Ph_4Sn at $150\text{ }^\circ\text{C}$ for 30 mins.⁹¹ High molecular weight polymer film with 41 nm thickness was obtained (figure 1.14).

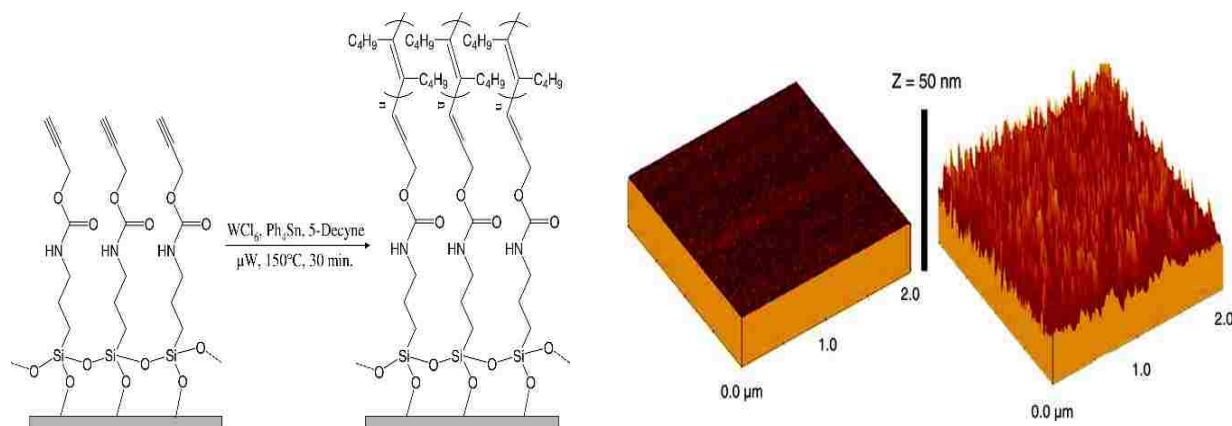


Figure 1.14 Synthesis of alkyne-functionalized SiO_2 substrates and formation of surface-confined polyacetylene film using tungsten catalyzed polymerization. Reproduced with permission from ref. 91. Copyright © 2007 American Chemical Society.

1.6 Research Focus

This dissertation is focused on the design of well-defined hybrid nanoparticle systems consisting of grafted conjugated polymers at the surface of inorganic nanosized core prepared by “grafting from” approach. Hybrid “hairy” materials have attracted attention due to their potential future technological applications (for example, for use in optoelectronic devices, sensors, etc.). This chapter mainly discusses the current state of the art and the progress achieved in the field so far.

In Chapter 2, novel hybrid materials consisting of silica core with grafted polymer and block copolymer shells were synthesized using surface-initiated Kumada catalyst transfer polymerization. Both synthesis of monodisperse silica particles and their characterization using various techniques are described. In addition, detailed photophysical studies, including time-

resolved spectroscopic studies are reported that revealed that energy transfer process between the components of the conjugated polymer shell varies with the order of the polymers.

Chapter 3 describes hybrid materials consisting of silica core and grafted triblock copolymer shell. This section discusses synthesis of the hybrid systems consisting of triblock copolymer, diblock copolymer and homopolymer shell grafted on silica nanoparticles. One of the subshells was polyallene, which provided stimuli responsive characteristics to the hybrid nanoparticles, such as response to solvent which affected the photophysical characteristics of the conjugated polymer shell.

In Chapter 4, a different core consisting of gold nanoparticles coated with a thin layer of silica was studied. This core was used to graft conjugated diblock copolymer, with the goal to investigate the effect of the fluorescence-quenching gold core on the photophysical characteristics of the conjugated polymer shell. This study was heavily focused on using time-resolved transient absorption spectroscopy to reveal the details of intra-shell energy transfer and the effect of the gold central core on this process.

1.7 References

1. Chiang, C. K.; Fincher, C. R., Jr.; Park, Y. W.; Heeger, A. J.; Shirakawa, H.; Louis, E. J.; Gau, S. C.; MacDiarmid, A. G., Electrical conductivity in doped polyacetylene. *Phys. Rev. Lett.* **1977**, *39* (17), 1098-101.
2. Sokolov, A. N.; Tee, B. C. K.; Bettinger, C. J.; Tok, J. B. H.; Bao, Z., Chemical and Engineering Approaches To Enable Organic Field-Effect Transistors for Electronic Skin Applications. *Acc. Chem. Res.* **2012**, *45* (3), 361-371.
3. Facchetti, A.; Vaccaro, L.; Marrocchi, A., Semiconducting Polymers Prepared by Direct Arylation Polycondensation. *Angew. Chem., Int. Ed.* **2012**, *51* (15), 3520-3523.
4. Marrocchi, A.; Lanari, D.; Facchetti, A.; Vaccaro, L., Poly(3-hexylthiophene): synthetic methodologies and properties in bulk heterojunction solar cells. *Energy Environ. Sci.* **2012**, *5* (9), 8457-8474.

5. Facchetti, A., π -Conjugated Polymers for Organic Electronics and Photovoltaic Cell Applications. *Chem. Mater.* **2011**, *23* (3), 733-758.
6. Marks, T. J., Materials for organic and hybrid inorganic/organic electronics. *MRS Bull.* **2010**, *35* (12), 1018-1027.
7. Hasegawa, M.; Iyoda, M., Conducting supramolecular nanofibers and nanorods. *Chem. Soc. Rev.* **2010**, *39* (7), 2420-2427.
8. Grimsdale, A. C.; Leok Chan, K.; Martin, R. E.; Jokisz, P. G.; Holmes, A. B., Synthesis of Light-Emitting Conjugated Polymers for Applications in Electroluminescent Devices. *Chem. Rev.* **2009**, *109* (3), 897-1091.
9. Dennler, G.; Scharber, M. C.; Brabec, C. J., Polymer-fullerene bulk-heterojunction solar cells. *Adv. Mater.* **2009**, *21* (13), 1323-1338.
10. Heremans, P.; Cheyns, D.; Rand, B. P., Strategies for Increasing the Efficiency of Heterojunction Organic Solar Cells: Material Selection and Device Architecture. *Acc. Chem. Res.* **2009**, *42* (11), 1740-1747.
11. Thompson, B. C.; Frechet, J. M. J., Polymer-fullerene composite solar cells. *Angew. Chem., Int. Ed.* **2008**, *47* (1), 58-77.
12. Yan, H.; Chen, Z.; Zheng, Y.; Newman, C.; Quinn, J. R.; Dotz, F.; Kastler, M.; Facchetti, A., A high-mobility electron-transporting polymer for printed transistors. *Nature* **2009**, *457* (7230), 679-686.
13. Collini, E.; Scholes, G. D., Coherent Intrachain Energy Migration in a Conjugated Polymer at Room Temperature. *Science* **2009**, *323* (5912), 369-373.
14. Hoppe, H.; Sariciftci, N. S., Morphology of polymer/fullerene bulk heterojunction solar cells. *J. Mater. Chem.* **2006**, *16* (1), 45-61.
15. Nguyen, T. Q.; Yee, R. Y.; Schwartz, B. J., Solution processing of conjugated polymers: the effects of polymer solubility on the morphology and electronic properties of semiconducting polymer films. *J. Photochem. Photobiol., A* **2001**, *144* (1), 21-30.
16. Lee, T.-W.; Park, O. O., The effect of different heat treatments on the luminescence efficiency of polymer light-emitting diodes. *Adv. Mater.* **2000**, *12* (11), 801-804.
17. Dennler, G.; Lungenschmied, C.; Neugebauer, H.; Sariciftci, N. S.; Latreche, M.; Czeremuszkin, G.; Wertheimer, M. R., A new encapsulation solution for flexible organic solar cells. *Thin Solid Films* **2006**, *511-512*, 349-353.

18. Helander, M. G.; Wang, Z. B.; Qiu, J.; Lu, Z. H., Band alignment at metal/organic and metal/oxide/organic interfaces. *Appl. Phys. Lett.* **2008**, *93* (19), 193310/1-193310/3.
19. Graetzel, M.; Janssen, R. A. J.; Mitzi, D. B.; Sargent, E. H., Materials interface engineering for solution-processed photovoltaics. *Nature* **2012**, *488* (7411), 304-312.
20. Edmondson, S.; Osborne, V. L.; Huck, W. T. S., Polymer brushes via surface-initiated polymerizations. *Chem. Soc. Rev.* **2004**, *33* (1), 14-22.
21. Li, G.; Shrotriya, V.; Huang, J.; Yao, Y.; Moriarty, T.; Emery, K.; Yang, Y., High-efficiency solution processable polymer photovoltaic cells by self-organization of polymer blends. *Nat. Mater.* **2005**, *4* (11), 864-868.
22. Reiss, P.; Couderc, E.; De Girolamo, J.; Pron, A., Conjugated polymers/semiconductor nanocrystals hybrid materials-preparation, electrical transport properties and applications. *Nanoscale* **2011**, *3* (2), 446-489.
23. Skompska, M., Hybrid conjugated polymer/semiconductor photovoltaic cells. *Synth. Met.* **2010**, *160* (1-2), 1-15.
24. Xu, T.; Qiao, Q., Conjugated polymer-inorganic semiconductor hybrid solar cells. *Energy Environ. Sci.* **2011**, *4* (8), 2700-2720.
25. Gonzalez-Valls, I.; Lira-Cantu, M., Vertically-aligned nanostructures of ZnO for excitonic solar cells: a review. *Energy Environ. Sci.* **2009**, *2* (1), 19-34.
26. Ong, W. L.; Low, Q. X.; Huang, W.; van Kan, J. A.; Ho, G. W., Patterned growth of vertically-aligned ZnO nanorods on a flexible platform for feasible transparent and conformable electronics applications. *J. Mater. Chem.* **2012**, *22* (17), 8518-8524.
27. Greenham, N. C.; Peng, X.; Alivisatos, A. P., Charge separation and transport in conjugated-polymer/semiconductor-nanocrystal composites studied by photoluminescence quenching and photoconductivity. *Phys. Rev. B: Condens. Matter* **1996**, *54* (24), 17628-17637.
28. Saunders, B. R.; Turner, M. L., Nanoparticle-polymer photovoltaic cells. *Adv. Colloid Interface Sci.* **2008**, *138* (1), 1-23.
29. Oosterhout, S. D.; Koster, L. J. A.; van Bavel, S. S.; Loos, J.; Stenzel, O.; Thiedmann, R.; Schmidt, V.; Campo, B.; Cleij, T. J.; Lutzen, L.; Vanderzande, D.; Wienk, M. M.; Janssen, R. A. J., Controlling the morphology and efficiency of hybrid ZnO:polythiophene solar cells via side chain functionalization. *Adv. Energy Mater.* **2011**, *1* (1), 90-96.
30. Feng, J.; Li, Y.; Yang, M., Conjugated polymer-grafted silica nanoparticles for the sensitive detection of TNT. *Sens. Actuators, B* **2010**, *145* (1), 438-443.

31. Advincula, R. C.; Brittain, W. J.; Baster, K. C.; Ruhe, J., *Polymer Brushes: Synthesis, Characterization, Applications*. Wiley-VCH Verlag GmbH & Co. KGaA: 2004; p 483 pp.
32. Ma, H.; Yip, H.-L.; Huang, F.; Jen, A. K. Y., Interface Engineering for Organic Electronics. *Adv. Funct. Mater.* **2010**, *20* (9), 1371-1388.
33. Hains, A. W.; Ramanan, C.; Irwin, M. D.; Liu, J.; Wasielewski, M. R.; Marks, T. J., Designed Bithiophene-Based Interfacial Layer for High-Efficiency Bulk-Heterojunction Organic Photovoltaic Cells: Importance of Interfacial Energy Level Matching. *ACS Appl. Mater. Interfaces* **2010**, *2* (1), 175-185.
34. De Gennes, P. G., Conformations of polymers attached to an interface. *Macromolecules* **1980**, *13* (5), 1069-75.
35. Mansky, P.; Liu, Y.; Huang, E.; Russell, T. P.; Hawker, C., Controlling polymer-surface interactions with random copolymer brushes. *Science* **1997**, *275* (5305), 1458-1460.
36. Kopf, A.; Baschnagel, J.; Wittmer, J.; Binder, K., On the Adsorption Process in Polymer Brushes: A Monte Carlo Study. *Macromolecules* **1996**, *29* (5), 1433-41.
37. Ulman, A., Formation and Structure of Self-Assembled Monolayers. *Chem. Rev.* **1996**, *96* (4), 1533-1554.
38. Kango, S.; Kalia, S.; Celli, A.; Njuguna, J.; Habibi, Y.; Kumar, R., Surface modification of inorganic nanoparticles for development of organic-inorganic nanocomposites-A review. *Prog. Polym. Sci.* **2013**, *38* (8), 1232-1261.
39. Belanger, D.; Pinson, J., Electrografting: a powerful method for surface modification. *Chem. Soc. Rev.* **2011**, *40* (7), 3995-4048.
40. Pieters, G.; Prins, L. J., Catalytic self-assembled monolayers on gold nanoparticles. *New J. Chem.* **2012**, *36* (10), 1931-1939.
41. Queffelec, C.; Petit, M.; Janvier, P.; Knight, D. A.; Bujoli, B., Surface Modification Using Phosphonic Acids and Esters. *Chem. Rev.* **2012**, *112* (7), 3777-3807.
42. de Groot, G. W.; Santonicola, M. G.; Sugihara, K.; Zambelli, T.; Reimhult, E.; Voeroes, J.; Vancso, G. J., Switching Transport through Nanopores with pH-Responsive Polymer Brushes for Controlled Ion Permeability. *ACS Appl. Mater. Interfaces* **2013**, *5* (4), 1400-1407.
43. Santonicola, M. G.; Memesa, M.; Meszynska, A.; Ma, Y.; Vancso, G. J., Surface-grafted zwitterionic polymers as platforms for functional supported phospholipid membranes. *Soft Matter* **2012**, *8* (5), 1556-1562.

44. Rastogi, A.; Paik, M. Y.; Tanaka, M.; Ober, C. K., Direct Patterning of Intrinsically Electron Beam Sensitive Polymer Brushes. *ACS Nano* **2010**, *4* (2), 771-780.
45. Takahashi, H.; Nakayama, M.; Yamato, M.; Okano, T., Controlled Chain Length and Graft Density of Thermoresponsive Polymer Brushes for Optimizing Cell Sheet Harvest. *Biomacromolecules* **2010**, *11* (8), 1991-1999.
46. Lang, A. S.; Neubig, A.; Sommer, M.; Thelakkat, M., NMRP versus "Click" Chemistry for the Synthesis of Semiconductor Polymers Carrying Pendant Perylene Bisimides. *Macromolecules* **2010**, *43* (17), 7001-7010.
47. Stenzel, M. H., Hairy Core-Shell Nanoparticles via RAFT: Where are the Opportunities and Where are the Problems and Challenges? *Macromol. Rapid Commun.* **2009**, *30* (19), 1603-1624.
48. Barbey, R.; Lavanant, L.; Paripovic, D.; Schuwer, N.; Sugnaux, C.; Tugulu, S.; Klok, H.-A., Polymer Brushes via Surface-Initiated Controlled Radical Polymerization: Synthesis, Characterization, Properties, and Applications. *Chem. Rev.* **2009**, *109* (11), 5437-5527.
49. Matyjaszewski, K.; Spanswick, J., Controlled/living radical polymerization. *Mater. Today* **2005**, *8* (3), 26-33.
50. Rutenberg, I. M.; Scherman, O. A.; Grubbs, R. H.; Jiang, W.; Garfunkel, E.; Bao, Z., Synthesis of Polymer Dielectric Layers for Organic Thin Film Transistors via Surface-Initiated Ring-Opening Metathesis Polymerization. *J. Am. Chem. Soc.* **2004**, *126* (13), 4062-4063.
51. Iovu, M. C.; Sheina, E. E.; Gil, R. R.; McCullough, R. D., Experimental Evidence for the Quasi-"Living" Nature of the Grignard Metathesis Method for the Synthesis of Regioregular Poly(3-alkylthiophenes). *Macromolecules* **2005**, *38* (21), 8649-8656.
52. Stefan, M. C.; Javier, A. E.; Osaka, I.; McCullough, R. D., Grignard Metathesis Method (GRIM): Toward a Universal Method for the Synthesis of Conjugated Polymers. *Macromolecules* **2009**, *42* (1), 30-32.
53. Chen, T.-A.; Wu, X.; Rieke, R. D., Regiocontrolled Synthesis of Poly(3-alkylthiophenes) Mediated by Rieke Zinc: Their Characterization and Solid-State Properties. *J. Am. Chem. Soc.* **1995**, *117* (1), 233-44.
54. Miyakoshi, R.; Yokoyama, A.; Yokozawa, T., Catalyst-Transfer Polycondensation. Mechanism of Ni-Catalyzed Chain-Growth Polymerization Leading to Well-Defined Poly(3-hexylthiophene). *J. Am. Chem. Soc.* **2005**, *127* (49), 17542-17547.
55. Yokozawa, T.; Adachi, I.; Miyakoshi, R.; Yokoyama, A., Catalyst-transfer condensation polymerization for the synthesis of well-defined polythiophene with hydrophilic side chain

- and of diblock copolythiophene with hydrophilic and hydrophobic side Chains. *High Perform. Polym.* **2007**, *19* (5/6), 684-699.
56. Lanni, E. L.; McNeil, A. J., Mechanistic Studies on Ni(dppe)Cl₂-Catalyzed Chain-Growth Polymerizations: Evidence for Rate-Determining Reductive Elimination. *J. Am. Chem. Soc.* **2009**, *131* (45), 16573-16579.
 57. Lanni, E. L.; McNeil, A. J., Evidence for Ligand-Dependent Mechanistic Changes in Nickel-Catalyzed Chain-Growth Polymerizations. *Macromolecules* **2010**, *43* (19), 8039-8044.
 58. Tkachov, R.; Senkovskyy, V.; Komber, H.; Sommer, J.-U.; Kiriy, A., Random Catalyst Walking along Polymerized Poly(3-hexylthiophene) Chains in Kumada Catalyst-Transfer Polycondensation. *J. Am. Chem. Soc.* **2010**, *132* (22), 7803-7810.
 59. Okamoto, K.; Luscombe, C. K., Controlled polymerizations for the synthesis of semiconducting conjugated polymers. *Polym. Chem.* **2011**, *2* (11), 2424-2434.
 60. Chavez, C. A.; Choi, J.; Nesterov, E. E., One-Step Simple Preparation of Catalytic Initiators for Catalyst-Transfer Kumada Polymerization: Synthesis of Defect-Free Polythiophenes. *Macromolecules* **2014**, *47* (2), 506-516.
 61. Yokoyama, A.; Yokozawa, T., Converting Step-Growth to Chain-Growth Condensation Polymerization. *Macromolecules* **2007**, *40* (12), 4093-4101.
 62. Elmalem, E.; Biedermann, F.; Johnson, K.; Friend, R. H.; Huck, W. T. S., Synthesis and Photophysics of Fully π -Conjugated Heterobis-Functionalized Polymeric Molecular Wires via Suzuki Chain-Growth Polymerization. *J. Am. Chem. Soc.* **2012**, *134* (42), 17769-17777.
 63. Kang, S.; Ono, R. J.; Bielawski, C. W., Controlled Catalyst Transfer Polycondensation and Surface-Initiated Polymerization of a p-Phenyleneethynylene-Based Monomer. *J. Am. Chem. Soc.* **2013**, *135* (13), 4984-4987.
 64. Lanni, E. L.; Locke, J. R.; Gleave, C. M.; McNeil, A. J., Ligand-Based Steric Effects in Ni-Catalyzed Chain-Growth Polymerizations Using Bis(dialkylphosphino)ethanes. *Macromolecules* **2011**, *44* (13), 5136-5145.
 65. Bryan, Z. J.; Smith, M. L.; McNeil, A. J., Chain-Growth Polymerization of Aryl Grignards Initiated by a Stabilized NHC-Pd Precatalyst. *Macromol. Rapid Commun.* **2012**, *33* (9), 842-847.
 66. Tamba, S.; Shono, K.; Sugie, A.; Mori, A., C-H Functionalization Polycondensation of Chlorothiophenes in the Presence of Nickel Catalyst with Stoichiometric or Catalytically Generated Magnesium Amide. *J. Am. Chem. Soc.* **2011**, *133* (25), 9700-9703.

67. Bridges, C. R.; McCormick, T. M.; Gibson, G. L.; Hollinger, J.; Seferos, D. S., Designing and Refining Ni(II)diimine Catalysts Toward the Controlled Synthesis of Electron-Deficient Conjugated Polymers. *J. Am. Chem. Soc.* **2013**, *135* (35), 13212-13219.
68. Senkovskyy, V.; Tkachov, R.; Komber, H.; Sommer, M.; Heuken, M.; Voit, B.; Huck, W. T. S.; Kataev, V.; Petr, A.; Kiriya, A., Chain-Growth Polymerization of Unusual Anion-Radical Monomers Based on Naphthalene Diimide: A New Route to Well-Defined n-Type Conjugated Copolymers. *J. Am. Chem. Soc.* **2011**, *133* (49), 19966-19970.
69. Senkovskyy, V.; Tkachov, R.; Komber, H.; John, A.; Sommer, J.-U.; Kiriya, A., Mechanistic Insight into Catalyst-Transfer Polymerization of Unusual Anion-Radical Naphthalene Diimide Monomers: An Observation of Ni(0) Intermediates. *Macromolecules* **2012**, *45* (19), 7770-7777.
70. Senkovskyy, V.; Khanduyeva, N.; Komber, H.; Oertel, U.; Stamm, M.; Kuckling, D.; Kiriya, A., Conductive Polymer Brushes of Regioregular Head-to-Tail Poly(3-alkylthiophenes) via Catalyst-Transfer Surface-Initiated Polycondensation. *J. Am. Chem. Soc.* **2007**, *129* (20), 6626-6632.
71. Khanduyeva, N.; Senkovskyy, V.; Beryozkina, T.; Bocharova, V.; Simon, F.; Nitschke, M.; Stamm, M.; Groetzschel, R.; Kiriya, A., Grafting of Poly(3-hexylthiophene) from Poly(4-bromostyrene) Films by Kumada Catalyst-Transfer Polycondensation: Revealing of the Composite Films Structure. *Macromolecules* **2008**, *41* (20), 7383-7389.
72. Khanduyeva, N.; Senkovskyy, V.; Beryozkina, T.; Horecha, M.; Stamm, M.; Uhrich, C.; Riede, M.; Leo, K.; Kiriya, A., Surface Engineering Using Kumada Catalyst-Transfer Polycondensation (KCTP): Preparation and Structuring of Poly(3-hexylthiophene)-Based Graft Copolymer Brushes. *J. Am. Chem. Soc.* **2009**, *131* (1), 153-161.
73. Senkovskyy, V.; Tkachov, R.; Beryozkina, T.; Komber, H.; Oertel, U.; Horecha, M.; Bocharova, V.; Stamm, M.; Gevorgyan, S. A.; Krebs, F. C.; Kiriya, A., "Hairy" poly(3-hexylthiophene) particles prepared via surface-initiated Kumada catalyst-transfer polycondensation. *J. Am. Chem. Soc.* **2009**, *131* (45), 16445-16453.
74. Sontag, S. K.; Sheppard, G. R.; Usselman, N. M.; Marshall, N.; Locklin, J., Surface-Confining Nickel Mediated Cross-Coupling Reactions: Characterization of Initiator Environment in Kumada Catalyst-Transfer Polycondensation. *Langmuir* **2011**, *27* (19), 12033-12041.
75. Tkachov, R.; Senkovskyy, V.; Horecha, M.; Oertel, U.; Stamm, M.; Kiriya, A., Surface-initiated Kumada catalyst-transfer polycondensation of poly(9,9-dioctylfluorene) from organosilica particles: chain-confinement promoted β -phase formation. *Chem. Commun.* **2010**, *46* (9), 1425-1427.

76. Tkachov, R.; Senkovskyy, V.; Oertel, U.; Synytska, A.; Horecha, M.; Kiriy, A., Microparticle-Supported Conjugated Polyelectrolyte Brushes Prepared by Surface-Initiated Kumada Catalyst Transfer Polycondensation for Sensor Applications. *Macromol. Rapid Commun.* **2010**, *31* (24), 2146-2150.
77. Senkovskyy, V.; Senkovska, I.; Kiriy, A., Surface-Initiated Synthesis of Conjugated Microporous Polymers: Chain-Growth Kumada Catalyst-Transfer Polycondensation at Work. *ACS Macro Lett.* **2012**, *1* (4), 494-498.
78. Sontag, S. K.; Marshall, N.; Locklin, J., Formation of conjugated polymer brushes by surface-initiated catalyst-transfer polycondensation. *Chem. Commun.* **2009**, (23), 3354-3356.
79. Marshall, N.; Sontag, S. K.; Locklin, J., Substituted Poly(p-phenylene) Thin Films via Surface-Initiated Kumada-Type Catalyst Transfer Polycondensation. *Macromolecules* **2010**, *43* (5), 2137-2144.
80. Doubina, N.; Jenkins, J. L.; Paniagua, S. A.; Mazzio, K. A.; MacDonald, G. A.; Jen, A. K. Y.; Armstrong, N. R.; Marder, S. R.; Luscombe, C. K., Surface-Initiated Synthesis of Poly(3-methylthiophene) from Indium Tin Oxide and its Electrochemical Properties. *Langmuir* **2012**, *28* (3), 1900-1908.
81. Ratcliff, E. L.; Zacher, B.; Armstrong, N. R., Selective Interlayers and Contacts in Organic Photovoltaic Cells. *J. Phys. Chem. Lett.* **2011**, *2* (11), 1337-1350.
82. Beryozkina, T.; Boyko, K.; Khanduyeva, N.; Senkovskyy, V.; Horecha, M.; Oertel, U.; Simon, F.; Stamm, M.; Kiriy, A., Grafting of polyfluorene by surface-initiated Suzuki polycondensation. *Angew. Chem., Int. Ed.* **2009**, *48* (15), 2695-2698.
83. Huddleston, N. E.; Sontag, S. K.; Bilbrey, J. A.; Sheppard, G. R.; Locklin, J., Palladium-Mediated Surface-Initiated Kumada Catalyst Polycondensation: A Facile Route Towards Oriented Conjugated Polymers. *Macromol. Rapid Commun.* **2012**, *33* (24), 2115-2120.
84. Huynh, W. U.; Dittmer, J. J.; Alivisatos, A. P., Hybrid nanorod-polymer solar cells. *Science* **2002**, *295* (5564), 2425-2427.
85. Lee, J.; Sundar, V. C.; Heine, J. R.; Bawendi, M. G.; Jensen, K. F., Full color emission from II-VI semiconductor quantum dot-polymer composites. *Adv. Mater.* **2000**, *12* (15), 1102-1105.
86. Pathak, S.; Choi, S.-K.; Arnheim, N.; Thompson, M. E., Hydroxylated Quantum Dots as Luminescent Probes for in Situ Hybridization. *J. Am. Chem. Soc.* **2001**, *123* (17), 4103-4104.
87. Helfferich, F., Ligand exchange: a novel separation technique. *Nature* **1961**, *189*, 1001-2.

88. Odoi, M. Y.; Hammer, N. I.; Sill, K.; Emrick, T.; Barnes, M. D., Observation of Enhanced Energy Transfer in Individual Quantum Dot-Oligophenylene Vinylene Nanostructures. *J. Am. Chem. Soc.* **2006**, *128* (11), 3506-3507.
89. Skaff, H.; Sill, K.; Emrick, T., Quantum Dots Tailored with Poly(para-phenylene vinylene). *J. Am. Chem. Soc.* **2004**, *126* (36), 11322-11325.
90. Ogawa, K.; Chemburu, S.; Lopez, G. P.; Whitten, D. G.; Schanze, K. S., Conjugated Polyelectrolyte-Grafted Silica Microspheres. *Langmuir* **2007**, *23* (8), 4541-4548.
91. Jhaveri, S. B.; Carter, K. R., Disubstituted polyacetylene brushes grown via surface-directed tungsten-catalyzed polymerization. *Langmuir* **2007**, *23* (16), 8288-8290.

CHAPTER 2. SYNTHESIS OF HYBRID CORE-SHELL PARTICLES CONSISTING OF SILICA CORE AND CONJUGATED BLOCK COPOLYMER SHELL PREPARED BY SURFACE-INITIATED POLYMERIZATION

2.1 Introduction

Recent advances in materials science have enabled the fabrication of various nanomaterials with attractive physico-chemical properties due to their enhanced surface to volume ratio compared to similar bulk materials. These nanomaterials with controlled sizes and structure found applications in the development of sensory materials,¹⁻⁸ photovoltaics,⁹ optoelectronics¹⁰ and biomedical applications such as drug delivery, bioimaging,¹¹ etc.

Organic/inorganic hybrid nanomaterials have attracted attention due to their fascinating optical, electronic, magnetic and catalytic properties. Hybrid materials consist of an inorganic core with a polymer shell. Organic polymer shells generally determine the chemical properties of nanoparticles and how they respond to external stimuli, whereas physical properties of nanoparticles are governed by size and shape of the inorganic core and the surrounding polymer shell layer. Chemical and physical properties of polymers are tuned according to the desired final properties and applications. Hybrid materials can provide extensive opportunities for the development of new materials with improved physical and chemical properties than their single-component counterpart. Hybrid nanoparticles are synthesized either by physical adsorption or using covalent grafting techniques such as *grafting to* or *grafting from* approach. Generally, homo- or copolymers can be grown from or attached to the surface of the substrate to get hybrid materials. These polymers form surface-tethered polymers which stretch out in good solvents to form brush-like polymer.¹² Polymer brushes have been widely explored due to their importance for fabrication of stimuli-responsive materials, sensors, and various biomedical applications.^{8, 11}

Conjugated polymers (CPs) are a class of polymers which possess delocalized π -electrons along the polymer backbone and they have been widely studied for application in optoelectronic devices and fluorescent probes due to their typically large absorption coefficient and excellent fluorescence properties. They are more flexible and exhibit complex self-assembly behavior which may lead to poorly defined meso- and microstructures in thin films which diminish their efficiency in photovoltaic and other optoelectronic applications.¹³ Controlled or directed self-assembly of these functional structures thus presents a challenge and requires higher degree of control to give an ordered 3-dimensional nanostructures.^{10, 14}

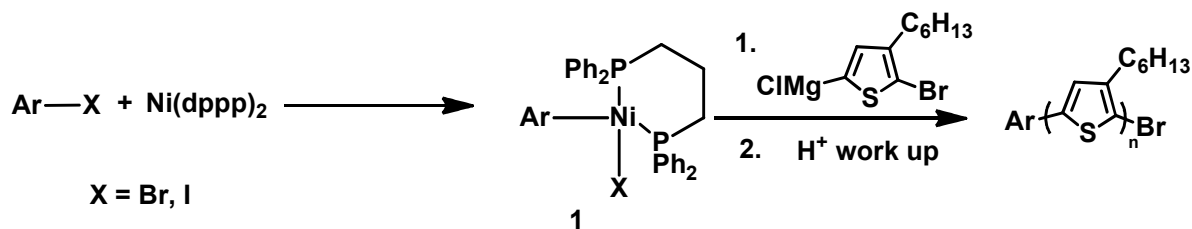
Thus, hybrid hairy nanoparticles can be an alternative approach in which CP brushes are attached to the central core and stretched out to solvent to form spherical shells. These complex multicomponent functional hybrid particles can self-assemble to give higher-complexity structures and can provide additional degree of control, form unconventional structures and act as covalently pre-organized building blocks and therefore would be an interesting alternative to linear conventional CPs. The “grafting-to” approach is one of the methods to attach end-functionalized polymer to a complementary functionalized inorganic surfaces; the examples include attachment of thiol end-functionalized polythiophenes to gold nanoparticles or amino-functionalized P3HT to quantum dots.¹⁵ The *grafting to* approaches, however, usually result in low grafting density. Schanze’s group performed grafting of polyacetylene that resulted in polymer brushes that were limited to just 12 nm thickness.¹⁶

Surface-initiated (also called surface-confined) polymerization or the ‘*grafting from*’ approach is one of the powerful techniques to prepare hairy particles with variable compositions and polymer grafting densities.¹⁷ Surface-initiated polymerization is initiated from the surface directly rather than having a pre-synthesized polymer attached to the functional group immobilized

on the particle surface (as in *grafting to* approach). This gives more control over brush thickness and thus the higher grafting density can be achieved. Polythiophenes (PT) can be prepared via step-growth polymerization methods as well as oxidative chemical polymerization which results in higher polydispersities. An important discovery by Yokozawa¹⁸⁻¹⁹ and McCullough²⁰⁻²¹ that regioregular poly(3-hexylthiophene) (P3HT) can be prepared by controlled chain-growth Kumada catalyst-transfer polycondensation (KCTP) has opened a possibility for surface-confined chemical polymerization. Mechanistic studies showed that the polymerization process occurs in a quasi-“living” chain-growth fashion and involves typical transition metal catalyzed series of consecutive transmetallation, oxidative addition and reductive elimination steps. Due to lower reactivity of traditionally used Ni(II) catalysts, the polymerization gives lower molecular weight polymers. In addition, there is a possibility of the occurrence of transfer of the Ni(II) reactive center to another chain of polymerization or chain termination via disproportionation. Recently, Kiriya,²²⁻²⁵ Locklin,²⁶⁻²⁷ and others carried out surface-confined *in situ* preparation of regioregular poly(3-alkylthiophene) brushes through Kumada polymerization using surface-immobilized Ni(II) catalytic initiators. This resulted in mechanically stable surface-grafted CP thin films; however with seemingly low surface density, and limited degree of polymerization, possibly due to instability and lower activity of the metal catalytic site and dominance of side reactions. Kiriya carried out surface-confined *in situ* preparation of P3HT on silica particles surface.²⁵ Using Kiriya’s methodology and a modified Ni catalyst to improve “living” nature of the polymerization process, Locklin has demonstrated preparation of relatively thick (up to 42 nm) surface-attached poly(3-methylthiophene) films.²⁸ Nevertheless, all the reported systems suffer either from the low activity of the surface-immobilized Ni(II) catalyst, or its instability, as well as from the complexity of the catalyst preparation; therefore, practical implementation of the surface-initiated polymerization

still remains a challenge. In addition, very little is known about molecular organization and morphology of surface-confined CP thin films and methods which can be used to control it.

Recently, Nesterov's group found that the reaction of aryl bromides or aryl iodides with Ni(0) complex Ni(dppp)₂ (where dppp is 1,3-bis(diphenylphosphino)propane) at moderate temperatures produces a stable Ni(II) complex 1 that can be used as a highly efficient catalytic initiator of Kumada catalyst-transfer polymerization (KCTP) of 5-bromo-2-thienylmagnesium monomers (Scheme 2.1).²⁹ The polymerization efficiently produces highly regioregular (regioregularity, as a fraction of head-to-tail (HT) coupled 3-alkylthienyl units, close to 100%) P3HT with the number average molecular weight (*M_n*) being linearly dependent on the monomer/catalyst 1 ratio. These and other experimental findings pointed out on the controlled chain-growth mechanism of the polymerization initiated/catalyzed by 1. In good agreement with this mechanism, each polymer chain was found to be terminated with the aryl group from catalyst 1 at one end, and (somewhat unexpectedly) predominantly with Br at the other end (Scheme 2.1).



Scheme 2.1 Synthesis of regioregular poly(3-hexyl thiophene) using external catalytic initiator 1.

The experimental simplicity of preparation of the catalytic initiator 1 and the efficiency of the 1-catalyzed KCTP prompted us to systematically investigate preparation of surface-attached polythiophenes (PT) and poly(*p*-phenylenes) (PPP) shells on silica nanoparticles via surface-confined *in situ* polymerization. Colloidal silica nanoparticles were chosen due to their well-studied preparation chemistry and processability. They have many desirable characteristics such

as low cytotoxicity, facile and convenient preparation, ability to control over interparticle interactions, and high stability.

Conjugated polymers (CPs) are well-suited for applications in chemo- and biosensors and optoelectronic devices due to efficient transport of excitons along and between the conjugated polymer chains. The intramolecular energy migration strongly depends on the extent of π -electron conjugation within the CP chain, which is determined by how polymers self-organize to form highly planar conjugated backbone conformations. Dilute solutions of conjugated polymers are a good model where energy transfer processes can take place via combination of intramolecular through-space dipole-induced dipole (Förster) and through-bond (Dexter-type) exchange mechanisms. More planarized conformations of CPs tend to form intermolecular aggregates whereas more twisted conformations lead to lower conjugation length and less aggregation. These conformational changes can deplanarize and affect the energy transfer process in donor-acceptor conjugated polymer systems.

The novel class of hybrid materials, silica nanoparticles grafted with conjugated polymer (including diblock copolymers), was synthesized via surface-confined polymerization. In addition to preparation, we studied energy transfer processes between the subshell in the case of diblock copolymer polymer shells and showed that irrespective of the order of the subshells, energy transfer always takes place as a unidirectional process from the higher energy poly(*p*-phenylene) (PPP) chromophore to the lower energy polythiophene (PT) chromophore.

2.2 Results and Discussion

2.2.1 Synthesis of conjugated polymer grafted silica particles

Monodisperse silica particles were prepared by the well-known Stöber process. They were prepared by polycondensation of tetraorthosilicates and ammonium hydroxide to give a porous

network of polysilicates. However, Stöber process leads to more polydisperse particles.³⁰ To obtain silica particles with more uniform size, Bogush's group has used reverse microemulsion method to get uniform silica particles.³¹ pH was maintained around 9 to control the unwanted silica particles formation and give narrow size distribution. FT-IR spectroscopy confirmed the formation of silica particles by showing peaks at 1100 cm^{-1} (Si–O stretching), 465 cm^{-1} (Si–O bending), 945 cm^{-1} (Si–OH bending), and 800 cm^{-1} (Si–O–Si bending) characteristic of silica formation. TEM image (Figure 2.1) showed that the prepared particles were monodisperse with an average size of 58 nm with standard deviation of 4.3 nm. Growth of the nanoparticles followed lognormal distribution and particles formed were highly monodisperse (1019 particles were measured to get average size).

The TEM results were also comparable with the results of the SANS experiments (figure 2.1). The size obtained by fitting the SANS data for colloidal solution of nanoparticles in D₂O solution was 60.2 nm which was close to the TEM results. The data were fitted by log normal sphere model which corresponds to the local density fluctuation of the silica particles in suspensions. The monodisperse core-shell model worked and directly caught all the oscillations in the scattering profile. The slightly higher diameter by SANS can be explained by solvation of the nanoparticles in the solvent, which effectively increases their measured size.

The preparation of conjugated polymer coated silica nanoparticles was based upon the surface-initiated polymerization strategy developed in the Nesterov's group (Scheme 2.2).¹⁵ It is based on covalent immobilization of 5-(triethoxysilyl)-2-iodothiophene precursor on silica nanoparticle surface followed by the reaction of the surface-immobilized iodothiophene monolayer with Ni(0) complex Ni(dppp)₂ to yield the surface-immobilized Ni(II) initiator.

$\text{Ni}(\text{dppp})_2$ can be easily prepared in large scale and is stable for a few months. The heterogeneous reaction occurs through oxidative addition of $\text{Ni}(\text{dppp})_2$ complex to iodothiophene.

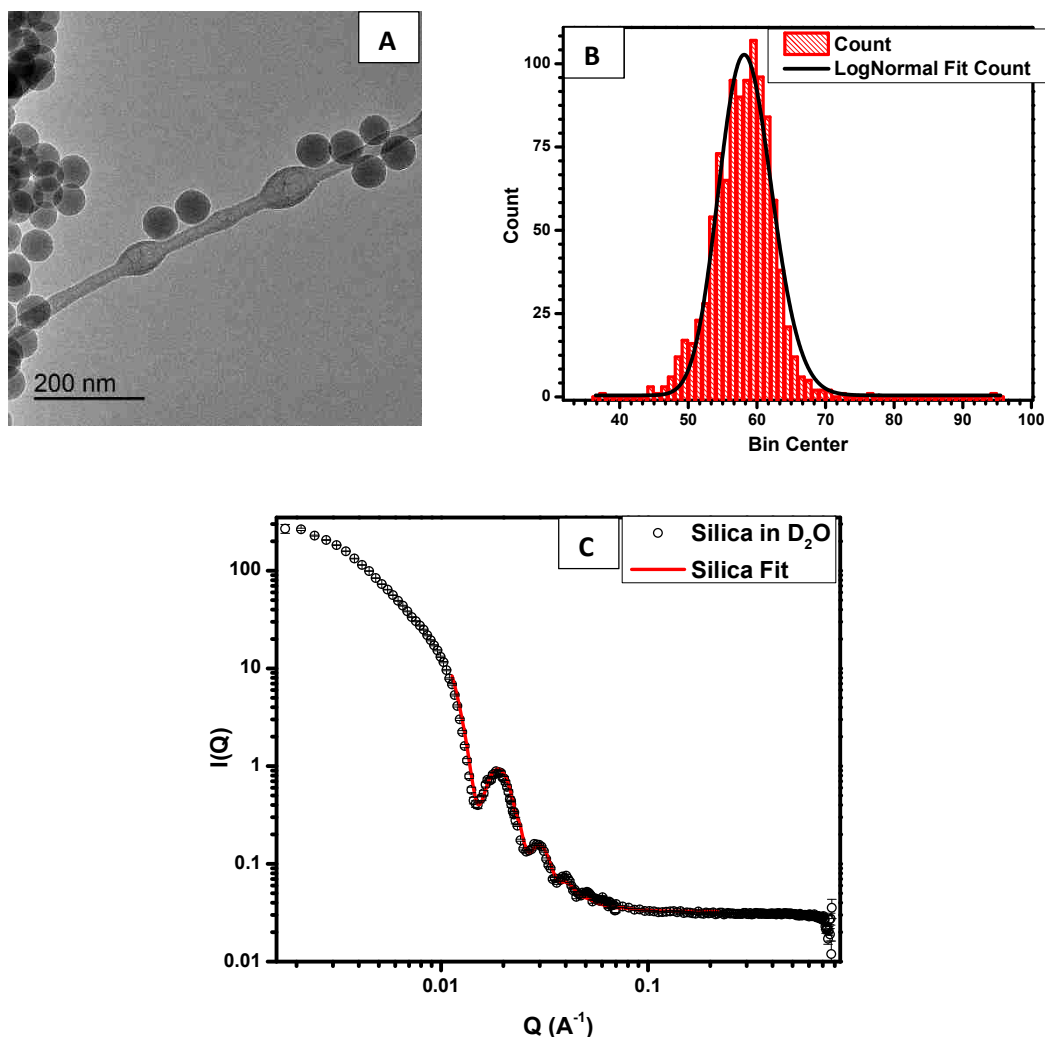
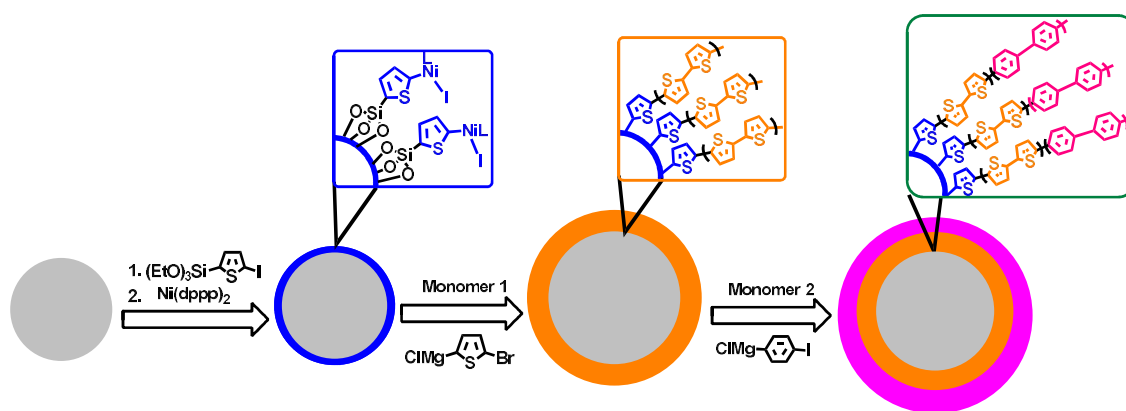


Figure 2.1 (A) TEM image of as synthesized silica nanoparticles; (B) Size distribution histogram of the nanoparticles; (C) SANS analysis of silica nanoparticles in D_2O solution (10 mg/mL).

This method allowed us to obtain an efficient catalytic system for surface-initiated Kumada catalyst transfer polymerization yielding surface-immobilized brushes of defect-free polymers, e.g. polythiophene, poly-*p*-phenylene, and block copolymers. Upon completion of the formation of surface-immobilized Ni(II) catalyst, the resulting nanoparticles were thoroughly washed with toluene to get rid of excess of reagents.

Surface-confined initiator upon exposure to a solution of suitable monomer initiates controlled quasi-“living” polymerization to form a conjugated polymer shell. For preparing a block copolymer shell, after 1 day of polymerization, initiating sites were regenerated with Ni(dppp)₂ followed by addition of a 2nd Grignard monomer. It was shown previously, that regeneration of active catalytic sites at the end of surface-confined polymer with Ni(dppp)₂ gives a higher catalytic initiator density. For the case of homopolymers, such a regeneration helped to reinstate an incomplete terminated polymerization.¹⁶ As a proof-of concept, we chose Ni-initiated Kumada polycondensation of (5-bromothiophen-2-yl)magnesium chloride, or (4-iodophenyl)magnesium chloride to form polythiophene (PT), or poly-*p*-phenylene (PPP) shells, respectively.



Scheme 2.2 Preparation of silica nanoparticles grafted with shell composed of conjugated polymer or block copolymer.

PT and PPP are among the most convenient conjugated polymers for various electronic and optoelectronic applications, and their photophysical properties are well-studied and characterized in detail. Therefore, both polymers were a convenient model for our proof-of-concept study. Final polymer-functionalized silica nanoparticles were successively washed upon ultrasonication in a series of organic solvents to get rid of unbound oligomers, metal impurities and other unwanted by-products. In particular, particles were washed sequentially with methanol, THF, hexane, chloroform, and finally redispersed in 1,2-dichlorobenzene.

The amount of surface-confined polymer was determined using TGA in air. Heating the hybrid particles in air to high temperature (1000 °C) was anticipated to result in complete loss of the organic polymer shell, but should not affect silica core. TGA in figure 2.2 shows the expected trend. Although the hybrid particles were previously dried *in vacuo*, the bare SiO₂ nanoparticles showed approximately 10% loss of weight at the temperature up to 100 °C due to adsorbed water. Loss due to precursor was 17%. This allowed to calculate a grafting density of 1.03 molecules/nm².

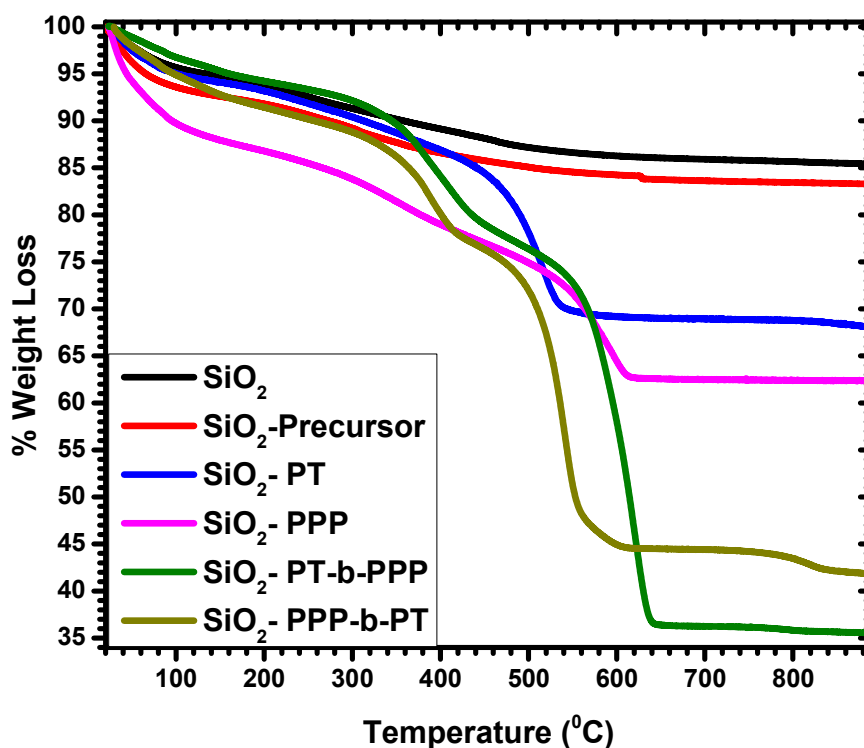


Figure 2.2 TGA of %weight loss with temperature change of hybrid particles.

Assuming that living chain growth polymerization started from each molecule of precursor, we calculated the surface-immobilized molecular weight of polymer along with degree of polymerization based on amount of loss of weight corresponding to each subshell. Thus, there was loss of 15% and 35% in total weight for PT and PT-b-PPP hybrid nanoparticles, respectively. Similarly, 20% and 41% weight loss was found for PPP and PPP-b-PT nanoparticles. The results

showed an expected trend thus confirming successful formation of each subshell. Table 2.1 shows molecular weight and corresponding degree of polymerization obtained from TGA data.

Table 2.1: Molecular weight and DP of conjugated polymer shell hybrid particles from TGA

Type of Polymer shell	PT	PPP	PT-b-PPP	PPP-b-PT
Molecular Weight	2627	3931	10752	5785
Degree of Polymerization	32	51	141	71

Small-angle neutron scattering (SANS) is a noninvasive technique which not only gives useful information about the shape and morphology of colloidal particles but also how the particles interact with each other. Size of bare silica core particles, along with hybrid particles with homopolymer and diblock copolymer grafted subshells were studied by SANS (Figure 2.4). Conjugated polymers, especially those without long-chain alkyl solubilizing groups, are prone to aggregate in solution. Indeed, from SANS data we did observe inter-particle aggregation in the case of both homopolymer and diblock copolymer functionalized nanoparticles.

The experimental SANS datasets were fitted using core-shell model (figure 2.3) plus a structural fractal dimension to take into account the effect from inter-particle aggregation. In this data fitting, there were four free parameters to vary: pre-factors, polymer shell thickness, neutron scattering length density (SLD) of the shell, and the fractal dimension. The scattering intensity of a polymer can be fit using the following equation:

$$I(q) = KP(q) S(q) + I_{inc} \quad (1)$$

where K is a scaling factor, P(q) is the form factor of a single chain, and I_{inc} is the incoherent scattering intensity which is assumed independent of q.

$$P(q) = \frac{1}{V_s} \left[\frac{(3V_c(\rho_c - \rho_s)j_1(qr_c))}{qr_c} + \frac{(3V_s(\rho_s - \rho_{solv})j_1(qr_s))}{qr_s} \right]^2 + bkg \quad (2)$$

Where $j_1(x) = (\sin x - x \cos x) / x^2$; $r_s = r_c + t$; $V_i = (4\pi/3)$; bkg is incoherent background, solv is solvent, s is shell, c is core

$$S(q) = 1 + \frac{\sin[(D_f - 1)\tan^{-1}(q\xi)]}{(qR_0)^{D_f}} \frac{D_f \Gamma(D_f - 1)}{[1 + 1/(q^2 \xi^2)]^{(D_f - 1)/2}} \quad (3)$$

Where ξ is correlation length, D_f is fractal dimension

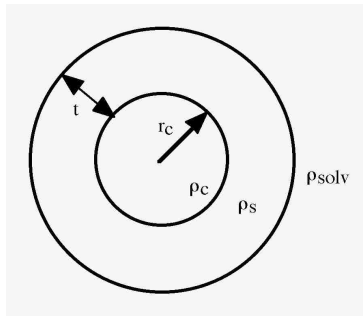


Figure 2.3 Core-Shell Model

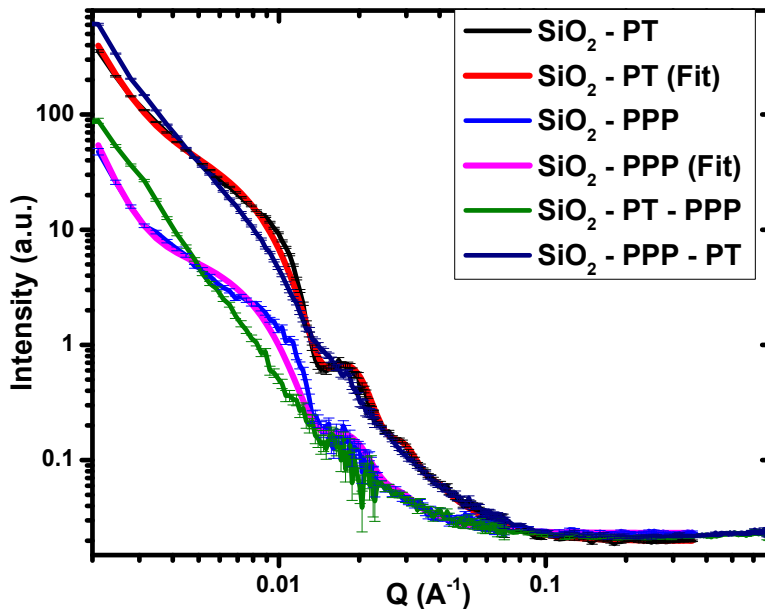


Figure 2.4 SANS analysis of grafted conjugated homopolymer and diblock copolymers on SiO_2 hybrid nanoparticles in DCB (10 mg/ml). Fitting curves were obtained using models described in the text.

In case of homopolymer-functionalized nanoparticles, aggregation features were not dominant and we did observe characteristic oscillations in the data indicating relatively low polydispersity of the hybrid particles. The polymer shell thickness obtained from data fitting for the case of homopolymers were 2 nm for PT nanoparticles and 2.5 nm for PPP nanoparticles.

The relatively low values for the shell thickness indicated significantly tilted polymer chains. Indeed, based on our previous studies on thin films, the surface-confined polymer chains likely were oriented near-parallel to the nanoparticle surface, forming in-plane aligned layers of twisted and folded chains. SANS data for nanoparticles with grafted diblock copolymers shells, PPP-b-PT and PT-b-PPP, were found featureless, which might be due to strong interparticle aggregation in the system, which could bring the observed feature to too low Q value, out of SANS region, and we were not able to fit the data. That the diblock copolymers did form, was confirmed by TGA which showed a significantly higher amount of weight loss for the case of diblock copolymer shells relative to homopolymer shells.

2.2.2 Photophysical properties of hybrid nanoparticles

Steady state absorption, excitation and fluorescence spectra of hybrid particles in DCB were taken. Figure 2.5 shows absorption, excitation and emission spectra of conjugated polymers grown on silica particles dispersed in DCB. Absorption spectra (figure 2.5) display max of 420 nm for SiO₂-PT-b-PPP and 620 nm for SiO₂-PPP-b-PT.

Absorption and emission spectra of diblock copolymers showed no appreciable variations in the poly(*p*-phenylene) spectra region. On the other hand, any changes that occur due to energy transfer between the subshells were to be seen in the polythiophene spectral region. To understand the effect of energy transfer, we closely looked at the emission spectrum of block copolymer

grafted nanoparticles in solution and in thin films separately. The following two different cases of conjugated polymers grafted on silica cores were studied:

- (a) PT-b-PPP; (b) PPP-b-PT;

Absorption of light by diblock copolymer leads to delocalized primary photoexcitation which then relaxes to a more localized exciton state. Several processes contribute to the relaxation of the primary photoexcitation of polymer to the relaxed singlet exciton: (1) self-localization; (2) exciton formation; (3) exciton hopping, and (4) slow torsional rearrangements.

Upon photoexcitation, fast decay was observed which resulted from intrachain excitation energy transfer along the π -conjugated system by a torsional relaxation process which leads to an emission from lower energy conformer or structure. In this case, visible absorption spectrum showed allowed π - π^* vertical transition. Emission, on the other hand, always occurs from the relaxed singlet excited state.³²

The difference between the absorption spectrum and the fluorescence excitation spectrum indicated that the fluorescence quantum yield varied within the distribution of absorbing conformations. The shape of the emission spectrum in solution was independent of excitation wavelength. Even if a large distribution of conformations was created upon initial excitation, relaxation eventually should occur to a common emitting intrachain exciton state with less torsional disorder.

Absorption profiles were found to be broad with some vibronic features. Silica is transparent to light and therefore any features seen in the spectra were solely due to CPs. This is due to the ordering and possible chain rigidity increase of surface-confined polythiophene and poly(*p*-phenylene) via π - π stacking, possibly due to the folding of the elongated surface-confined polymer chain to form alignment parallel to the silica core surface. In case of all surface-confined

diblock copolymer series, there was no change in absorption or emission features of poly(*p*-phenylene), i.e. the absorption band stayed within 300 – 500 nm, and emission band remained at 400 – 550 nm. The only change that has been observed was due to emission band at 500 – 850 nm, i.e. the polythiophene emission band.

Absorption profile of diblock polymers showed pronounced dependence on the ordering of block copolymer subshells. When polythiophene subshell was introduced as the first (inner) subshell on silica core, intensity of absorption for polythiophene was substantially lower as compared when it was placed as a second (outer) subshell. For polythiophene band, vibronic peaks at 510, 550 and 610 nm were observed. The peak at 510 nm had been assigned to intrachain π - π transition of polythiophene block whereas the peak at 550 nm was attributed to 0-0 vibrational peak which can be associated with the increased conjugation length due to ordered (even crystalline) stacking of polythiophene chains that restricted the rotational motion of the conjugated backbones. The peak at 610 nm was assigned to 0-1 vibrational peak resulting from the interchain π - π interaction via electron hopping and its intensity correlated with the degree of interchain order.

Polythiophene without side solubilizing groups is generally insoluble in common organic solvents. But it has been observed that chlorinated solvents are better in dispersing these diblock copolymer functionalized nanoparticles. In chlorinated solvents, the grafted polymer chains likely are better dispersed and even stretched into solvent environment, as compared to other solvents. However, due to generally low solubility, the polythiophene chains form tightly packed and uniformly oriented layer of stretched polymer backbones. Such a packing should result in planarization of the polythiophene chains with delocalization of π -conjugated electrons, and efficient energy migration within the subshell – both by intra- and intermolecular pathways. In the case of PT-b-PPP, absorption peaks are a combination of poly(*p*-phenylene) and polythiophene in

which poly(*p*-phenylene) peak dominate. This can be related to the higher extinction coefficient of PPP. Poly(*p*-phenylene) is a polymer with higher rigidity of the conjugated backbone, which forms a rigid outer subshell over polythiophene inner subshell.

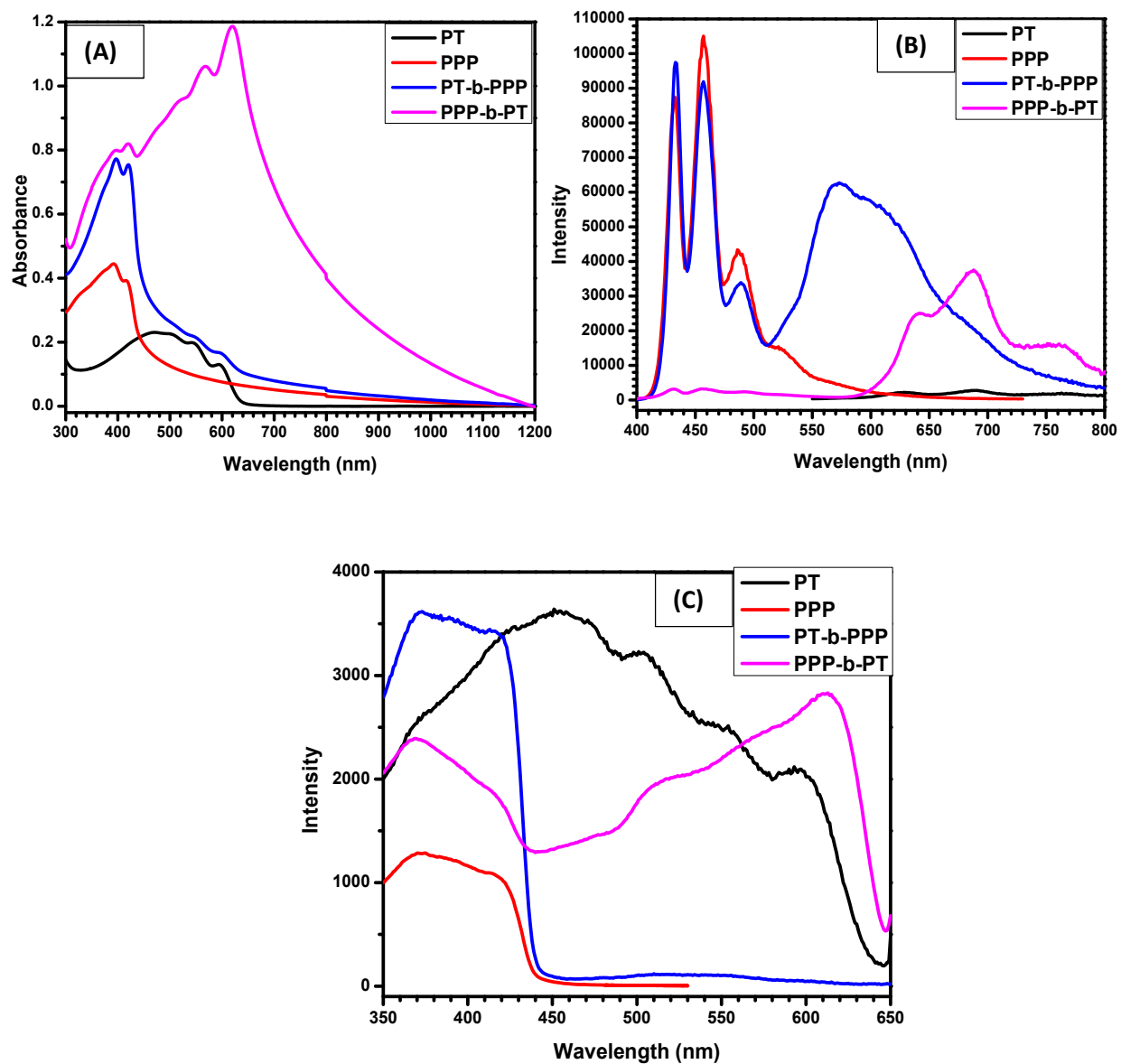


Figure 2.5 Absorption (A), excitation (B), emission (C) spectra of SiO₂@PT-b-PPP and SiO₂@PPP-b-PT in 1,2-dichlorobenzene (DCB). Fluorescence quantum yield (%) SiO₂@PT (0.1); SiO₂@PPP (26.32); SiO₂@PT-b-PPP (1.55); SiO₂@PPP-b-PT (0.13)

Fluorescence excitation spectra (figure 2.5) were found to be substantially different from absorption spectra. This indicated there were different intermediate processes taking place during excitation other than just a vertical Frank-Condon transition. This indicates that fluorescence quantum yield differs within the distribution of absorbing conformations. λ_{max} at 380 nm and 460 nm were due to contribution from poly(*p*-phenylene) and polythiophene respectively. Diblock copolymers were also excited around 500 nm (PT excitation) which produced weak PT emission. Thus, this proves that emission spectra do show significant energy transfer from poly(*p*-phenylene) to polythiophene. Poly(*p*-phenylene) absorbs more than polythiophene and transfer energy to polythiophene as seen by its emission spectra.

Emission spectra of the block copolymer – silica hybrid nanoparticles showed two distinct bands, one band from poly(*p*-phenylene) subshell (400 – 550 nm) and the other band from polythiophene subshell (550 – 850 nm). It can be seen that when poly(*p*-phenylene) subshell was inside (PT-b-PPP), there was more energy transfer occurring towards polythiophene subshell. Energy transfer in emissive conjugated polymers can occur at distances ranging from 0.1 nm to more than 5 nm, and it can take place via both intermolecular and intramolecular energy transfer processes, directing from an excited donor chromophore to an acceptor chromophore. Conjugated polymer chains have several hundred repeating units but their effective conjugation length may be decreased due to structural, topological and chemical defects. Thus, the excitation energy transfer can be described as a combination of intrachain and interchain processes occurring by Förster and Dexter mechanisms. Emission spectra show energy transfer from poly(*p*-phenylene) to polythiophene. Energy transfer processes can be either by “through space” (Förster) or “through bond” (Dexter) type. The former takes place with effective spectral overlap of donor absorption with acceptor emission.³³

That the sequence of diblock copolymer subshells can significantly affect the energy transfer processes was observed in emission spectra. In the case of PT-b-PPP shell, energy transfer from the PPP subshell chromophore was not prominent as could be seen from excitation spectra in figure 2.5. We can explain this by considering higher chain rigidity of PPP molecules, which likely prevents close packing of the surface-confined PPP chains. This should effectively place PPP chromophore further away from the inner PT subshell, and therefore diminish the efficiency of energy transfer through Förster (i.e. through space) pathway. In the case of PPP-b-PT grafted silica nanoparticles, less rigid PT chains in the outer subshell could effectively pack in a compact shell, which would place it closer to the PPP donor chromophore thus allowing effective funneling energy via through-space (Förster) as well as via through-bond (Dexter) pathways.³⁴

Absorption profiles of PPP-b-PT grafted silica nanoparticles showed increase in absorption intensity for the polythiophene chromophore, as compared for PT-b-PPP grafted nanoparticles. This observation may be related to the reactivity of 5-bromothiophen-2-yl over 4-iodophenyl Grignard monomers in the Kumada catalyst-transfer polymerization reaction. Yokozawa demonstrated that sequence of carrying polymerization of these two monomers was important in getting well-ordered and well-defined block copolymers. Thus, when polythiophene subshell was grown as the inner layer followed by poly(*p*-phenylene) as the outer subshell, low molecular weight polymers were formed, whereas the reverse sequence of polymerization resulted in well-defined block copolymers of poly(*p*-phenylene) (inner subshell) and polythiophene (outer subshell). The markedly different reactivity was probably due to the relative π - donor abilities of polythiophene and poly(*p*-phenylene). When 4-iodophenylmagnesium chloride monomer was added to the reaction mixture where Ni(II)-functionalized polythiophene shell on silica nanoparticles was formed first, Ni(II) reactive center on the termini of surface-confined

polythiophene chains would be difficult to migrate to the terminal C-Br bond of a *p*-phenylene ring because the thiophene ring has stronger π -donor ability than the *p*-phenylene ring. On the other hand, when 5-bromothiophene-2-ylmagnesium chloride monomer was added to the solution of the nanoparticles initially modified with poly(*p*-phenylene) shell, Ni catalyst would be able to migrate more effectively to the C-Br end of the thiophene ring possessing stronger π -donor ability.

2.2.3 Photophysical properties of thin films prepared from hybrid nanoparticles

Figure 2.6 shows normalized excitation and emission spectra of diblock copolymer functionalized silica nanoparticles in drop-casted film. They demonstrate that energy transfer occurs from higher energy to lower energy subshell chromophores irrespective of the order of subshells. The process of photoexcitation energy migration takes place via intermolecular or intramolecular pathways with the former being more prominent in the case of an aggregated state such as in thin films of conjugated polymers. Intermolecular exciton migration takes place via Förster dipole – induced dipole mechanism which depends upon intermolecular excitation migration distance as $1/R^6$ where R is the distance between delocalized chromophores segments of the polymer chains. The efficiency of energy transfer in conjugated polymers also depends upon how these polymer chains are aligned which means how transition dipole moments of these chains are mutually oriented. In the case of thin films, polymer chains are aggregated and chains are in close proximity to each other, and hence three-dimensional interchain exciton migration via exciton random walk takes place.¹⁸ Conjugated polymers are very efficient in funneling these excitons from higher energy sites to lower energy sites, so only a small concentration of defect sites is required to alter the polymer film emission. Thus if the low-energy exciton trap sites are emissive such as thiophene defect sites, then it can change its emission spectra.^{32-33, 35}

Emission spectra of thin films of hybrid nanoparticles showed again two distinct bands, one coming from the poly(*p*-phenylene) subshell (400 – 550 nm), and the other band characteristic of polythiophene subshell (550 – 850 nm). Both emission bands were vibronically structured indicating rigid and relatively well-ordered structure of the conjugated polymer shells. It can be seen that with poly(*p*-phenylene) being an inner subshell, there was more efficient energy transfer to polythiophene subshell. In contrast, when polythiophene was an outer subshell, a very intense band at around 700 nm could be observed, possibly resulted from an excimer or aggregated state formation, stemming from more ordering and rigidification of PT subshell polymer chains. In case when PT was inside, a broad featureless emission band was observed, which could indicate less ordering and more twisted structure accompanying with loss of conjugated backbone planarity and more blue shifted emission band than PT alone.

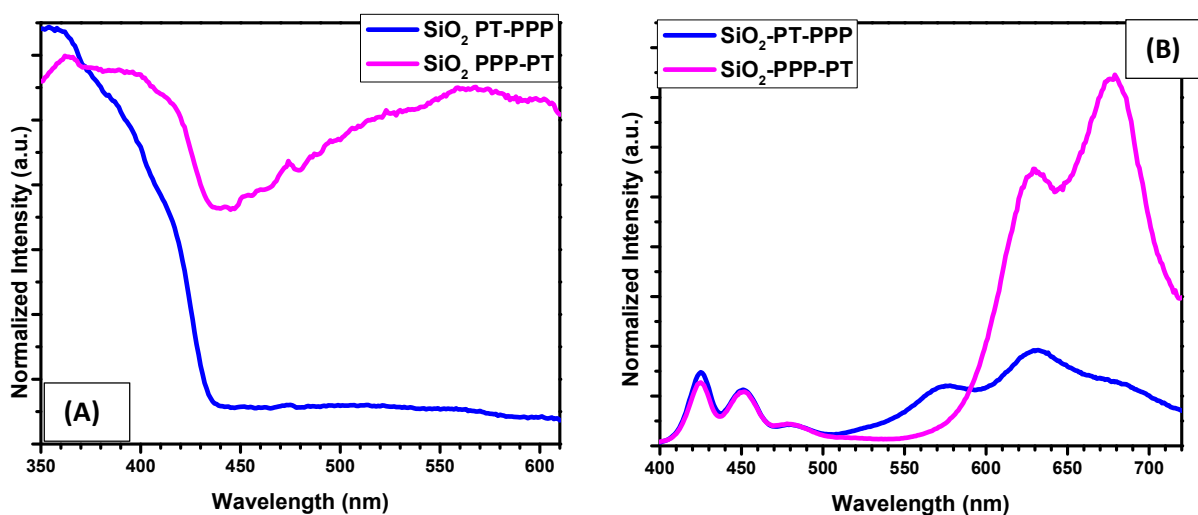


Figure 2.6 Excitation (A), emission (B) spectra of SiO₂@PT-b-PPP and SiO₂@PPP-b-PT drop-casted on glass slide.

2.2.4 Transient absorption studies of hybrid materials

Transient absorption spectra of hybrid conjugated polymer nanoparticles can provide information about the dynamics of photophysical processes occurring in the polymer shell. Conjugated

polymers such as polythiophene were well studied due to their importance in optoelectronics, solar cells, etc. Time-resolved optical spectroscopy studies can provide important information about the dynamic mechanisms such as exciton and free-charge carrier formation and migration in conjugated polymers.³⁷ Similar types of studies was also previously done on P3HT films and aggregated solutions.³⁸ Recently, Larsen studied ground state relaxation dynamics of P3HT by pump-dump-pump spectroscopy.³⁶ It was observed from the studies that primary photodynamics of P3HT films and aggregated solutions with comparable morphologies goes through following steps: (1) primary photoexcitation of conjugated polymer generates a single exciton which is delocalized over approximately 15 repeating units; (2) this exciton self-localizes to less than 10 repeating units via structural distortion processes; (3) exciton further relaxes through C=C vibrational relaxation, larger torsional relaxation and excitonic energy transfer. Transient absorption and emission studies of amorphous and solution-phase polythiophene systems showed that exciton localization can occur via conformational disorder. In this project, we studied four hybrid nanoparticles: Silica@PT, Silica@PPP; Silica@PT-PPP and Silica@PPP-PT.

The transient absorption spectroscopy of hybrid nanoparticles consisting of a homopolymer shell attached to the surface of SiO₂ in colloidal suspension in 1,2-dichlorobenzene (DCB) was investigated using 380 nm excitation in order to understand the ultrafast excited-state dynamics. Figure 2.7 (a) shows representative transient absorption spectra of colloidal SiO₂-poly(*p*-phenylene) nanoparticles. A negative band centered at 470 nm was attributed to ground state depletion. Two positive bands near 400 nm and 600 nm were due to excited-state absorption. The transient absorption time profile of the SiO₂-poly(*p*-phenylene) nanoparticles measured at 470 nm is shown in Figure 2.7 (b). The wavelength-dependent decay spectra obtained from the global analysis of the transient absorption time-profiles,³⁹⁻⁴⁰ described by a sum of exponentials to recover

the lifetimes and corresponding spectra of the relaxation dynamics, are shown in Figure 2.7 (c). Two lifetimes of $\tau_1 = 8 \pm 3$ ps and $\tau_2 = 20 \pm 4$ ps were needed to accurately describe the ultrafast excited-state relaxation dynamics of poly(*p*-phenylene) on the surface of SiO₂ nanoparticles, and the corresponding decay spectra were both convolutions of ground-state depletion and excited-state absorption.

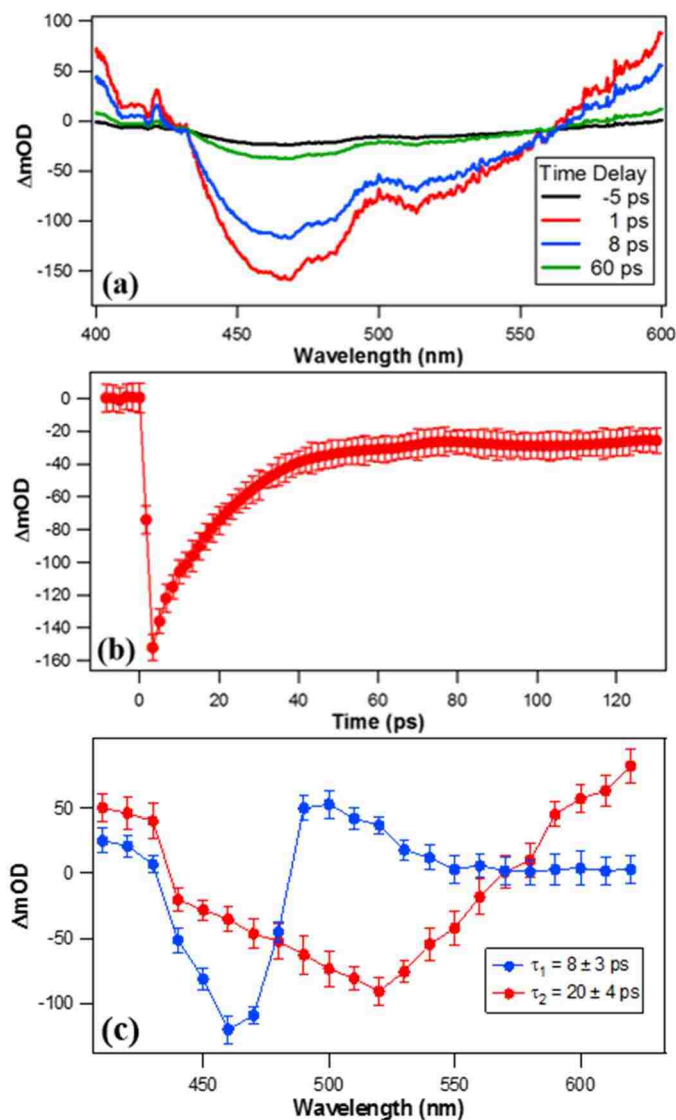


Figure 2.7 (a) Representative transient absorption spectra of colloidal SiO₂-poly(*p*-phenylene) nanoparticles in 1,2-dichlorobenzene using 380 nm pump pulses (conc. 0.5 mg/ml). (b) Transient absorption time-profiles of the SiO₂-poly(*p*-phenylene) nanoparticles measured at 470 nm. (c) Decay spectra obtained using global analysis of the time-dependent transient absorption spectra.

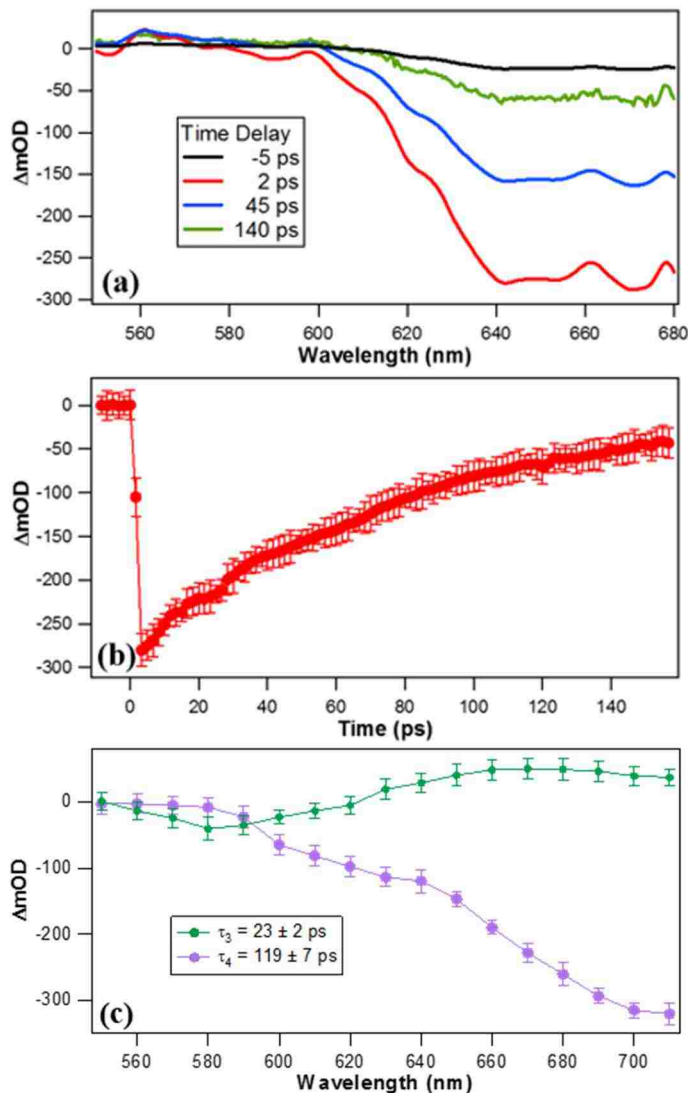


Figure 2.8 (a) Representative transient absorption spectra of colloidal SiO_2 -polythiophene nanoparticles in 1,2-dichlorobenzene using 380 nm pump pulses (conc. 0.5 mg/ml). (b) Transient absorption time profiles of the SiO_2 -polythiophene nanoparticles measured at 700 nm. (c) Decay spectra obtained using global analysis of the time-dependent transient absorption spectra.

Figure 2.8 (a) shows representative transient absorption spectra of hybrid nanoparticles consisting of polythiophene shell attached to the surface of SiO_2 core in colloidal solution in 1,2-dichlorobenzene using 380 nm excitation pulses. A broad depletion band was observed at wavelengths range from 580 nm and above. The corresponding transient absorption time profile measured at 700 nm is shown in Figure 2.8 (b). Two lifetimes were needed to accurately describe

the excited-state relaxation dynamics of the colloidal SiO₂-polythiophene nanoparticles. A positive band characterized mainly by excited-state absorption and a negative band characterized mainly by ground-state depletion were measured with lifetimes of $\tau_3 = 23 \pm 2$ ps and $\tau_4 = 119 \pm 7$ ps, respectively. Additional relaxation pathways with lifetimes that are longer than our experimental pump-probe temporal range were observed as an offset to the wavelength-dependent time profiles, as discussed in more detail later.

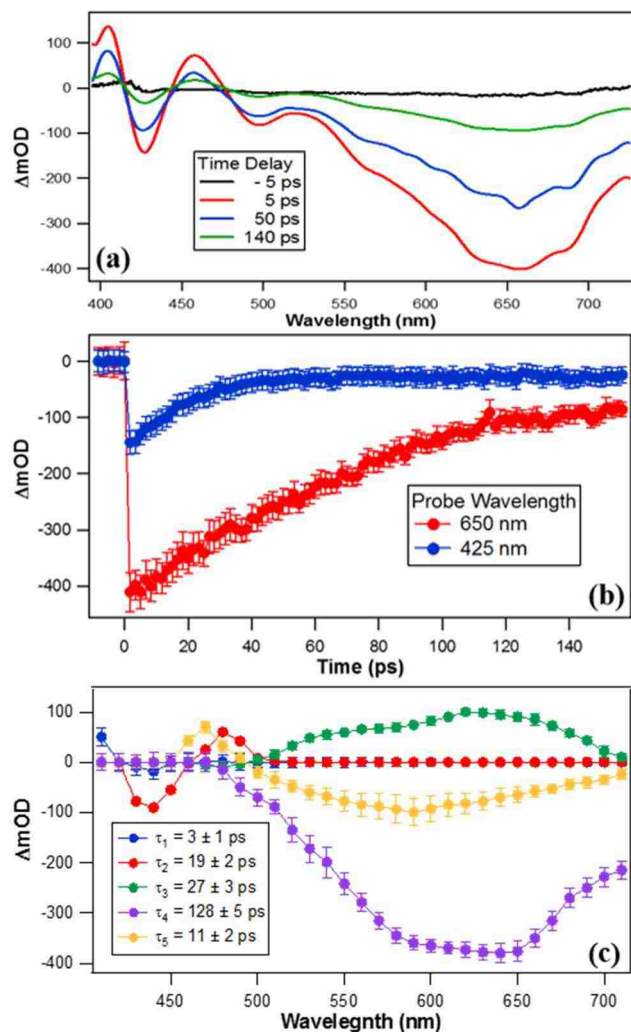


Figure 2.9 (a) Representative transient absorption spectra of colloidal SiO₂-poly(*p*-phenylene)-*b*-polythiophene hybrid nanoparticles in 1,2-dichlorobenzene (conc. 0.5 mg/ml) using 380 nm excitation pulses. (b) Transient absorption time-profiles of the SiO₂-poly(*p*-phenylene)-*b*-polythiophene nanoparticles measured at 425 nm and 650 nm. (c) Decay spectra obtained from global analysis of the time-dependent transient absorption spectra.

The transient absorption spectra of diblock copolymer functionalized hybrid nanoparticles (SiO_2 -poly(*p*-phenylene)-*b*-polythiophene) are shown in Figure 2.9 (a) and were obtained using 380 nm excitation pulses. Here the poly(*p*-phenylene) was an inner subshell directly attached to the SiO_2 nanoparticle surface. The transient absorption time-profiles of the SiO_2 -poly(*p*-phenylene)-*b*-polythiophene nanoparticles measured at 425 nm and 650 nm are shown in Figure 2.9 (b). The corresponding decay spectra from global analysis are shown in Figure 2.9 (c), where five lifetimes of $\tau_1 = 3 \pm 1$ ps, $\tau_2 = 19 \pm 2$ ps, $\tau_3 = 27 \pm 3$ ps, $\tau_4 = 128 \pm 5$ ps, and $\tau_5 = 11 \pm 2$ ps were needed to accurately describe the ultrafast excited-state relaxation dynamics. The decay spectra associated with τ_1 and τ_2 were assigned to the poly(*p*-phenylene) subshell chromophore while the decay spectra associated with τ_3 and τ_4 were assigned to the polythiophene subshell, using a direct comparison with the results shown in Figures 2.7 and 2.8. The remaining fifth lifetime τ_5 likely describes the kinetics of the energy transfer from poly(*p*-phenylene) to polythiophene subshells.

The transient absorption spectra of hybrid block copolymer nanoparticles consisting of polythiophene-*b*-poly(*p*-phenylene) shell attached to the SiO_2 core surface are shown in Figure 2.10 (a) and were obtained using 380 nm excitation pulses. Here the polythiophene was an inner subshell directly attached to the SiO_2 nanoparticle surface. Two negative bands centered near 480 and 650 nm were attributed to ground state depletion separated by a positive, excited-state absorption band centered near 630 nm. The transient absorption time-profiles of the SiO_2 -polythiophene-*b*-poly(*p*-phenylene) nanoparticles measured at 450 nm and 650 nm are shown in Figure 2.10 (b). As shown in the decay spectra in Figure 2.10 (c), five lifetimes of $\tau_1 = 7 \pm 1$ ps, $\tau_2 = 21 \pm 3$ ps, $\tau_3 = 23 \pm 1$ ps, and $\tau_4 = 118 \pm 4$ ps, and $\tau_5 = 8 \pm 1$ ps were required to accurately describe the ultrafast excited-state relaxation dynamics of the SiO_2 -polythiophene-*b*-poly(*p*-

phenylene) nanoparticles. Again, τ_1 and τ_2 could be assigned to poly(*p*-phenylene) chromophore, τ_3 and τ_4 were assigned to polythiophene, and τ_5 was attributed to describe kinetics of intraparticle energy transfer between poly(*p*-phenylene) and polythiophene subshells.

The transient absorption results shown in Figures 2.9 and 2.10 demonstrate the important changes in excited state dynamics that occur upon changing the order of the two subshells within the diblock copolymer shell. In Figure 2.9 (c), the decay spectrum associated with τ_1 and τ_2 , assigned to poly(*p*-phenylene), showed very small amplitudes compared to the decay spectrum associated with τ_3 and τ_4 , which were assigned to polythiophene. In this case, the polythiophene subshell dominated the excited-state dynamics due to its placement on the outside of the polymer shell. In contrast, in Figure 2.10 (c), the decay spectra associated with τ_1 and τ_2 showed much higher amplitudes, indicating that the poly(*p*-phenylene) subshell dominated the excited-state dynamics when it was placed on the outside of the polymer shell. The decay spectra associated with energy transfer between poly(*p*-phenylene) and polythiophene have spectral features from both polymers, with excited-state absorption near 475 nm from poly(*p*-phenylene) and a broad ground-state depletion band from polythiophene. In addition, the global analysis results of the diblock copolymers attached to the SiO₂ nanoparticles were altered with respect to the single polymer spectra shown in figures 2.9 (c) and 2.10 (c), and were characterized by blue shifting of the broad excited-state absorption and ground-state depletion bands in polythiophene chromophore and a suppression of excited-state absorption signal in poly(*p*-phenylene) chromophore. The polythiophene lifetimes of τ_3 and τ_4 were the same both for the SiO₂-polythiophene (homopolymer) nanoparticles and the SiO₂-polythiophene-*b*-poly(*p*-phenylene) (diblock copolymer) nanoparticles but became slightly longer in the case of SiO₂-poly-*p*-phenylene-*b*-polythiophene nanoparticles. The first lifetime of poly(*p*-phenylene), τ_1 , was the same both for the

homopolymer SiO₂-poly(*p*-phenylene) and diblock copolymer SiO₂-polythiophene-*b*-poly(*p*-phenylene) nanoparticles, but it became much faster in the case of reversed order SiO₂-poly(*p*-phenylene)-*b*-polythiophene nanoparticles, while the second lifetime, τ_2 , remained the same (within experimental uncertainty) for all polymer configurations. The fifth lifetime, τ_5 , was associated with the energy transfer between poly(*p*-phenylene) and polythiophene subshells; it was slightly faster in the case of SiO₂-polythiophene-*b*-poly(*p*-phenylene) nanoparticles which showed broader, red-shifted decay spectra compared to SiO₂-poly(*p*-phenylene)-*b*-polythiophene nanoparticles.

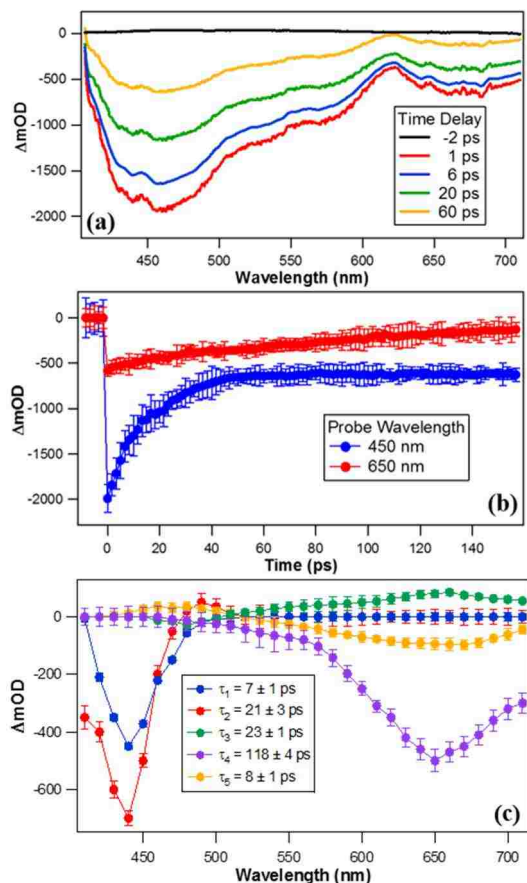


Figure 2.10 (a) Representative transient absorption spectra of SiO₂-polythiophene-*b*-poly(*p*-phenylene) nanoparticles in 1,2-dichlorobenzene (conc. 0.5 mg/ml) using 380 nm excitation pulses. (b) Transient absorption time-profiles of the SiO₂-polythiophene-*b*-poly(*p*-phenylene) nanoparticles measured at 450 nm and 650 nm. (c) Decay spectra obtained from global analysis of the time-dependent transient absorption spectra.

If we closely look at the lifetimes of block copolymers, it may be seen that the excited state decay mechanism may involve charge transfer from polythiophene to poly(*p*-phenylene). This is reflected in a longer lifetime of polythiophene than poly(*p*-phenylene). This contradicts our observation from steady-state fluorescence analysis where clearly energy transfer from PPP to PT takes place irrespective of ordering of polymer growth.

But when we closely look into global analysis spectra of diblock polymers, we got see a better picture of excited state dynamics. In both cases, for lifetime τ_5 , we see that there was a positive peak at PPP spectral region followed by depletion of the PT region. Positive peak of PPP clearly shows energy transfer process. Thus, we can safely conclude that at such time scale, both energy transfer and electron transfer process may takes place, although overall process was dominated by energy transfer from PPP to PT. Much slower charge transfer process couldnot be seen in the time scale of our experiment. Further detailed experiments are underway to get more detailed understanding of this process.

Overall, the transient absorption spectroscopy of the hybrid nanoparticles consisting of different polymers and diblock copolymers attached to SiO₂ core in 1,2-dichlorobenzene provided an important insight into the excited-state dynamics and energy transfer within the conjugated polymer shell that occurs upon photoexcitation.

2.3 Conclusions

Controlled Kumada catalyst transfer polymerization occurring by the chain-growth mechanism was employed for the synthesis of hybrid nanoparticles consisting of homopolymer or diblock copolymer shell attached to the central silica core. Although controlled synthesis of well-defined conjugated polymers via Kumada catalyst transfer polymerization became an established technique for solution polymerization, carrying out the same reaction in heterogeneous conditions

(as surface-confined process) to reliably form surface-attached uniform polymer chains still remains challenging. We developed and described a simple and efficient approach to the preparation of surface-immobilized layer of catalytic Ni(II) initiator, and demonstrated using it to prepare layers of homopolymers and well-defined block copolymers on silica nanoparticles. The resulting hybrid nanoparticles were characterized using electron microscopy, small angle neutron scattering and thermal analysis which allowed to observe controlled formation of the polymer shells. Finally, photophysical properties, and, in particular, photoexcitation energy transfer processes, were studied via steady-state fluorescence and absorption spectroscopies, and time-resolved transient absorption spectroscopy. Irrespective of the sequence of conjugated polymer chromophores in the organic shell, energy transfer always takes place from the higher energy poly-*p*-phenylene donor chromophore to the lower energy polythiophene acceptor chromophore, although its efficiency strongly depends on the order of the CP subshells. From the transient absorption spectroscopy studies, we observed that the energy transfer process was only effected in the polythiophene subshell chromophore and was unaffected in the PPP subshell chromophore. This could be due to the rigid expanded structure of PPP subshell, whereas PT subshell was strongly folded to form a tightly packed crystalline phase. We are currently investigating the opportunities to use these hybrid nanoparticles in design of solar cells and LED devices, as well as for chemo- and biosensing applications.

2.4 References

1. Hoppe, H.; Sariciftci, N. S., Morphology of polymer/fullerene bulk heterojunction solar cells. *J. Mater. Chem.* **2006**, *16* (1), 45-61.
2. Thompson, B. C.; Frechet, J. M. J., Polymer-fullerene composite solar cells. *Angew. Chem., Int. Ed.* **2008**, *47* (1), 58-77.

3. Kroon, R.; Lenes, M.; Hummelen, J. C.; Blom, P. W. M.; de Boer, B., Small Bandgap Polymers for Organic Solar Cells (Polymer Material Development in the Last 5 Years). *Polym. Rev.* **2008**, *48* (3), 531-582.
4. Kiriya, N.; Bocharova, V.; Kiriya, A.; Stamm, M.; Krebs, F. C.; Adler, H.-J., Designing Thiophene-Based Azomethine Oligomers with Tailored Properties: Self-assembly and Charge Carrier Mobility. *Chem. Mater.* **2004**, *16* (23), 4765-4771.
5. Kiriya, N.; Kiriya, A.; Bocharova, V.; Stamm, M.; Richter, S.; Ploetner, M.; Fischer, W.-J.; Krebs, F. C.; Senkowska, I.; Adler, H.-J., Conformation, molecular packing, and field effect mobility of regioregular β,β' -Dihexylsexithiophene. *Chem. Mater.* **2004**, *16* (23), 4757-4764.
6. Boucle, J.; Ravirajan, P.; Nelson, J., Hybrid polymer-metal oxide thin films for photovoltaic applications. *J. Mater. Chem.* **2007**, *17* (30), 3141-3153.
7. Peet, J.; Salvatore, M. L.; Heeger, A. J.; Bazan, G. C., The Role of Processing in the Fabrication and Optimization of Plastic Solar Cells. *Adv. Mater.* **2009**, *21* (14-15), 1521-1527.
8. McQuade, D. T.; Pullen, A. E.; Swager, T. M., Conjugated polymer-based chemical sensors. *Chem. Rev.* **2000**, *100* (7), 2537-2574.
9. Bundgaard, E.; Krebs, F. C., Low band gap polymers for organic photovoltaics. *Sol. Energy Mater. Sol. Cells* **2007**, *91* (11), 954-985.
10. Cavallini, M.; Stolar, P.; Moulin, J.-F.; Surin, M.; Leclere, P.; Lazzaroni, R.; Breiby, D. W.; Andreasen, J. W.; Nielsen, M. M.; Sonar, P.; Grimsdale, A. C.; Muellen, K.; Biscarini, F., Field-Effect Transistors Based on Self-Organized Molecular Nanostripes. *Nano Lett.* **2005**, *5* (12), 2422-2425.
11. Ho, H. A.; Dore, K.; Boissinot, M.; Bergeron, M. G.; Tanguay, R. M.; Boudreau, D.; Leclerc, M., Direct Molecular Detection of Nucleic Acids by Fluorescence Signal Amplification. *J. Am. Chem. Soc.* **2005**, *127* (36), 12673-12676.
12. Brittain, W. J.; Minko, S., A structural definition of polymer brushes. *J. Polym. Sci., Part A: Polym. Chem.* **2007**, *45* (16), 3505-3512.
13. Sokolov, A. N.; Tee, B. C. K.; Bettinger, C. J.; Tok, J. B. H.; Bao, Z., Chemical and Engineering Approaches To Enable Organic Field-Effect Transistors for Electronic Skin Applications. *Acc. Chem. Res.* **2012**, *45* (3), 361-371.
14. Ulman, A., Formation and Structure of Self-Assembled Monolayers. *Chem. Rev.* **1996**, *96* (4), 1533-1554.

15. Monnaie, F.; Brulot, W.; Verbiest, T.; De Winter, J.; Gerbaux, P.; Smeets, A.; Koeckelberghs, G., Synthesis of End-Group Functionalized P3HT: General Protocol for P3HT/Nanoparticle Hybrids. *Macromolecules* **2013**, *46* (21), 8500-8508.
16. Ogawa, K.; Chemburu, S.; Lopez, G. P.; Whitten, D. G.; Schanze, K. S., Conjugated Polyelectrolyte-Grafted Silica Microspheres. *Langmuir* **2007**, *23* (8), 4541-4548.
17. Edmondson, S.; Osborne, V. L.; Huck, W. T. S., Polymer brushes via surface-initiated polymerizations. *Chem. Soc. Rev.* **2004**, *33* (1), 14-22.
18. Miyakoshi, R.; Yokoyama, A.; Yokozawa, T., Catalyst-Transfer Polycondensation. Mechanism of Ni-Catalyzed Chain-Growth Polymerization Leading to Well-Defined Poly(3-hexylthiophene). *J. Am. Chem. Soc.* **2005**, *127* (49), 17542-17547.
19. Yokozawa, T.; Adachi, I.; Miyakoshi, R.; Yokoyama, A., Catalyst-transfer condensation polymerization for the synthesis of well-defined polythiophene with hydrophilic side chain and of diblock copolythiophene with hydrophilic and hydrophobic side Chains. *High Perform. Polym.* **2007**, *19* (5/6), 684-699.
20. Stefan, M. C.; Javier, A. E.; Osaka, I.; McCullough, R. D., Grignard Metathesis Method (GRIM): Toward a Universal Method for the Synthesis of Conjugated Polymers. *Macromolecules* **2009**, *42* (1), 30-32.
21. Iovu, M. C.; Sheina, E. E.; Gil, R. R.; McCullough, R. D., Experimental Evidence for the Quasi-"Living" Nature of the Grignard Metathesis Method for the Synthesis of Regioregular Poly(3-alkylthiophenes). *Macromolecules* **2005**, *38* (21), 8649-8656.
22. Senkovskyy, V.; Khanduyeva, N.; Komber, H.; Oertel, U.; Stamm, M.; Kuckling, D.; Kiriya, A., Conductive Polymer Brushes of Regioregular Head-to-Tail Poly(3-alkylthiophenes) via Catalyst-Transfer Surface-Initiated Polycondensation. *J. Am. Chem. Soc.* **2007**, *129* (20), 6626-6632.
23. Khanduyeva, N.; Senkovskyy, V.; Beryozkina, T.; Bocharova, V.; Simon, F.; Nitschke, M.; Stamm, M.; Groetzschel, R.; Kiriya, A., Grafting of Poly(3-hexylthiophene) from Poly(4-bromostyrene) Films by Kumada Catalyst-Transfer Polycondensation: Revealing of the Composite Films Structure. *Macromolecules* **2008**, *41* (20), 7383-7389.
24. Tkachov, R.; Senkovskyy, V.; Komber, H.; Sommer, J.-U.; Kiriya, A., Random Catalyst Walking along Polymerized Poly(3-hexylthiophene) Chains in Kumada Catalyst-Transfer Polycondensation. *J. Am. Chem. Soc.* **2010**, *132* (22), 7803-7810.
25. Senkovskyy, V.; Tkachov, R.; Beryozkina, T.; Komber, H.; Oertel, U.; Horecha, M.; Bocharova, V.; Stamm, M.; Gevorgyan, S. A.; Krebs, F. C.; Kiriya, A., "Hairy" poly(3-

- hexylthiophene) particles prepared via surface-initiated Kumada catalyst-transfer polycondensation. *J. Am. Chem. Soc.* **2009**, *131* (45), 16445-16453.
26. Marshall, N.; Sontag, S. K.; Locklin, J., Substituted Poly(p-phenylene) Thin Films via Surface-Initiated Kumada-Type Catalyst Transfer Polycondensation. *Macromolecules* **2010**, *43* (5), 2137-2144.
 27. Sontag, S. K.; Marshall, N.; Locklin, J., Formation of conjugated polymer brushes by surface-initiated catalyst-transfer polycondensation. *Chem. Commun.* **2009**, (23), 3354-3356.
 28. Sontag, S. K.; Sheppard, G. R.; Usselman, N. M.; Marshall, N.; Locklin, J., Surface-Confined Nickel Mediated Cross-Coupling Reactions: Characterization of Initiator Environment in Kumada Catalyst-Transfer Polycondensation. *Langmuir* **2011**, *27* (19), 12033-12041.
 29. Chavez, C. A.; Choi, J.; Nesterov, E. E., One-Step Simple Preparation of Catalytic Initiators for Catalyst-Transfer Kumada Polymerization: Synthesis of Defect-Free Polythiophenes. *Macromolecules* **2014**, *47* (2), 506-516.
 30. Stoeber, W.; Fink, A.; Bohn, E., Controlled growth of monodisperse silica spheres in the micron size range. *J. Colloid Interface Sci.* **1968**, *26* (1), 62-9.
 31. Bogush, G. H.; Tracy, M. A.; Zukoski, C. F. I., Preparation of monodisperse silica particles: control of size and mass fraction. *J. Non-Cryst. Solids* **1988**, *104* (1), 95-106.
 32. Levitsky, I. A.; Kim, J.; Swager, T. M., Energy Migration in a Poly(phenylene ethynylene): Determination of Interpolymer Transport in Anisotropic Langmuir-Blodgett Films. *J. Am. Chem. Soc.* **1999**, *121* (7), 1466-1472.
 33. Satrijo, A.; Kooi, S. E.; Swager, T. M., Enhanced Luminescence from Emissive Defects in Aggregated Conjugated Polymers. *Macromolecules* **2007**, *40* (25), 8833-8841.
 34. Duvanel, G.; Grilj, J.; Vauthey, E., Ultrafast Long-Distance Excitation Energy Transport in Donor-Bridge-Acceptor Systems. *J. Phys. Chem. A* **2013**, *117* (5), 918-928.
 35. Hwang, I.; Scholes, G. D., Electronic Energy Transfer and Quantum-Coherence in π -Conjugated Polymers. *Chem. Mater.* **2011**, *23* (3), 610-620.
 36. Wells, N. P.; Blank, D. A., Correlated Exciton Relaxation in Poly(3-hexylthiophene). *Phys. Rev. Lett.* **2008**, *100* (8), 086403/1-086403/4.
 37. Banerji, N.; Cowan, S.; Vauthey, E.; Heeger, A. J., Ultrafast Relaxation of the Poly(3-hexylthiophene) Emission Spectrum. *J. Phys. Chem. C* **2011**, *115* (19), 9726-9739.

38. Brown, P. J.; Thomas, D. S.; Kohler, A.; Wilson, J. S.; Kim, J.-S.; Ramsdale, C. M.; Sirringhaus, H.; Friend, R. H., Effect of interchain interactions on the absorption and emission of poly(3-hexyl-thiophene). *Phys. Rev. B: Condens. Matter Mater. Phys.* **2003**, *67* (6), 064203/1-064203/16.
39. Karam, T. E.; Smith, H. T.; Haber, L. H., Enhanced Photothermal Effects and Excited-State Dynamics of Plasmonic Size-Controlled Gold-Silver-Gold Core-Shell-Shell Nanoparticles. *J. Phys. Chem. C* **2015**, *119* (32), 18573-18580.
40. Karam, T. E.; Siraj, N.; Warner, I. M.; Haber, L. H., Anomalous Size-Dependent Excited-State Relaxation Dynamics of NanoGUMBOS. *J. Phys. Chem. C* **2015**, *119* (50), 28206-28213.

CHAPTER 3. SYNTHESIS OF HYBRID CORE-SHELL PARTICLES CONSISTING OF SILICA CORE AND TRIBLOCK COPOLYMER SHELL PREPARED BY SURFACE-INITIATED POLYMERIZATION

3.1 Introduction

Self-assembly of conjugated polymers has been at the center of numerous investigations to prepare well-defined ordered structures which can have potential applications in bulk heterojunction solar cells. Self-assembly is an efficient and cost-effective approach for fabrication of complex nanostructures.¹⁻⁷ Conjugated polymers with side groups are more flexible, bulkier and display complex self-assembly behavior relative to their small-molecule counterparts. Thus, self-assembly of these complex multicomponent systems would be subject to higher precision, a greater degree of control to give well-defined 3-dimensional ordered nanoscale structures. These assemblies can act as the building blocks for well-ordered semiconducting materials and have potential applications in optoelectronic devices, sensors, etc.^{3, 8} Thus, solution-phase colloidal self-assembly of these polymers may offer a new pathway to control and fabricate nanoscale building blocks of conjugated polymers with well-ordered packing structures.⁹⁻¹⁰

Polythiophene-based block copolymers self-assemble to form different nanostructures such as nanowires,¹¹ nanospheres,¹²⁻¹⁹ helical nanowires,¹⁴ nanorings and vesicles,²⁰ all of them being potential materials for optoelectronic applications. Very recently, Choi's group showed one pot synthesis of fully conjugated poly(*p*-phenylene)-block polythiophene and polythiophene block copolymers which make use of substituted poly(*p*-phenylene) or poly(3-(2-ethylhexyl) thiophene) as the first block and unsubstituted polythiophene as the second block.²¹⁻²² These materials self-assemble to form various 1D nanostructures such as nano-caterpillar, nanostar and nanonetwork crystals.²¹ However, to form such well-defined nanostructures post-synthetic processes such as

aging, temperature annealing, and the solvent annealing are required to promote self-assembly of these materials to get defined structures.

Organic-inorganic hybrid systems could be an excellent alternative to conventional conjugated polymers. Organic-inorganic hybrid systems have gained popularity due to the synergism of the properties of inorganic core and organic shell.²³⁻²⁵ Due to such unique properties, they find applications in optoelectronic and electrochemical devices such as a photovoltaic cells, light-emitting diodes, chemosensors, electrochromic devices and field-effect transistors. These materials are prepared by attaching organic polymer shells onto inorganic cores either by the “*grafting to*” or “*grafting from*” approach. Though “*grafting to*” approach is an attractive method to attach a polymer onto a surface-functionalized inorganic core, it typically leads to poor or low grafting density.²⁶⁻²⁹ Schanze’s group tried to graft conjugated polyacetylene onto silica particles to form polymer brushes, but it resulted in a lower thickness of 12 nm polymer on silica surface and spotty coverage.³⁰ Many other *grafting to* approaches were tried; for example, attachment of thiol-end functionalized polythiophene on gold nanoparticles or amino-functionalized quantum dots,³¹ but they also did not accomplish the desired surface coverage density.

“*Grafting from*” approach is a method of growing polymer from end-functionalized surfaces or particles by chain-growth addition of monomers to the surface-functionalized initiator. This is one of the best methods not only to get different shell composition but also to have the ability to tune grafting density on the surface by changing the initial initiator concentration. Ground-breaking discovery by McCullough³²⁻³³ and Yokozawa³⁴⁻³⁵ showing that Ni-catalyzed Kumada polymerization of thiophene monomer formed regioregular P3HT by a quasi-living mechanism (rather than via step growth), it opened up the possibility of surface-initiated polymerization on different substrates. Recently, Kiriy used an external initiator to initiate the

polymerization of P3HT on silica micro and nanoparticles.³⁶⁻³⁷ Though it produced mechanically stable silica grafted P3HT, it also achieved low surface density. Based on this strategy, Locklin demonstrated preparation of thicker (up to 42 nm) poly(3-methyl thiophene) films.³⁸⁻³⁹ Nevertheless, all of these systems suffer from low activity and relative instability of the surface-immobilized Ni(II) catalyst; therefore, practical implementation of surface-initiated polymerization still remains a challenge. Recently, Nesterov's group⁴⁰ demonstrated that the reaction of aryl bromides or aryl iodides with Ni(0) complex Ni(dppp)₂ (where dppp is 1,3-bis(diphenylphosphino)propane) at moderate temperatures produces a stable Ni (II) complex that can be used as a highly efficient catalytic initiator of Kumada catalyst transfer polymerization (KCTP) of 5-bromo-2-thienylmagnesium monomers. The polymerization gives a high yield of close to 100% regioregular poly(3-alkylthiophene) with number average molecular weight being linearly dependent on the monomer/catalyst ratio. This technique was applied by Nesterov's group to grow polythiophene, poly(p-phenylene), and diblock polymers on silica nanoparticles, as described in chapter 2.

Although the *grafting from* approach has an advantage over the *grafting to* approach for its suitable control of grafting density, it still requires more elaborate group modifications needed for chain extension with second block. This leads to reduced overall yield, as all end groups might not be converted to the required functionality. Therefore, the development of novel synthetic methods for efficient synthesis of various block copolymers still remains important.

Recently, Wu's group⁴¹⁻⁴² had reported that the Ni(II)-terminated P3HT could initiate block copolymerization of various monomers such as phenyl isocyanide and alkoxyallene in a controlled chain-growth manner to afford P3HT-b-poly(aryl isocyanide) and P3HT-b-poly(alkoxyallene) block copolymers⁴³ with controlled molecular weights and tunable compositions.

Polyallenes are reactive polymers with C=C double bond within each repeating unit in the main chains.⁴⁴⁻⁴⁶ They have been used to induce particular self-assembly morphology. Well-defined poly(alkoxyallene)s are usually prepared through living coordination polymerization of alkoxyallene monomers with Ni(II) complexes as initiators/catalysts through 1,2 or 2,3 polymerization of the cumulative double bonds.⁴⁷⁻⁴⁹

Similarly, Nesterov group has recently demonstrated the possibility to grow different block copolymers on the surfaces of silica nanoparticles and thin films. So, we envisioned that our surface-immobilized catalyst can polymerize allene as well as 3-hexylthiophene to give complex block copolymers consisting of dissimilar blocks (e.g. conjugated and non-conjugated) on silica nanoparticles yielding a hybrid material. These materials would be important model systems to study self-assembly of rod-coil structures and formation of different macromolecular systems to control the energy transfer process in complex conjugated polymer systems. This strategy was further extended for the preparation of P3HT block copolymers and other semiconducting materials on surfaces with novel structures and functions.

In this chapter, we describe our studies on hybrid inorganic-organic nanomaterial consisting of conjugated polymers and insulating polyallene polymer. Incorporation of the polyallene subshell made the energy transfer process in this hybrid system affected by the change in a solvent, pH, and type of conjugated polymer involved.

3.2 Results and Discussion

3.2.1 Synthesis and characterization

Monodisperse silica particles were prepared by the well-known Stöber process. They were prepared by polycondensation of tetraorthosilicates and ammonium hydroxide to give a porous network of polysilicates. However, Stöber⁵⁰ process leads to more polydisperse particles. To get

silica particles with more uniform size, Bogush et. al.⁵¹ designed a reverse microemulsion method. pH was maintained around 9 to control the unwanted silica particles formation and provide uniform size distribution. TEM image (figure 3.1) shows formation of silica particles with a diameter of 74 ± 4 nm.

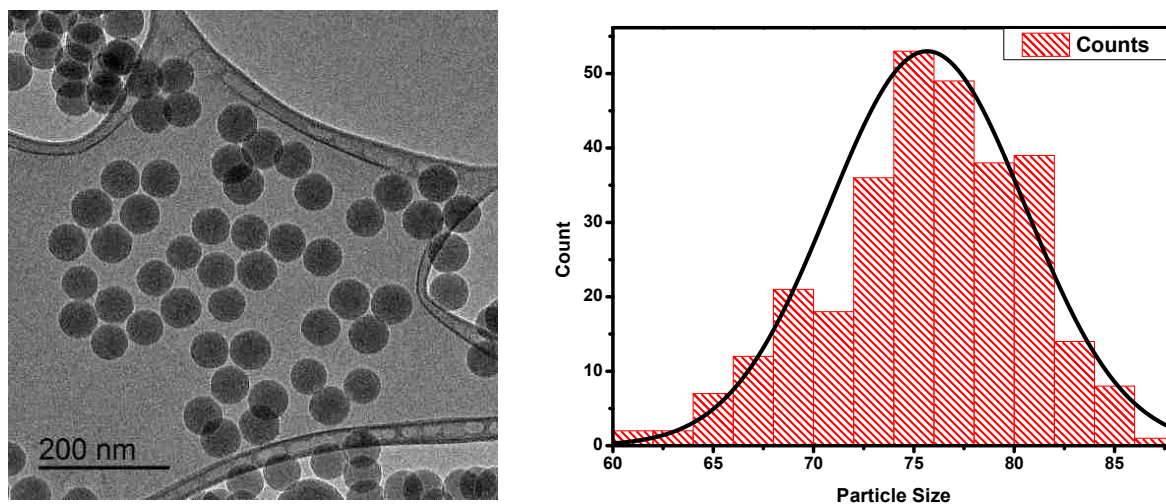
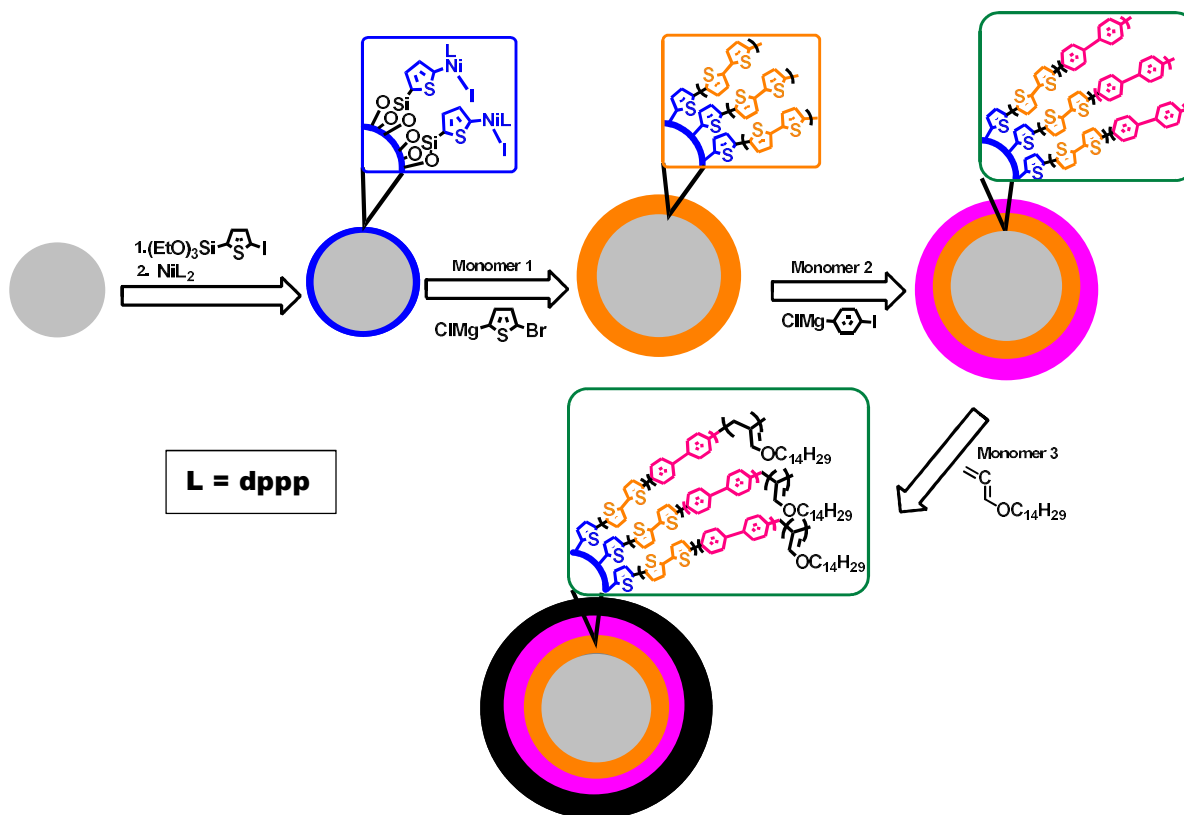


Figure 3.1 TEM images of silica particles with size distribution

The preparation of conjugated polymer-silica nanoparticles was based upon the surface-initiated polymerization strategy developed in the Nesterov's group (Scheme 3.1).⁴⁰ It is based on immobilization of silyl-functionalized bromothiophene precursor onto the silica surface, followed by further treatment with $\text{Ni}(\text{dppp})_2$ to yield Ni initiator. $\text{Ni}(\text{dppp})_2$ can be easily prepared in large scale and is stable for few months. The reaction occurs through oxidative addition of $\text{Ni}(\text{dppp})_2$ complex to iodothiophene precursor to give efficient Ni(II) catalytic initiator. This methods allowed us to obtain an efficient catalytic system for Kumada polymerization providing defect free polymers e.g. polythiophenes, poly(p-phenylenes), and block copolymers.



Scheme 3.1: Synthesis of homopolymer, diblock copolymer and triblock copolymer shells grafted on silica particles

Activate Ni(II) catalytic initiator upon exposure to a solution of suitable Grignard monomer starts living polymerization to form a conjugated polymer film. For co-block polymerization, after 1 day of polymerization, initiating sites were regenerated with additional amount of Ni(dppp)₂ followed by addition of 2nd Grignard monomer, followed by regeneration with Ni(dppp)₂ and the addition of 3rd (allene) monomer. It was previously shown that regeneration of polymer with Ni(0) gives better catalytic initiator density, and it helped to reinstate an incomplete terminated polymerization. As a proof-of-concept, we chose Ni-initiated Kumada polycondensation of (2-bromo 3-hexylthiophen-5-yl)magnesium chloride, or (4-iodo-phenyl)magnesium chloride to form poly(3hexylthiophene) (P3HT), or poly(*p*-phenylene) (PPP), respectively. P3HT and PPP are two of the most common conjugated polymers for various electronic and optoelectronic applications,

and their photophysical properties are well-known and well-documented. Therefore, it was a convenient model for our proof-of-concept study. Depending on the sequential order of these polymers on the silica particles, photophysical properties could be modified and fine-tuned.

Small-angle neutron scattering (SANS) is an important tool to characterize nanomaterials. Using SANS, Berry et al. found P3HT to possess rod-like structure.⁵² Segalman group studied various P3ATs and found that persistence length of P3AT is affected by synthesis method, regioregularity and side chain chemistry.⁵³ These factors can decrease the persistence length by 60-70%.

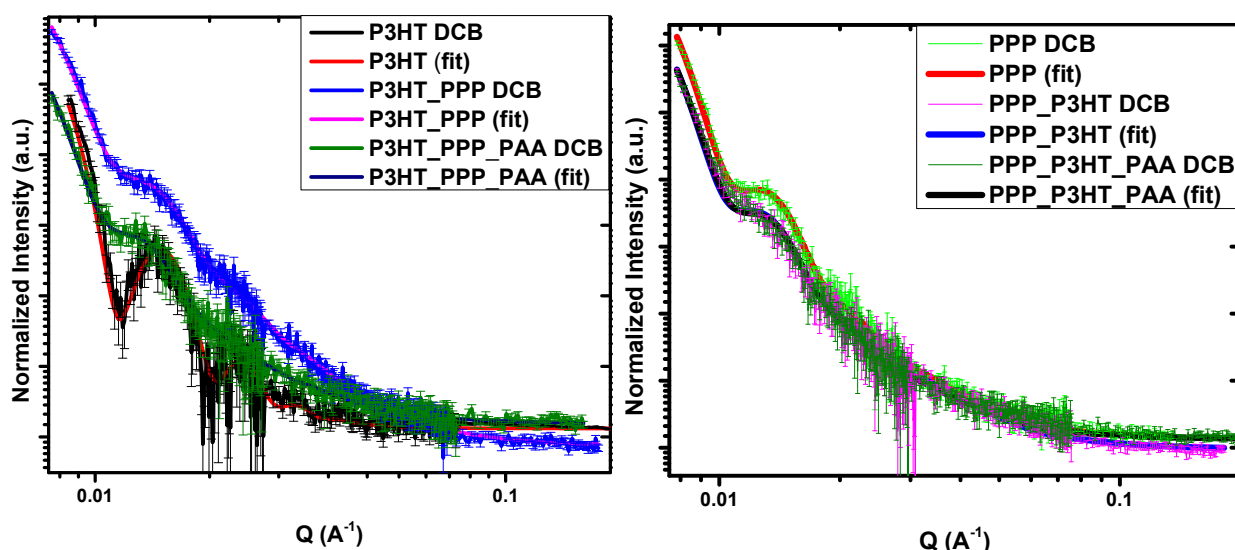


Figure 3.2 SANS analysis of hybrid particles consisting of homopolymer, diblock copolymer and triblock copolymer shells grafted on silica cores, dispersed in 1,2-dichlorobenzene (DCB).

Formation of each sublayer of polymer was studied by SANS. Small angle scattering has become a powerful tool to analyze macromolecules in solution. It had been used to study self-assembly and formation of aggregates of macromolecules as well as for the investigation of complex fluids. Polymer grafted silica particles were dispersed in d4-dichlorobenzene (DCB) to get more contrast. The SiO₂ core radius was fixed at 37 nm based on the data obtained from

the TEM image. The data was fitted by the core-shell model which corresponds to the local density fluctuation of the polymers in suspensions. The monodisperse core-shell model worked and directly caught all the oscillations in the scattering profile. Silica size obtained from TEM data was fixed to fit the data for grafted polymers on the surface.

The scattering intensity of a polymer can be fit using the following equation:

$$I(q) = KP(q) S(q) + I_{inc} \quad (1)$$

where K is a scaling factor, P(q) is the form factor of a single chain, and I_{inc} is the incoherent scattering intensity which is assumed independent of q.

$$P(q) = \frac{1}{V_s} \left[\frac{(3V_c(\rho_c - \rho_s)j_1(qr_c))}{qr_c} + \frac{(3V_s(\rho_s - \rho_{solv})j_1(qr_s))}{qr_s} \right]^2 + bkg \quad (2)$$

Where $j_1(x) = (\sin x - x \cos x) / x^2$; $r_s = r_c + t$; $V_i = (4\pi/3)$; bkg is incoherent background, solv is solvent, s is shell, c is core

There are only 3 fitting parameters: prefactor, shell thickness and the scattering length density of the polymer shell. The monodispersity of the grafted polymer on the surface of SiO₂ was excellent. Shell thickness obtained by fitting the data was as follows: P3HT 2.2 nm; P3HT-PPP 12.7 nm; P3HT-PPh-PAA 13.6 nm; PPP 12.3 nm; PPP-P3HT 13.2 nm; PPP-P3HT-PAA 13.2 nm.

3.2.2 Photophysical properties of hybrid silica-conjugated polymers

Photoexcitation of conjugated polymers creates an electron-hole pair, or exciton, by absorbing photon of light, through moving an electron from an occupied orbital to an unoccupied orbital. This exciton will then delocalize over the whole chain but is not confined within the chain. This exciton then relaxes along the excited state potential surface into a cold exciton which then decays radiatively back to the ground state.⁵⁴ In general, conjugated polymers after photoexcitation

undergo conformational changes from aromatic to quinoidal type of geometry. This results in a change in torsional constants between each repeat units. This change results in Stokes shifts which are greater in solutions than in thin films.⁵⁵

Particles functionalized with triblock copolymer, SiO₂- P3HT-PPP-PAA, were dissolved in DCB. DCB is a good solvent for P3HT and PPP, and thus, overall solvent-polymer interaction is good and stabilizes the polymer. Absorption spectra show broad spectra with maxima around 380 nm with a shoulder at 425 nm. A slight decrease in the shoulder intensity of triblock copolymer P3HT-PPP-PAA with respect to diblock copolymer P3HT- PPP grafted silica particles shows an increase in solubility of the polymer due to the incorporation of PAA layer. Absorption spectra showed less vibronic features than luminescence spectra because absorption spectra correspond to vertical frank-condon transition of ground state whereas emission spectra reflect conformations of relaxed excited state. Comparison of absorption spectra with excitation spectra demonstrated the effect of aggregation of P3HT. Order-disorder transition of P3HT has been extensively studied. Köhler's group had shown that aggregation is a first order transition from coil to a more ordered phase which changes with the difference in a polydispersity of polymer chains and molecular weight.⁵⁶ Study of aggregation in solution is important as it is well known that such aggregates in solution can later act as nucleation points for aggregate formation in thin films for spin-coating samples.⁵⁷ Comparison of λ_{max} of absorption and excitation shows that there is a 20 nm blue shift. Blue shift in the excitation spectra compared to absorption spectra may be understood as indicating energy transfer from poly(*p*-phenylene) to P3HT. With initial photoexcitation for most π -conjugated systems, energy is transferred via downhill process within the density of states. A structural disorder caused by kinks or twists in polymer chain leads to an inhomogeneous distribution of conformational states.⁵⁷ Thus, excitation at 380 nm (blue edge) will result in

excitation of high energy poly(*p*-phenylene) segments by rapid unidirectional energy migration to low energy P3HT layers. This results in the channeling of all excitation energy to the lowest energy emissive state regardless of the excitation wavelength.⁵⁸ Change in the solvent from DCB to THF does not alter absorbance and excitation spectra of poly(*p*-phenylene) segment appreciably. Thus, PPP block is least affected as it does not have any solubilizing group and is solvophobic. There is no change in absorbance for diblock copolymer but for triblock copolymer the appearance of shoulder at around 470 nm reflected possibly better solubility of polymers and overall planarization of the π -conjugated backbone which resulted in the formation of more ordered conformation. The appearance of 470 nm peak indicated that there were such conformational changes. Inter-chain interaction would relax the molecular symmetry, and thus, the 0-0 transition will be allowed and correspondingly increased.

In the case of PPP-P3HT-PAA series, it showed the same behavior for poly(*p*-phenylene) segment i.e. excitation maximum was blue shifted with respect to absorbance (395nm for absorbance and 375 nm for excitation). This clearly proved that there was an energy transfer taking place from higher energy poly(*p*-phenylene) segments to lower energy P3HT segment. Increase of the intensity in 470 nm peak for PPP, PPP-P3HT and PPP-P3HT-PAA in DCB relative to that in THF solution may be attributed to the incorporation of P3HT and PAA blocks. This is because THF is a nonaromatic solvent which tends to separate the polymer chains from each other and helps to collapse into coils. On the other hand, in the case of DCB, polymer chains would prefer to have extended conformations which help in aggregate formation.⁵⁹ The appearance of shoulder peak at 600 nm for the solution of PPP-P3HT-PAA in DCB and THF may correspond to P3HT 0-0 transition peak. This may be due to better planarization of the triblock copolymer upon the incorporation of PAA segment. This would result in more efficient energy transfer from poly(*p*-

phenylene) to P3HT segment. This was seen by the appearance of more vibronic structures in excitation spectra.

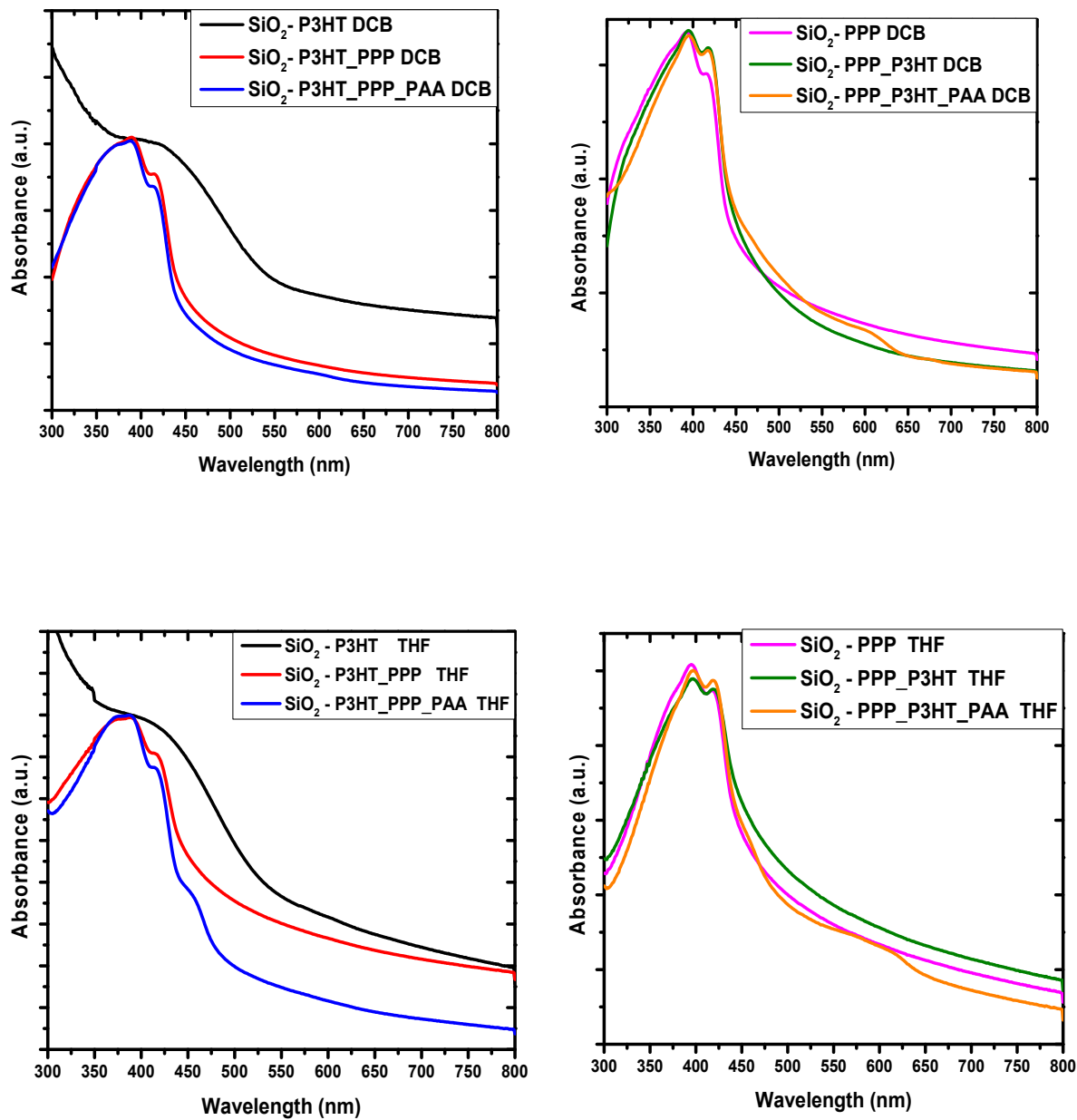


Figure 3.3 Absorbance spectra of homopolymer, diblock copolymer and triblock copolymer shells grafted on silica particles in 1,2-dichlorobenzene and THF (0.3 mg/ml).

As stated earlier, in the case of DCB, polymers may prefer to adopt a planar conformation with more electronic delocalization and more vibronic features appearing in the excitation spectra

of polymers in DCB than in THF. In the case of the diblock copolymer, there were almost no vibronic peaks observed in P3HT segment which mean that the solvent molecules tend to collapse P3HT polymer chains into coils on top of poly(*p*-phenylene) shell. Similar types of vibronic features have been documented in other conjugated polymers.⁶⁰⁻⁶³ This may be due to overall increasing solubility of polymer hybrid particles caused because of hexyl side chains of P3HT which prefer to stay in coil conformation.

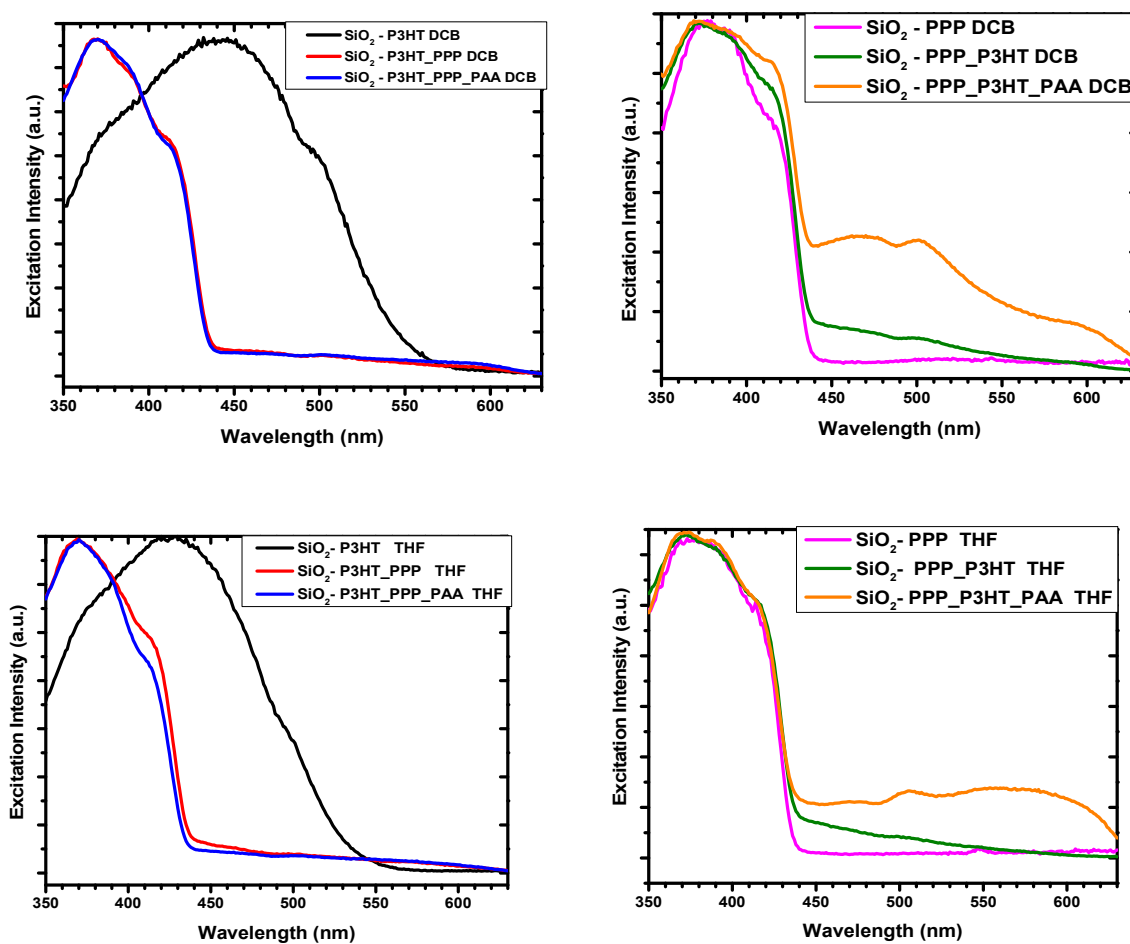


Figure 3.4 Excitation spectra of homopolymer, diblock copolymer and triblock copolymer shells grafted on silica particles in 1,2-dichlorobenzene and THF (emission at 650 nm) (0.3 mg/ml).

Emission spectra (figure 3.5) showed strikingly different behavior for the two polymer series in DCB and THF. In general, absorption spectra were mostly structureless whereas emission spectra were more structured. These suggest that the excited state geometry was more ordered compared to the ground state geometry. The rotational energy barrier was smaller in the ground state and thus contributed molecular disorder that lead to inhomogeneous broadening and almost featureless absorption band.⁶⁴ In the case of emission, on the other hand, it showed a narrow distribution of excited-state molecular geometries which is characterized by more rigid planar quinoid electronic structure contribution to the singlet excited state. Thus more structurally defined luminescence spectra originated from the conformational relaxation of the excited state to more ordered rigid molecular structure prior to the radiative decay.⁶²

Single step energy transfer occurs in conjugated polymers at distances ranging from 0.1 nm to more than 5 nm which can take place via intermolecular or intramolecular energy transfer processes from an excited donor molecule to an acceptor molecule. Conjugated polymer chains have several hundred repeat units, but their effective π -electron conjugation may be altered due to structural, topological and chemical defects.⁶² Thus, the excitation energy transfer can be described as a combination of intrachain and interchain energy transfer which can occur by Förster and Dexter mechanisms. Emission spectra clearly showed energy transfer from poly(*p*-phenylene) to polythiophene chromophores. Energy transfer process can be either by through space (Förster) or through bond (Dexter) type. The former takes place when an efficient spectral overlap of donor emission with acceptor absorption exists.

Emission spectra of diblock and triblock polymers can be divided into two regions: one from 400- 550 nm and the other from 550-850 nm. The first region (400-550 nm) originates from the contribution of the poly(*p*-phenylene) polymer segment, and the other region (from 550 – 850

nm) corresponds to P3HT chromophore. Energy transfer process is unidirectional irrespective of the order of poly(*p*-phenylene) and P3HT, but the efficiency of energy transfer is affected by the sequence of the two blocks. When P3HT was grown as the first block on silica core, energy transfer from PPP to P3HT was minimal due to twisting of bonds caused by steric repulsions between hexyl groups. Due to high grafting density near silica surface, sterically bulky hexyl groups in P3HT would hamper the subsequent growth of polymeric chains. This was confirmed by SANS where P3HT shell size was found to be 2 nm. Thus, the steric hindrance could result in more twisting of the π -conjugated bonds, thus breaking the electronic conjugation in P3HT. Also, presence of hexyl side chain does affect the polymerization growth process as could be seen from our previous results. The unsubstituted polythiophene shells grow to bigger size during the same polymerization time. Thus, energy transfer via Dexter mechanism will be hampered, and only the intramolecular Förster energy transfer process will take place. PPP is solvophobic to both the solvents and will thus form a protective layer covering P3HT. As soon as the polyallene layer was introduced as an outer layer, which is solvophilic to DCB as well as THF, it helped the overall polymer to stretch and thus enhancing the backbone planarization of triblock copolymer. This could assist in funneling the energy from PPP to P3HT and minimizing the conformational defects caused by twisting of bonds.

It can be seen that when poly(*p*-phenylene) was inside, there was more energy transfer occurring to P3HT chromophore. The appearance of two peaks at 625 and 675 nm confirmed the formation of ordered structures of P3HT. The peak at 675 nm was less pronounced in THF than in DCB. Again this is because of interaction of aromatic solvent, DCB, with polymer chain where polymer chains prefer to adopt an extended planar ordered structure, as opposed to THF, where polymer chains collapse and prefer to have coil conformation.⁷ Higher grafting density near the

surface could not affect the polymerization process toward poly(*p*-phenylene) as it has a rigid and symmetric structure which prefers to stay in planar extended conformation. Also, absence of solubilizing side groups on repeating units will give more room and a less steric hindrance to the polymer growth. This could be confirmed by SANS data where poly(*p*-phenylene) size was 12 nm in comparison to 2 nm for P3HT in DCB.

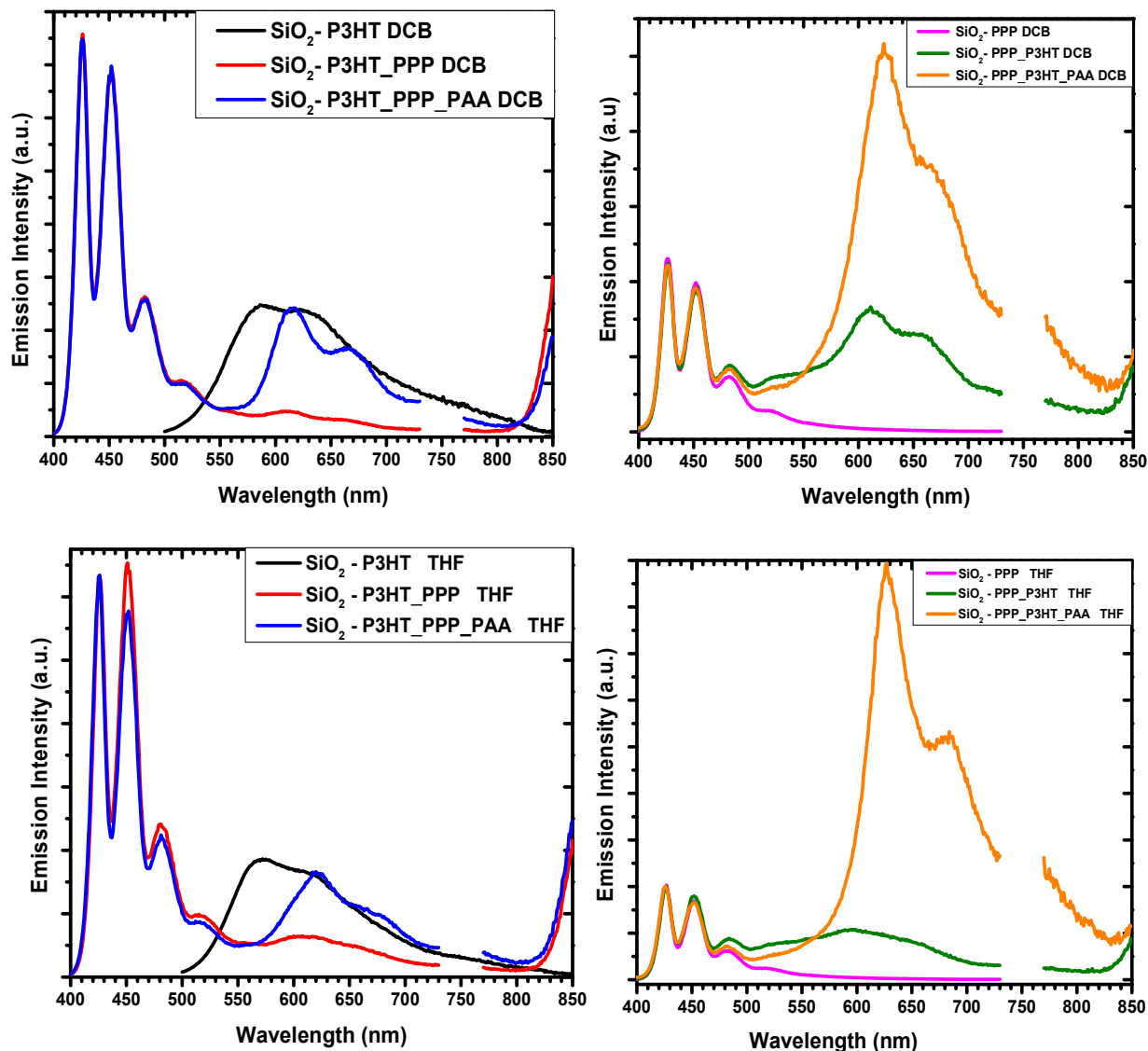


Figure 3.5: Emission spectra of homopolymer, diblock copolymer and triblock copolymer shells grafted on silica particles in 1,2-dichlorobenzene and THF (0.3 mg/ml).

3.2.3 Solvatochromism

The solvent effect was also studied. Three different solvents were chosen, 1,2-dichlorobenzene, THF, and chloroform. Figure 3.6 shows that energy transfer process was more efficient for THF than in DCB and chloroform at the same concentration of polymer in solution (0.3 mg/ml). Also, vibronic features were missing in chloroform but were present in DCB and THF. This is because chloroform solvent molecules tend to enhance polymer-polymer interactions and thus, polymer molecules would adopt a coil conformation to minimize the interaction with solvent molecules. Also, in the case of 1,2-dichlorobenzene, the polymer would adopt an extended conformation that would enhance aggregation or formation of more ordered structure. THF is also a good solvent for both P3HT as well as polyallene because it facilitates ordered and planarized structure.

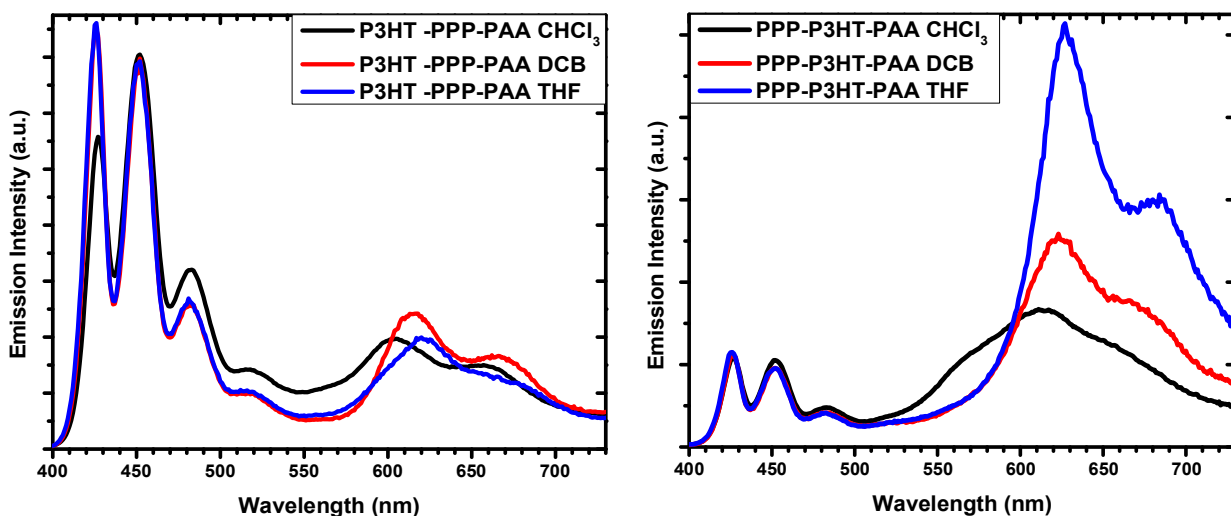


Figure 3.6: Emission spectra of hybrid silica-triblock copolymer particles in chloroform, 1,2-dichlorobenzene, and THF showing effect of solvent on spectroscopic properties of these hybrid silica polymer nanoparticles (0.3 mg/mL).

Both PPP and P3HT get affected by solvent quality. Though in the case of poly(*p*-phenylene) chromophore there was no change in shift in wavelength but there was a change in intensity of vibronic 0-0 peak which directly relates to the packing and interaction of this molecule

with solvent. Thus, in the case of chloroform, 0-0 peak was weak in comparison to 0-1 peak, which indicates strong interaction between the polymer and the solvent due to extra stability incorporated by polyallene block attached to the end of PPP. P3HT molecule prefers to be in different conformations depending upon the type of solvents. In THF, it tends to planarize which results in a more bathochromic shift as seen in figure 3.6. In chloroform, P3HT tries to adopt a coil structure which results in broad featureless P3HT emission spectrum with overall spectra blue shifted in comparison to DCB and THF.

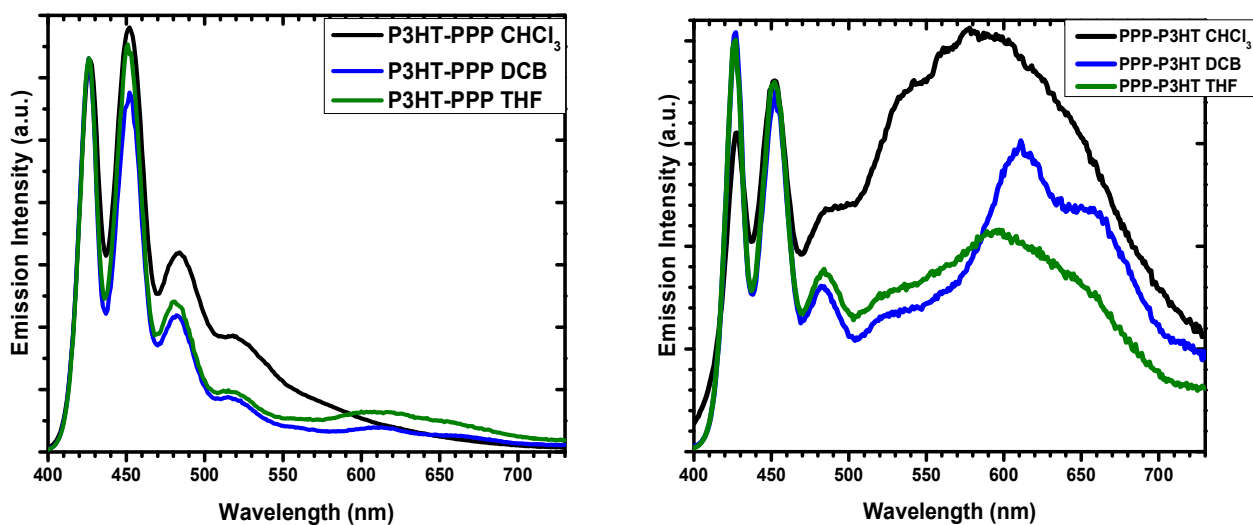


Figure 3.7: Emission spectra of hybrid silica-diblock copolymer nanoparticles in chloroform, 1,2-dichlorobenzene, and THF showing effect of solvent on spectroscopic properties of these nanoparticles (0.3 mg/mL).

To get more insight into the structure of these nanoparticles and how they behave in solvents, emission spectra of diblock polymer in different solvents were recorded (figure 3.7). The trend became entirely opposite as compared to the triblock copolymer. Though there was almost no effect for the P3HT-PPP diblock polymer; PPP-P3HT polymer showed substantial effect. Chloroform is a good solvent for P3HT, and thus, it would tend to planarize the molecule by increasing solvent-polymer interactions. As a result, the entire polymer molecule will stretch into extended conformation which would help to funnel energy from poly(*p*-phenylene) to P3HT

chromophores effectively, and thus energy transfer via both Förster and Dexter mechanism pathways could take place. Energy transfer process for the PPP-P3HT polymer was observed to be less efficient in THF, as THF is not an as good solvent for P3HT as chloroform and thus results in minimizing the energy by collapsing polymer chains into globular conformations. This results in twisting of bonds and breaking of π - electron conjugation. This will decrease the overall efficiency of energy transfer process from PPP to P3HT chromophores.

3.3 Conclusions

Controlled Kumada catalyst transfer polymerization occurring by the chain-growth mechanism was employed for the synthesis of homoblock and diblock copolymer from the surface of an inorganic material such as silica. Though synthesis of conjugated polymers via Kumada-type polymerization became an established method in solution, carrying out the same reaction in heterogeneous surface conditions to achieve a uniform polymer chain length still remains a challenge. We developed a simple and efficient approach to the preparation of a nanoparticle surface-immobilized layer of catalytic Ni(II) initiator, and demonstrated using it to grow block copolymers on silica nanoparticles. The hybrid nanoparticles were characterized by small angle neutron scattering which showed formation of polymer shells in each step. Effect of solvent on energy transfer processes was also studied. It was found that energy transfer took place via a combination of Dexter and Förster mechanisms, but the Dexter through-bond transfer was affected by the change in solvent quality as well as the sequence of conjugated polymer segments. The efficiency of energy transfer was greater for a polymer with P3HT segment as an outer block, grown over PPP block

3.4 References

1. Thompson, B. C.; Frechet, J. M. J., Polymer-fullerene composite solar cells. *Angew. Chem., Int. Ed.* **2008**, *47* (1), 58-77.
2. Kroon, R.; Lenes, M.; Hummelen, J. C.; Blom, P. W. M.; de Boer, B., Small Bandgap Polymers for Organic Solar Cells (Polymer Material Development in the Last 5 Years). *Polym. Rev.* **2008**, *48* (3), 531-582.
3. Kiriya, N.; Bocharova, V.; Kiriya, A.; Stamm, M.; Krebs, F. C.; Adler, H.-J., Designing Thiophene-Based Azomethine Oligomers with Tailored Properties: Self-assembly and Charge Carrier Mobility. *Chem. Mater.* **2004**, *16* (23), 4765-4771.
4. Kiriya, N.; Kiriya, A.; Bocharova, V.; Stamm, M.; Richter, S.; Ploetner, M.; Fischer, W.-J.; Krebs, F. C.; Senkowska, I.; Adler, H.-J., Conformation, molecular packing, and field effect mobility of regioregular β,β' -Dihexylsexithiophene. *Chem. Mater.* **2004**, *16* (23), 4757-4764.
5. Bundgaard, E.; Krebs, F. C., Low band gap polymers for organic photovoltaics. *Sol. Energy Mater. Sol. Cells* **2007**, *91* (11), 954-985.
6. Boucle, J.; Ravirajan, P.; Nelson, J., Hybrid polymer-metal oxide thin films for photovoltaic applications. *J. Mater. Chem.* **2007**, *17* (30), 3141-3153.
7. Peet, J.; Senatore, M. L.; Heeger, A. J.; Bazan, G. C., The Role of Processing in the Fabrication and Optimization of Plastic Solar Cells. *Adv. Mater.* **2009**, *21* (14-15), 1521-1527.
8. Cavallini, M.; Stoliar, P.; Moulin, J.-F.; Surin, M.; Leclere, P.; Lazzaroni, R.; Breiby, D. W.; Andreasen, J. W.; Nielsen, M. M.; Sonar, P.; Grimsdale, A. C.; Muellen, K.; Biscarini, F., Field-Effect Transistors Based on Self-Organized Molecular Nanostripes. *Nano Lett.* **2005**, *5* (12), 2422-2425.
9. McQuade, D. T.; Pullen, A. E.; Swager, T. M., Conjugated polymer-based chemical sensors. *Chem. Rev.* **2000**, *100* (7), 2537-2574.
10. Ho, H. A.; Dore, K.; Boissinot, M.; Bergeron, M. G.; Tanguay, R. M.; Boudreau, D.; Leclerc, M., Direct Molecular Detection of Nucleic Acids by Fluorescence Signal Amplification. *J. Am. Chem. Soc.* **2005**, *127* (36), 12673-12676.
11. Li, Z.; Ono, R. J.; Wu, Z.-Q.; Bielawski, C. W., Synthesis and self-assembly of poly(3-hexylthiophene)-block-poly(acrylic acid). *Chem. Commun.* **2011**, *47* (1), 197-199.

12. Wu, P.-T.; Ren, G.; Li, C.; Mezzenga, R.; Jenekhe, S. A., Crystalline Diblock Conjugated Copolymers: Synthesis, Self-Assembly, and Microphase Separation of Poly(3-butylthiophene)-b-poly(3-octylthiophene). *Macromolecules* **2009**, *42* (7), 2317-2320.
13. He, M.; Zhao, L.; Wang, J.; Han, W.; Yang, Y.; Qiu, F.; Lin, Z., Self-Assembly of All-Conjugated Poly(3-alkylthiophene) Diblock Copolymer Nanostructures from Mixed Selective Solvents. *ACS Nano* **2010**, *4* (6), 3241-3247.
14. Lee, E.; Hammer, B.; Kim, J.-K.; Page, Z.; Emrick, T.; Hayward, R. C., Hierarchical Helical Assembly of Conjugated Poly(3-hexylthiophene)-block-poly(3-triethylene glycol thiophene) Diblock Copolymers. *J. Am. Chem. Soc.* **2011**, *133* (27), 10390-10393.
15. Patra, S. K.; Ahmed, R.; Whittell, G. R.; Lunn, D. J.; Dunphy, E. L.; Winnik, M. A.; Manners, I., Cylindrical Micelles of Controlled Length with a π -Conjugated Polythiophene Core via Crystallization-Driven Self-Assembly. *J. Am. Chem. Soc.* **2011**, *133* (23), 8842-8845.
16. Gilroy, J. B.; Lunn, D. J.; Patra, S. K.; Whittell, G. R.; Winnik, M. A.; Manners, I., Fiber-like Micelles via the Crystallization-Driven Solution Self-Assembly of Poly(3-hexylthiophene)-block-Poly(methyl methacrylate) Copolymers. *Macromolecules* **2012**, *45* (14), 5806-5815.
17. Kamps, A. C.; Fryd, M.; Park, S.-J., Hierarchical Self-Assembly of Amphiphilic Semiconducting Polymers into Isolated, Bundled, and Branched Nanofibers. *ACS Nano* **2012**, *6* (3), 2844-2852.
18. Gwyther, J.; Gilroy, J. B.; Rugar, P. A.; Lunn, D. J.; Kynaston, E.; Patra, S. K.; Whittell, G. R.; Winnik, M. A.; Manners, I., Dimensional Control of Block Copolymer Nanofibers with a π -Conjugated Core: Crystallization-Driven Solution Self-Assembly of Amphiphilic Poly(3-hexylthiophene)-b-poly(2-vinylpyridine). *Chem. - Eur. J.* **2013**, *19* (28), 9186-9197.
19. Qian, J.; Li, X.; Lunn, D. J.; Gwyther, J.; Hudson, Z. M.; Kynaston, E.; Rugar, P. A.; Winnik, M. A.; Manners, I., Uniform, High Aspect Ratio Fiber-like Micelles and Block Co-micelles with a Crystalline π -Conjugated Polythiophene Core by Self-Seeding. *J. Am. Chem. Soc.* **2014**, *136* (11), 4121-4124.
20. Kim, J.; Song, I. Y.; Park, T., Polymeric vesicles with a hydrophobic interior formed by a thiophene-based all-conjugated amphiphilic diblock copolymer. *Chem. Commun.* **2011**, *47* (16), 4697-4699.
21. Lee, I.-H.; Amaladass, P.; Choi, T.-L., One-pot synthesis of nanocaterpillar structures via in situ nanoparticlization of fully conjugated poly(p-phenylene)-block-polythiophene. *Chem. Commun.* **2014**, *50* (59), 7945-7948.

22. Lee, I.-H.; Amaladass, P.; Yoon, K.-Y.; Shin, S.; Kim, Y.-J.; Kim, I.; Lee, E.; Choi, T.-L., Nanostar and Nanonetwork Crystals Fabricated by in Situ Nanoparticlization of Fully Conjugated Polythiophene Diblock Copolymers. *J. Am. Chem. Soc.* **2013**, *135* (47), 17695-17698.
23. Ravindranath, R.; Ajikumar, P. K.; Hanafiah, N. B. M.; Knoll, W.; Valiyaveetil, S., Synthesis and Characterization of Luminescent Conjugated Polymer-Silica Composite Spheres. *Chem. Mater.* **2006**, *18* (5), 1213-1218.
24. Montalti, M.; Prodi, L.; Zaccheroni, N.; Zatonni, A.; Reschiglian, P.; Falini, G., Energy Transfer in Fluorescent Silica Nanoparticles. *Langmuir* **2004**, *20* (7), 2989-2991.
25. Qu, Y.; Feng, L.; Tong, C.; Liu, B.; Lu, C., Poly(p-phenylenevinylene) functionalized fluorescent mesoporous silica nanoparticles for drug release and cell imaging. *Microporous Mesoporous Mater.* **2013**, *182*, 155-164.
26. Wu, Z.-Q.; Ono, R. J.; Chen, Z.; Li, Z.; Bielawski, C. W., Polythiophene-block-poly(γ -benzyl L-glutamate): synthesis and study of a new rod-rod block copolymer. *Polym. Chem.* **2011**, *2* (2), 300-302.
27. Tao, Y.; McCulloch, B.; Kim, S.; Segalman, R. A., The relationship between morphology and performance of donor-acceptor rod-coil block copolymer solar cells. *Soft Matter* **2009**, *5* (21), 4219-4230.
28. Yang, H.; Xia, H.; Wang, G.; Peng, J.; Qiu, F., Insights into poly(3-hexylthiophene)-b-poly(ethylene oxide) block copolymer: Synthesis and solvent-induced structure formation in thin films. *J. Polym. Sci., Part A: Polym. Chem.* **2012**, *50* (24), 5060-5067.
29. Urien, M.; Erothu, H.; Cloutet, E.; Hiorns, R. C.; Vignau, L.; Cramail, H., Poly(3-hexylthiophene) Based Block Copolymers Prepared by Click Chemistry. *Macromolecules* **2008**, *41* (19), 7033-7040.
30. Ogawa, K.; Chemburu, S.; Lopez, G. P.; Whitten, D. G.; Schanze, K. S., Conjugated Polyelectrolyte-Grafted Silica Microspheres. *Langmuir* **2007**, *23* (8), 4541-4548.
31. Monnaie, F.; Brullot, W.; Verbiest, T.; De Winter, J.; Gerbaux, P.; Smeets, A.; Koeckelberghs, G., Synthesis of End-Group Functionalized P3HT: General Protocol for P3HT/Nanoparticle Hybrids. *Macromolecules* **2013**, *46* (21), 8500-8508.
32. Iovu, M. C.; Sheina, E. E.; Gil, R. R.; McCullough, R. D., Experimental Evidence for the Quasi-"Living" Nature of the Grignard Metathesis Method for the Synthesis of Regioregular Poly(3-alkylthiophenes). *Macromolecules* **2005**, *38* (21), 8649-8656.

33. Stefan, M. C.; Javier, A. E.; Osaka, I.; McCullough, R. D., Grignard Metathesis Method (GRIM): Toward a Universal Method for the Synthesis of Conjugated Polymers. *Macromolecules* **2009**, *42* (1), 30-32.
34. Miyakoshi, R.; Yokoyama, A.; Yokozawa, T., Catalyst-Transfer Polycondensation. Mechanism of Ni-Catalyzed Chain-Growth Polymerization Leading to Well-Defined Poly(3-hexylthiophene). *J. Am. Chem. Soc.* **2005**, *127* (49), 17542-17547.
35. Yokozawa, T.; Adachi, I.; Miyakoshi, R.; Yokoyama, A., Catalyst-transfer condensation polymerization for the synthesis of well-defined polythiophene with hydrophilic side chain and of diblock copolythiophene with hydrophilic and hydrophobic side Chains. *High Perform. Polym.* **2007**, *19* (5/6), 684-699.
36. Senkovskyy, V.; Khanduyeva, N.; Komber, H.; Oertel, U.; Stamm, M.; Kuckling, D.; Kiriy, A., Conductive Polymer Brushes of Regioregular Head-to-Tail Poly(3-alkylthiophenes) via Catalyst-Transfer Surface-Initiated Polycondensation. *J. Am. Chem. Soc.* **2007**, *129* (20), 6626-6632.
37. Senkovskyy, V.; Tkachov, R.; Beryozkina, T.; Komber, H.; Oertel, U.; Horecha, M.; Bocharova, V.; Stamm, M.; Gevorgyan, S. A.; Krebs, F. C.; Kiriy, A., "Hairy" poly(3-hexylthiophene) particles prepared via surface-initiated Kumada catalyst-transfer polycondensation. *J. Am. Chem. Soc.* **2009**, *131* (45), 16445-16453.
38. Sontag, S. K.; Marshall, N.; Locklin, J., Formation of conjugated polymer brushes by surface-initiated catalyst-transfer polycondensation. *Chem. Commun. (Cambridge, U. K.)* **2009**, (23), 3354-3356.
39. Marshall, N.; Sontag, S. K.; Locklin, J., Substituted Poly(p-phenylene) Thin Films via Surface-Initiated Kumada-Type Catalyst Transfer Polycondensation. *Macromolecules* **2010**, *43* (5), 2137-2144.
40. Chavez, C. A.; Choi, J.; Nesterov, E. E., One-Step Simple Preparation of Catalytic Initiators for Catalyst-Transfer Kumada Polymerization: Synthesis of Defect-Free Polythiophenes. *Macromolecules* **2014**, *47* (2), 506-516.
41. Wu, Z.-Q.; Ono, R. J.; Chen, Z.; Bielawski, C. W., Synthesis of Poly(3-alkylthiophene)-block-poly(arylisocyanide): Two Sequential, Mechanistically Distinct Polymerizations Using a Single Catalyst. *J. Am. Chem. Soc.* **2010**, *132* (40), 14000-14001.
42. Wu, Z.-Q.; Radcliffe, J. D.; Ono, R. J.; Chen, Z.; Li, Z.; Bielawski, C. W., Synthesis of conjugated diblock copolymers: two mechanistically distinct, sequential living polymerizations using a single catalyst. *Polym. Chem.* **2012**, *3* (4), 874-881.

43. Wu, Z.-Q.; Chen, Y.; Wang, Y.; He, X.-Y.; Ding, Y.-S.; Liu, N., One pot synthesis of poly(3-hexylthiophene)-block-poly(hexadecyloxylallene) by sequential monomer addition. *Chem. Commun.* **2013**, 49 (73), 8069-8071.
44. McGrath, M. P.; Sall, E. D.; Tremont, S. J., Functionalization of Polymers by Metal-Mediated Processes. *Chem. Rev.* **1995**, 95 (2), 381-98.
45. Mochizuki, K.; Tomita, I., π -Allylnickel-catalyzed living coordination polymerization of allene having homochiral phenylcarbamoyloxy-substituted binaphthyl function. *Macromolecules* **2006**, 39 (19), 6336-6340.
46. Zhang, X.; Shen, Z.; Feng, C.; Yang, D.; Li, Y.; Hu, J.; Lu, G.; Huang, X., PMHDO-g-PEG Double-Bond-Based Amphiphilic Graft Copolymer: Synthesis and Diverse Self-Assembled Nanostructures. *Macromolecules* **2009**, 42 (12), 4249-4256.
47. Endo, T.; Tomita, I., Novel polymerization methods for allene derivatives. *Prog. Polym. Sci.* **1997**, 22 (3), 565-600.
48. Taguchi, M.; Tomita, I.; Endo, T., Living coordination polymerization of allene derivatives bearing hydroxy groups by π -allylnickel catalyst. *Angew. Chem., Int. Ed.* **2000**, 39 (20), 3667-3669.
49. Kino, T.; Taguchi, M.; Tazawa, A.; Tomita, I., Living Coordination Polymerization of Allene Derivatives in Protic Solvents: Remarkable Acceleration of Polymerization and Increase of 1,2-Polymerization Selectivity. *Macromolecules* **2006**, 39 (22), 7474-7478.
50. Stoeber, W.; Fink, A.; Bohn, E., Controlled growth of monodisperse silica spheres in the micron size range. *J. Colloid Interface Sci.* **1968**, 26 (1), 62-9.
51. Bogush, G. H.; Tracy, M. A.; Zukoski, C. F. I., Preparation of monodisperse silica particles: control of size and mass fraction. *J. Non-Cryst. Solids* **1988**, 104 (1), 95-106.
52. Yue, S.; Berry, G. C.; McCullough, R. D., Intermolecular Association and Supramolecular Organization in Dilute Solution. 1. Regioregular Poly(3-dodecylthiophene). *Macromolecules* **1996**, 29 (3), 933-9.
53. McCulloch, B.; Ho, V.; Hoarfrost, M.; Stanley, C.; Do, C.; Heller, W. T.; Segalman, R. A., Polymer Chain Shape of Poly(3-alkylthiophenes) in Solution Using Small-Angle Neutron Scattering. *Macromolecules* **2013**, 46 (5), 1899-1907.
54. Baessler, H.; Schweitzer, B., Site-Selective Fluorescence Spectroscopy of Conjugated Polymers and Oligomers. *Acc. Chem. Res.* **1999**, 32 (2), 173-182.
55. Heun, S.; Mahrt, R. F.; Greiner, A.; Lemmer, U.; Baessler, H.; Halliday, D. A.; Bradley, D. D. C.; Burn, P. L.; Holmes, A. B., Conformational effects in poly(p-

- phenylenevinylene)s revealed by low-temperature site-selective fluorescence. *J. Phys.: Condens. Matter* **1993**, *5* (2), 247-60.
56. Panzer, F.; Baessler, H.; Lohwasser, R.; Thelakkat, M.; Koehler, A., The Impact of Polydispersity and Molecular Weight on the Order-Disorder Transition in Poly(3-hexylthiophene). *J. Phys. Chem. Lett.* **2014**, *5* (15), 2742-2747.
 57. Guo, Z.; Lee, D.; Gao, H.; Huang, L., Exciton Structure and Dynamics in Solution Aggregates of a Low-Bandgap Copolymer. *J. Phys. Chem. B* **2015**, *119* (24), 7666-7672.
 58. Gao, J.; Chen, W.; Dou, L.; Chen, C.-C.; Chang, W.-H.; Liu, Y.; Li, G.; Yang, Y., Elucidating double aggregation mechanisms in the morphology optimization of diketopyrrolopyrrole-based narrow bandgap polymer solar cells. *Adv Mater* **2014**, *26* (19), 3142-7.
 59. Janssen, R. A. J.; Smilowitz, L.; Sariciftci, N. S.; Moses, D., Triplet-state photoexcitations of oligothiophene films and solutions. *J. Chem. Phys.* **1994**, *101* (3), 1787-98.
 60. Street, R. A.; Hawks, S. A.; Khlyabich, P. P.; Li, G.; Schwartz, B. J.; Thompson, B. C.; Yang, Y., Electronic Structure and Transition Energies in Polymer-Fullerene Bulk Heterojunctions. *J. Phys. Chem. C* **2014**, *118* (38), 21873-21883.
 61. Oliveira, F. A. C.; Cury, L. A.; Righi, A.; Moreira, R. L.; Guimaraes, P. S. S.; Matinaga, F. M.; Pimenta, M. A.; Nogueira, R. A., Temperature effects on the vibronic spectra of BEH-PPV conjugated polymer films. *J. Chem. Phys.* **2003**, *119* (18), 9777-9782.
 62. Brown, P. J.; Thomas, D. S.; Kohler, A.; Wilson, J. S.; Kim, J.-S.; Ramsdale, C. M.; Sirringhaus, H.; Friend, R. H., Effect of interchain interactions on the absorption and emission of poly(3-hexyl-thiophene). *Phys. Rev. B: Condens. Matter Mater. Phys.* **2003**, *67* (6), 064203/1-064203/16.
 63. Reid, O. G.; Nekuda Malik, J. A.; Latini, G.; Dayal, S.; Kopidakis, N.; Silva, C.; Stingelin, N.; Rumbles, G., The influence of solid-state microstructure on the origin and yield of long-lived photogenerated charge in neat semiconducting polymers. *J. Polym. Sci., Part B: Polym. Phys.* **2012**, *50* (1), 27-37.
 64. Lemmer, U.; Heun, S.; Mahrt, R. F.; Scherf, U.; Hopmeier, M.; Siegner, U.; Goebel, E. O.; Muellen, K.; Baessler, H., Aggregate fluorescence in conjugated polymers. *Chem. Phys. Lett.* **1995**, *240* (4), 373-8.

CHAPTER 4. RELATIONS BETWEEN STRUCTURE AND PHOTOPHYSICAL PROPERTIES IN HYBRID GOLD@SILICA NANOPARTICLES WITH CONJUGATED POLYMER SHELLS

4.1 Introduction

Nanostructured materials such as metals, metal oxides, and semiconductors, having unique physical and chemical properties, have become an exciting field of research due to their unique quantum properties at nanoscale dimension. In particular, they have promising applications in the areas of sensor technology, biomarkers, etc.¹ Metal nanoparticles such as gold can act as nanoantennas when excited by light and can partly transfer energy nonradiatively to the chromophores.²

Thus, the presence of gold nanoparticles in proximity to nanocrystals has been observed to influence the photoluminescence properties of nanocrystals. First, the excitation rates in the nanocrystal are changed due to the variation of electromagnetic field caused by surface plasmon of gold. Second, the decay rates of the nanocrystal, including radiative and non-radiative decay, are also changed. Thus, this competition will result either in PL enhancement or quenching.³⁻⁴

Polymer brushes are made by a surface-initiated polymerization reaction or *grafting-from*⁴ technique. The *grafting from* method is preferred and most widely used as polymerization is initiated from the surface directly rather than a pre-synthesized polymer is attached to the functionalized surface. This gives more control over brush thickness, and thus, higher grafting density can be achieved. An important discovery by Yokozawa⁵ and McCulloch⁶ that formation of regioregular poly(3-hexylthiophene), P3HT, takes place by chain growth mechanism made it possible to effectively grow this conjugated polymer from the surface. With such development, external-initiated catalyst-transfer polymerization with surface immobilized initiator was used to grow polymer from glass surface to form a thin film on spherical silica nanosurface to give well-

defined polymer brush.⁷⁻¹² These can provide well defined shells of polythiophene, PT, and other conducting polymers.

In the previous chapters, we described using of this methodology to prepare complex conjugated polymer shells on silica cores. Conjugated polymers (CP) due to their unique optical and electrical properties find applications in a variety of devices such as organic light-emitting diodes,¹³ solar cells,¹⁴⁻¹⁵ optically pumped lasers¹⁶ and fluorescent sensors for detection of various analytes.¹⁷⁻¹⁸ Recently Guy et al. have used *grafting to* approach to attach conjugated polymers to iron oxide, quantum dots.¹⁹

Quantum dots encapsulated iron oxides,²⁰ or organic dyes,²¹ are widely used as a labeling material for biological sensing and detection applications. Organic dyes proved to be useful but are still not a perfect candidate as they suffer from severe photobleaching during biodetection process. Conjugated polymer thin film sensory device, on other hand, has an advantage over organic dyes due to a highly extended π -conjugated system which, if properly aligned, gives better signal amplification due to the facile transport of excited states (excitons).²² Photoexcitation energy migration process in case of the thin film can occur either by intramolecular or intermolecular pathways where latter is more predominant due to the proximity of particles in the strongly aggregated system.^{20, 23-27} Use of magnetic field to orient this polymer hybrid brush can help in facilitating exciton migration.

Photoluminescence properties of conjugated polymers will also be affected by the presence of gold nanoparticles by altering the excitation decay rates of the conjugated polymer, thus changing the ratio of radiative and non-radiative decay rates.²⁸⁻³³ Heeger et al. showed the quenching of conjugated polymer emission by investigating the role of energy and electron transfer in the presence of gold nanoparticles. They found that quenching of emission depends on the size

of gold particles, and quenching takes place via energy transfer and not through electron transfer. In some cases, there was a huge enhancement in optical limiting performance when the conjugated polymer is coupled with gold nanoparticles.³⁴ Thus, to avoid quenching of these polymers, a spacer molecule is placed in between gold and chromophores.³⁵⁻³⁶

Thus, adding silica coating on gold nanoparticle is necessary not only to avoid quenching but also the silica shell provide a surface to grow polymer shells.³⁷⁻³⁸ Silica will also act as a spacer to transfer the energy from gold to polymers or vice-versa. FRET is an electrodynamic phenomenon that occurs between donor molecule in an excited state and acceptor molecule in the ground state.³⁹ The energy transfer rate depends on the extent at which donor emission spectra overlaps with acceptor absorption, and also depends on the orientation of the donor and acceptor chromophores and distance between donor and acceptor. Thus, the transfer of energy depends on the negative 6th power of distance (R^{-6}) and any condition that affects donor-acceptor distance will affect the transfer rate. In this chapter, we describe our studies on the energy transfer taking place between gold nanoparticles and conjugated block copolymers.

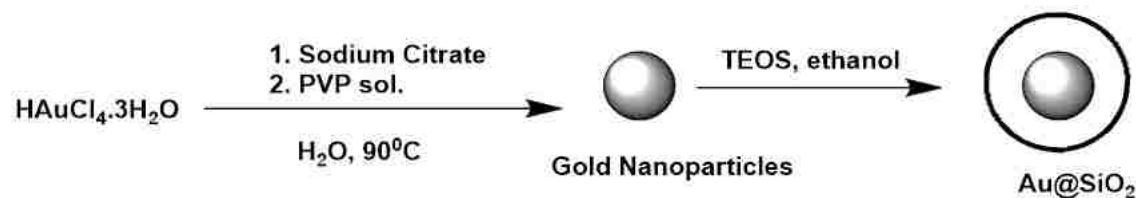
Herein we designed a unique series of block copolymers grown on gold nanoparticles coated with a thin layer of silica, showing more efficient energy transfer from one polymer to another. The energy transfer takes place between block copolymer segments irrespective on how conjugated block copolymers are attached on silica surface with or without gold core. We attempted to evaluate how energy transfer takes place between two attached polymer chromophores, and effect of the plasmon core on optical properties of these polymers.

4.2 Results and Discussion

4.2.1. Synthesis of Au@SiO₂-homopolymers and block copolymers

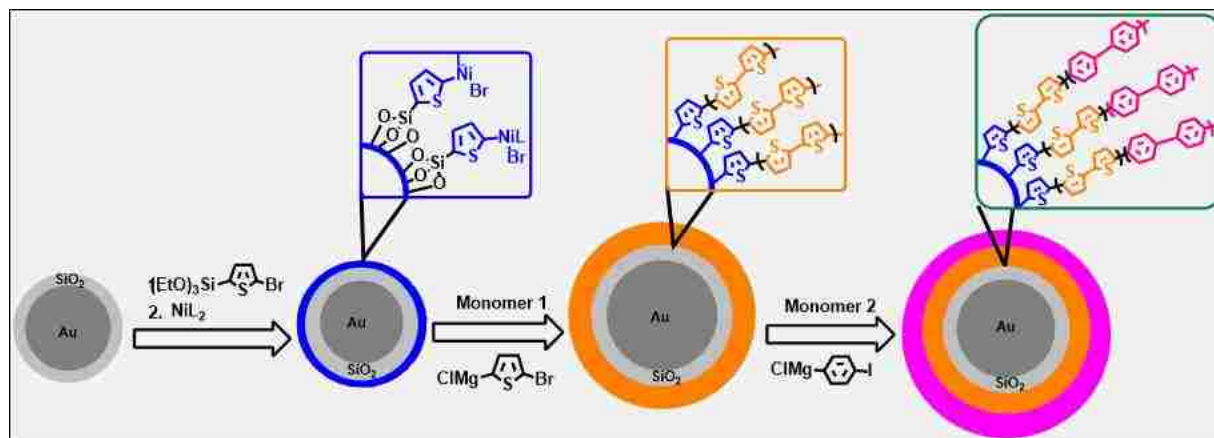
Gold nanoparticles were prepared by standard sodium citrate reduction method.⁴⁰

Au@SiO₂ was prepared by the method described by Kobayashi (Scheme 4.1).⁴¹



Scheme 4.1 Synthesis of Au and Au@SiO₂ nanoparticles

Au@SiO₂- homopolymer and block copolymer were synthesized by “grafting from” the surface of Au@SiO₂ by surface-initiated Kumada polymerization. It is based on surface immobilization of silyl-functionalized thiophene precursor on Au@SiO₂ followed by treatment with Ni(dppp)₂ to give surface-immobilized catalytic nickel initiator. This synthetic approach gives efficient catalytic initiator suitable for efficient and reliable surface-initiated polymerization.⁴² Particles were then washed with an excess of solvents to get rid of excess reagents. Activated hybrid particles were then transferred to a suitable Grignard monomer which initiated living polymerization to form conjugated polymer shell. Thus, 5-bromo-thiophen-2-ylmagnesium chloride or 4-iodo-phenylmagnesium chloride give polythiophene and poly(p-phenylene), respectively. After one day of polymerization, an aliquote of the polymer was taken out and quenched to give a homopolymer shell. Remaining reaction mixture was treated with Ni(0) for regeneration of active initiating sites followed by addition of 2nd Grignard monomer. Regeneration helps to activate incomplete terminated polymerization sites and thus increases efficiency of subsequent surface-initiated polymerization (scheme 4.2).



Scheme 4.2: Synthesis of multilayer shells of block copolymers on Au@SiO₂ nanoparticles by surface-initiated living Kumada polymerization technique

TEM image (figure 4.1) shows monodisperse gold particles with an increase in particle size upon the incorporation of each block of polymer

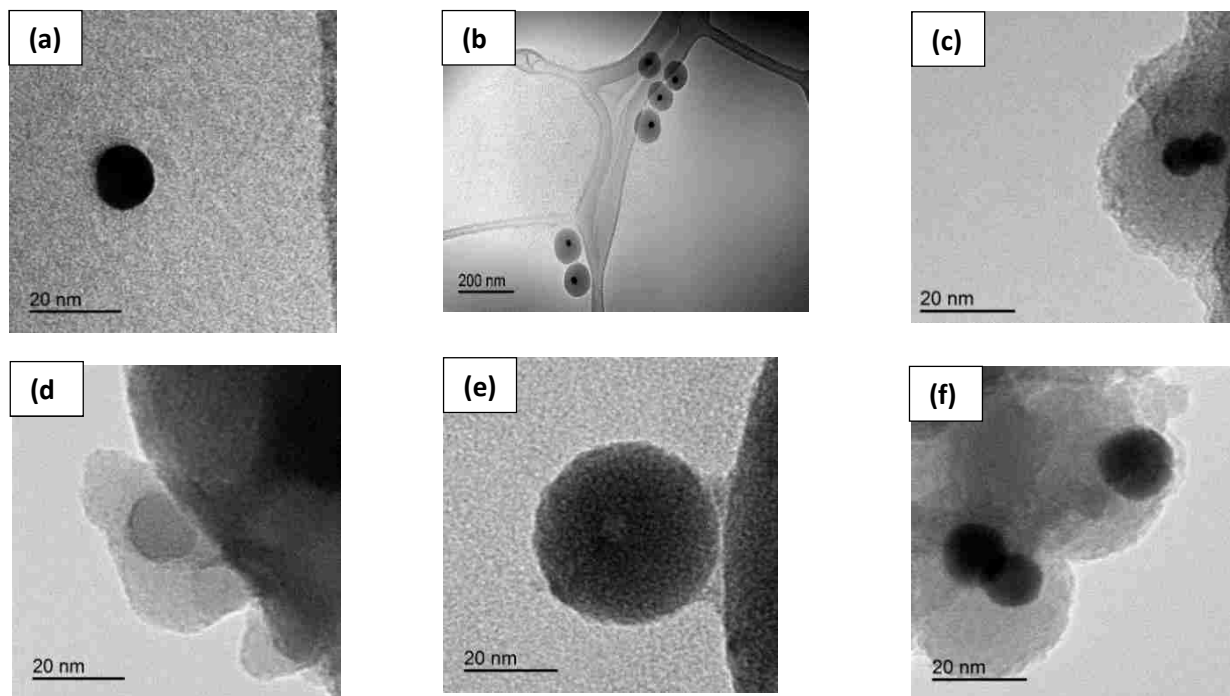


Figure 4.1 TEM images of nanoparticles: (a) Au; (b) Au@SiO₂; (c) Au@SiO₂-PT; (d) Au@SiO₂-PPP; (e) Au@SiO₂-PT-b-PPP; (f) Au@SiO₂-PPP-b-PT

4.2.2 Photophysical properties Gold@Silica- conjugated polymer nanoparticles

Figure 4.2 shows normalized absorption spectra of gold nanoparticles and gold@silica-conjugated homopolymer and block copolymers hybrid particles dispersed in chloroform. Gold@SiO₂ nanoparticles have a strong plasmonic band around 525 nm. In the case of Au@SiO₂-PPP, plasmon band of gold appears red-shifted at 536 nm. This is likely due to the strong electronic interaction between poly(*p*-phenylene) and gold nanoparticles which change both the surface plasmon band and the absorption band of poly(*p*-phenylene). Also, the formation of a dipole on the surface of the particles causes a red shift of the plasmon band.

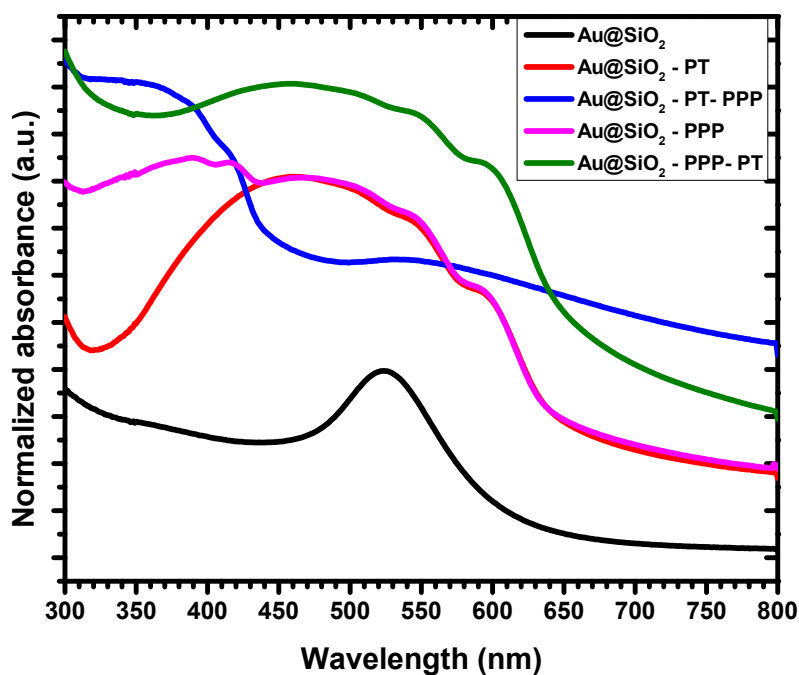


Figure 4.2 Normalized absorption spectra of Au@SiO₂-Conjugated polymer nanoparticles in 1,2-dichlorobenzene.

The dipolar band was blue shifted for hybrid particles. Au band was completely masked by PT absorption band for Au@SiO₂-PT hybrid particles, which appeared at λ_{\max} at 460 nm. It also showed two characteristic vibronic shoulder bands at 550 and 598 nm. Which were due to the intrachain π - π transition of PT chains arising because of the increasing order and crystallinity of

the PT shell. Indeed, such two peaks typically appear due to more ordered structures arising because of π - π stacking and resulting better electronic delocalization of polythiophene.⁴³ Polythiophene can self-organize to align polymer chains and form semi-crystalline lamellar morphologies which possess highly ordered packing and alignment, and also show high hole mobility and strong interchain and interlayer interactions. We observed that when poly(*p*-phenylene) was inside there was an efficient energy transfer taking place from poly(*p*-phenylene) to polythiophene chromophores. It was more efficient compared to the case when PT was on outside block.

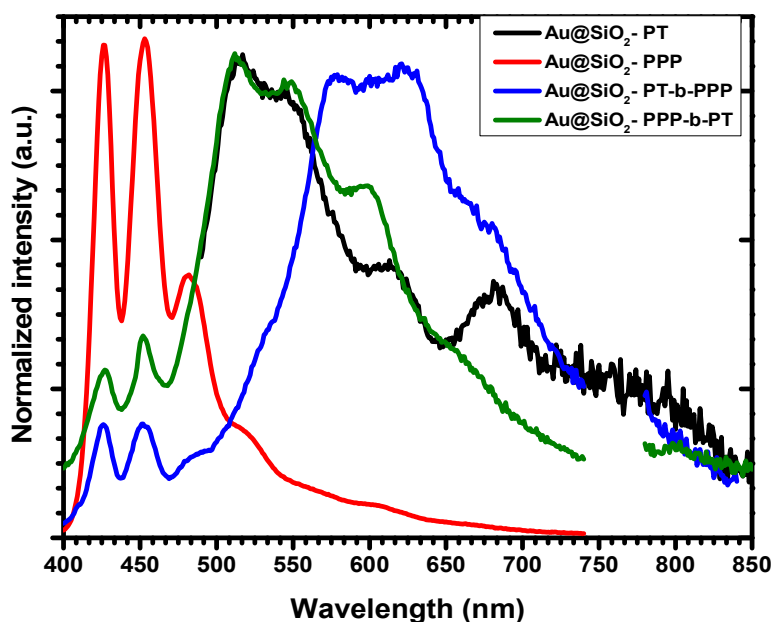


Figure 4.3 Normalized emission spectra of Au@SiO₂-Conjugated polymer nanoparticles in 1,2-dichlorobenzene solution.

Photoluminescence spectra (figure 4.3) of diblock copolymer-functionalized particles showed a different trend for each block copolymer. Irrespective of ordering of polymer block in the shell, there was always energy transfer from poly(*p*-phenylene) chromophore to polythiophene. In the case of PT placed as the first block, there was no change in λ_{max} of polythiophene absorption band. λ_{max} was found to be more red-shifted for poly(*p*-phenylene)-coblock-polythiophene than

for polythiophene-coblock-poly(*p*-phenylene). This might be due to more electronic delocalization and more ordering/planarization when polythiophene was outside. There was almost a 100 nm blue shift in λ_{\max} which could be explained by two considerations. First, in the case of Au@SiO₂-PPP-b-PT, there was an energy transfer from polythiophene chromophore to gold nanoparticles through surface plasmon-coupled emission (SPCE) via strong coupling between plasmonic field and conjugated polymer excitons which resulted in more blue shifted absorption band. Second, it could also result in more twisted or coil-like conformation with corresponding loss in planarity and lower electron delocalization.⁴⁴

4.2.3 Transient absorption studies of Gold@Silica- conjugated polymer nanoparticles

To gain more insight into effect of gold nanoparticle core on photophysical characteristics of conjugated polymers, transient absorption spectroscopy experiments were undertaken were taken.⁴⁵⁻⁴⁷ Figure 4.4 (a) shows representative transient absorption spectra of Au@SiO₂-PPP nanoparticles after excitation with 380 nm pulses. An intense negative band centered at 450 nm was observed. The transient absorption time profiles measured at 450 nm are shown in figure 4.4 (b). The decay spectra of Au@SiO₂-PPP generated by a global analysis technique using multi-exponential fits are shown in figure 4.4 (c). Two lifetimes of $\tau_1 = 17.2 \pm 0.8$ ps and $\tau_2 = 4.3 \pm 0.6$ ps were needed for the fit.

Figure 4.5 (a) shows representative transient absorption spectra of Au@SiO₂-PT nanoparticles after excitation with 380 nm pulses. A negative band centered at near 700 nm was observed. The transient absorption time profiles measured at 670 nm are shown in figure 4.5 (b). The decay spectra of Au@SiO₂-PT generated by a global analysis technique using multi-exponential fits are shown in figure 4.5 (c). Two lifetimes of $\tau_4 = 10 \pm 0.2$ ps and $\tau_5 = 74.3 \pm 1.1$ ps were needed for the fit.

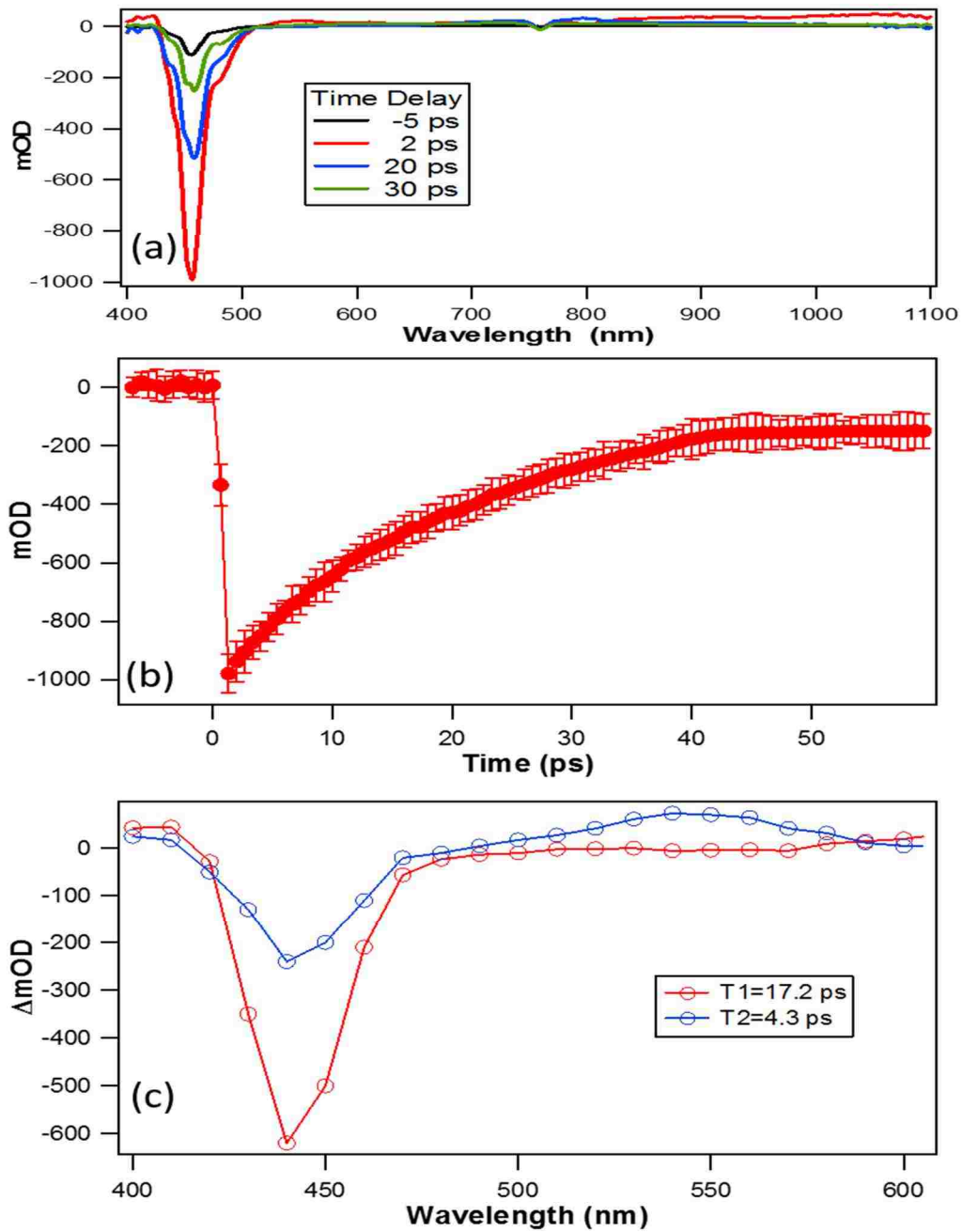


Figure 4.4. (a) Transient absorption spectra of Au@SiO₂-PPP after excitation with 380 nm excitation pulses. (b) Transient absorption time-profiles of Au@SiO₂-PPP. (c) Decay spectra of Au@SiO₂-PPP obtained by global analysis of the time profiles.

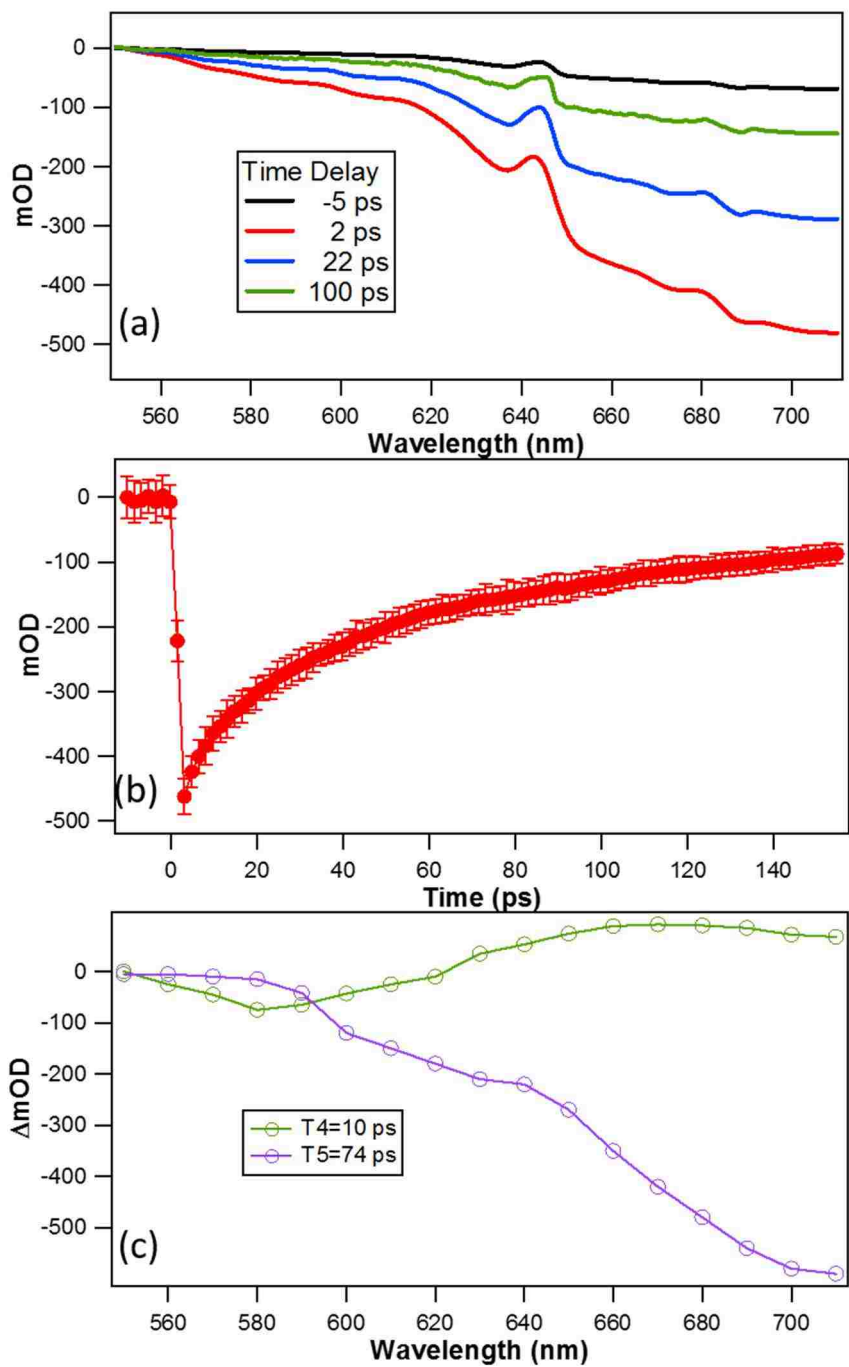


Figure 4.5. (a) Transient absorption spectra of Au@SiO₂-PT after excitation with 380 nm excitation pulses. (b) Transient absorption time-profiles of Au@SiO₂-PT. (c) Decay spectra of Au@SiO₂-PT obtained by global analysis of the time profiles.

Figure 4.6 (a) shows representative transient absorption spectra for Au@SiO₂-PPP-b-PT nanoparticles after excitation with 380 nm pulses. A small negative band appears at 450 nm followed by a second strong depletion band centered at 630 nm. The transient absorption time profiles measured at 450 and 650 nm are shown in figure 4.6 (b). The decay spectra of Au@SiO₂-PPP-b-PT nanoparticles generated by a global analysis technique using multi-exponential fits is shown in figure 4.6 (c). Five lifetimes of $\tau_1 = 52.3 \pm 1.1$ ps, $\tau_2 = 6.5 \pm 0.3$ ps, $\tau_3 = 9.3 \pm 0.1$ ps, $\tau_4 = 24.5 \pm 0.6$ ps, and $\tau_5 = 5.3 \pm 0.2$ ps were needed for the fit.

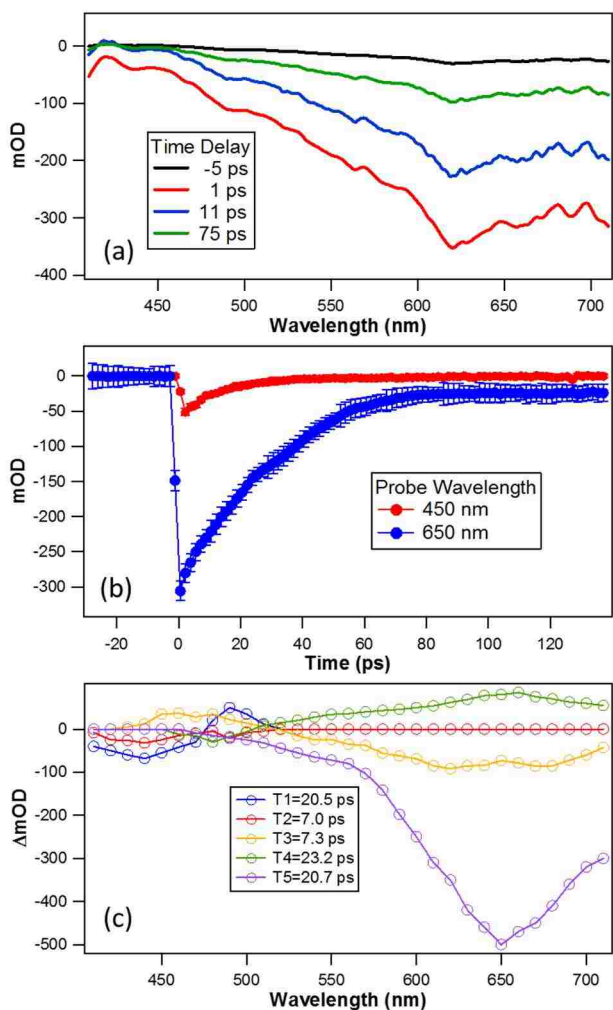


Figure 4.6. (a) Transient absorption spectra of Au@SiO₂-PPP-b-PT after excitation with 380 nm excitation pulses. (b) Transient absorption time-profiles of Au@SiO₂-PPP-b-PT. (c) Decay spectra of Au@SiO₂-PPP-b-PT obtained by global analysis of the time profiles.

Figure 4.7 (a) shows representative transient absorption spectra of Au@SiO₂-PT-b-PPP nanoparticles after excitation with 380 nm pulses. A negative band appears at 450 nm followed by a second smaller depletion band centered at 650 nm. The transient absorption time profiles measured at 450 and 650 nm are shown in figure 4.7 (b). The decay spectra of Au@SiO₂-PT-b-PPP nanoparticles generated by a global analysis technique using multi-exponential fits is shown in figure 4.7 (c). Five lifetimes of $\tau_1 = 78.9 \pm 0.4$ ps, $\tau_2 = 8.5 \pm 0.3$ ps, $\tau_3 = 14.2 \pm 0.2$ ps, $\tau_4 = 19.5 \pm 0.3$, and $\tau_5 = 4.7 \pm 0.2$ were needed for the fit.

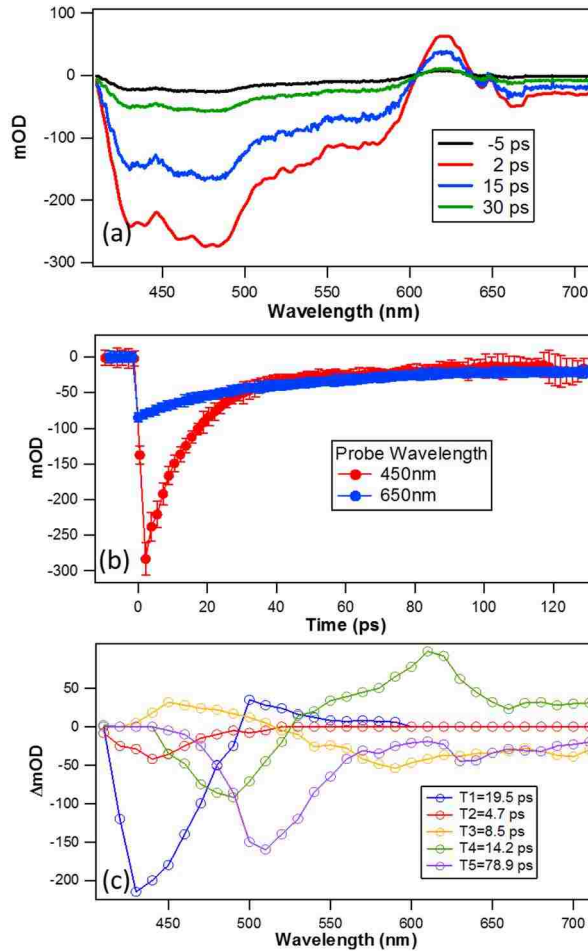


Figure 4.7. (a) Transient absorption spectra of Au@SiO₂-PT-b-PPP after excitation with 380 nm excitation pulses. (b) Transient absorption time-profiles of Au@SiO₂-PT-b-PPP. (c) Decay spectra of Au@SiO₂-PT-b-PPP obtained by global analysis of the time profiles.

In Au@SiO₂-PT-b-PPP nanoparticles, PT excited state ends up quenched on gold surface through the gold plasmon effect as well as energy transfer to PPP chromophore. In contrast, energy is additionally transferred to PPP chromophore, as compared to SiO₂-PT-PPP system. For Au@SiO₂-PPP-b-PT system, possibly a charge transfer between PPP chromophore and the plasmon surface diminishes the energy transfer from PPP to PT.

Table 4.1: Comparison of transient times of Silica@Conjugated polymers with Au@Silica-Conjugated polymers

	SiO ₂ -PPP-b-PT	SiO ₂ -PT-b-PPP	SiO ₂ -PT	SiO ₂ -PPP
650 nm	128.6 ± 1.4 ps	120.7 ± 0.9 ps	119.9 ± 1.1ps	
	27.1 ± 0.4 ps	23.2 ± 0.5 ps	23.1 ± 1.4 ps	
	11.4 ± 0.9 ps	7.3 ± 1.1 ps		
450 nm	18.7 ± 0.3 ps	20.5 ± 0.4 ps		20.0 ± 0.3 ps
	2.8 ± 0.4 ps	7.0 ± 0.5 ps		8.0 ± 0.6 ps
	Au@SiO ₂ -PPP-b-PT	Au@SiO ₂ -PT-b-PPP	Au@SiO ₂ -PT	Au@SiO ₂ -PPP
650 nm	52.3 ± 1.1 ps	78.9 ± 0.4 ps	74.3 ± 1.1 ps	
	9.3 ± 0.1 ps	14.2 ± 0.2 ps	10.8 ± 0.2 ps	
	6.5 ± 0.3 ps	8.5 ± 0.3 ps		
450 nm	24.5 ± 0.6 ps	19.5 ± 0.3 ps		4.3 ± 0.6 ps
	5.3 ± 0.2 ps	4.7 ± 0.2 ps		17.2 ± 0.8 ps

In contrast, in Au@SiO₂-PT-PPP system, PPP is far enough from the gold nanoparticle surface so that charge transfer from the plasmon surface to PPP is not observed.

These results were compared with control silica@conjugated polymers hybrid nanoparticles. Table 4.1 shows the results of transient absorption studies. It was evident gold quenches PT heavily. Thus, energy transfer takes place from PT chromophore to gold. When PT is the outer layer, energy transfer to gold is more efficient in comparison to when PT is an inner layer. One possibility is that PPP also transfers energy to PT, which slightly compensates for the energy transfer from PT to gold. In the case of PPP chromophore, there is always a gain in energy in PPP, which may be due to energy transfer from gold to PPP. No such effect was observed in silica particles as silica act as an insulator, so any changes in diblock copolymers should be due to the energy transfer between the polymers. This can be seen by an appearance of extra lifetime peak τ_5 which only was observed for diblock copolymer nanoparticles.

4.3 Conclusions

Polythiophene and poly(*p*-phenylene) based polymers were grown on Au@SiO₂ core using surface-initiated Kumada catalyst transfer polymerization. Photophysical studies showed that energy transfer from poly(*p*-phenylene) to polythiophene chromophore takes place irrespective of the order of polymer grown on the surface of Au@SiO₂. There is a strong coupling of gold and polythiophene which results in energy transfer from polythiophene to gold particles when polythiophene is placed as an outer block layer which resulted in blue spectroscopic shift. Transient absorption studies indicated that there was a gain in excitation energy for poly(*p*-phenylenes) whereas there was an efficient energy transfer occurring from polythiophene to gold at a picosecond time scale.

4.4 References

1. Lakowicz, J. R.; Malicka, J.; Gryczynski, I.; Gryczynski, Z.; Geddes, C. D., Radiative decay engineering: The role of photonic mode density in biotechnology. *J.Phys.D: Appl.Phys.* **2003**, *36* (14), R240-R249.
2. Heydari, E.; Pastoriza-Santos, I.; Flehr, R.; Liz-Marzan, L. M.; Stumpe, J., Nanoplasmonic Enhancement of the Emission of Semiconductor Polymer Composites. *J. Phys. Chem. C* **2013**, *117* (32), 16577-16583.
3. Aslan, K.; Gryczynski, I.; Malicka, J.; Matveeva, E.; Lakowicz, J. R.; Geddes, C. D., Metal-enhanced fluorescence: an emerging tool in biotechnology. *Curr. Opin. Biotechnol.* **2005**, *16* (1), 55-62.
4. Lakowicz, J. R., Radiative decay engineering 5: metal-enhanced fluorescence and plasmon emission. *Anal. Biochem.* **2005**, *337* (2), 171-194.
5. Miyakoshi, R.; Yokoyama, A.; Yokozawa, T., Catalyst-Transfer Polycondensation. Mechanism of Ni-Catalyzed Chain-Growth Polymerization Leading to Well-Defined Poly(3-hexylthiophene). *J. Am. Chem. Soc.* **2005**, *127* (49), 17542-17547.
6. Iovu, M. C.; Sheina, E. E.; Gil, R. R.; McCullough, R. D., Experimental Evidence for the Quasi-"Living" Nature of the Grignard Metathesis Method for the Synthesis of Regioregular Poly(3-alkylthiophenes). *Macromolecules* **2005**, *38* (21), 8649-8656.
7. Marshall, N.; Sontag, S. K.; Locklin, J., Surface-initiated polymerization of conjugated polymers. *Chem. Commun.* **2011**, *47* (20), 5681-5689.
8. Khanduyeva, N.; Senkovskyy, V.; Beryozkina, T.; Horecha, M.; Stamm, M.; Uhrich, C.; Riede, M.; Leo, K.; Kiriy, A., Surface Engineering Using Kumada Catalyst-Transfer Polycondensation (KCTP): Preparation and Structuring of Poly(3-hexylthiophene)-Based Graft Copolymer Brushes. *J. Am. Chem. Soc.* **2009**, *131* (1), 153-161.
9. Senkovskyy, V.; Tkachov, R.; Beryozkina, T.; Komber, H.; Oertel, U.; Horecha, M.; Bocharova, V.; Stamm, M.; Gevorgyan, S. A.; Krebs, F. C.; Kiriy, A., "Hairy" poly(3-hexylthiophene) particles prepared via surface-initiated Kumada catalyst-transfer polycondensation. *J. Am. Chem. Soc.* **2009**, *131* (45), 16445-16453.
10. Sontag, S. K.; Marshall, N.; Locklin, J., Formation of conjugated polymer brushes by surface-initiated catalyst-transfer polycondensation. *Chem. Commun.* **2009**, (23), 3354-3356.

11. Senkovskyy, V.; Senkovska, I.; Kiriy, A., Surface-Initiated Synthesis of Conjugated Microporous Polymers: Chain-Growth Kumada Catalyst-Transfer Polycondensation at Work. *ACS Macro Lett.* **2012**, *1* (4), 494-498.
12. Kiriy, A.; Senkovskyy, V.; Sommer, M., Kumada Catalyst-Transfer Polycondensation: Mechanism, Opportunities, and Challenges. *Macromol. Rapid Commun.* **2011**, *32* (19), 1503-1517.
13. Skotheim, T. A.; Reynolds, J. R., *Handbook of Conducting Polymers (3rd Edition)*. CRC Press LLC: 2007; Vol. 2, p 15/1-15/53.
14. Burroughes, J. H.; Bradley, D. D. C.; Brown, A. R.; Marks, R. N.; Mackay, K.; Friend, R. H.; Burns, P. L.; Holmes, A. B., Light-emitting diodes based on conjugated polymers. *Nature* **1990**, *347* (6293), 539-41.
15. Kraft, A.; Grimsdale, A. C.; Holmes, A. B., Electroluminescent conjugated polymers—seeing polymers in a new light. *Angew. Chem., Int. Ed.* **1998**, *37* (4), 403-428.
16. Halls, J. J. M.; Walsh, C. A.; Greenham, N. C.; Marseglia, E. A.; Friend, R. H.; Moratti, S. C.; Holmes, A. B., Efficient photodiodes from interpenetrating polymer networks. *Nature* **1995**, *376* (6540), 498-500.
17. Tessler, N.; Denton, G. J.; Friend, R. H., Lasing from conjugated-polymer microcavities. *Nature* **1996**, *382* (6593), 695-697.
18. McGehee, M. D.; Heeger, A. J., Semiconducting (conjugated) polymers as materials for solid-state lasers. *Adv. Mater.* **2000**, *12* (22), 1655-1668.
19. Monnaie, F.; Brullot, W.; Verbiest, T.; De Winter, J.; Gerbaux, P.; Smeets, A.; Koeckelberghs, G., Synthesis of End-Group Functionalized P3HT: General Protocol for P3HT/Nanoparticle Hybrids. *Macromolecules* **2013**, *46* (21), 8500-8508.
20. Thomas, S. W., III; Joly, G. D.; Swager, T. M., Chemical sensors based on amplifying fluorescent conjugated polymers. *Chem. Rev.* **2007**, *107* (4), 1339-1386.
21. Zhao, X.; Tapecc-Dytioco, R.; Tan, W., Ultrasensitive DNA detection using highly fluorescent bioconjugated nanoparticles. *J. Am. Chem. Soc.* **2003**, *125* (38), 11474-11475.
22. Cao, Y. C.; Jin, R.; Mirkin, C. A., Nanoparticles with Raman spectroscopic fingerprints for DNA and RNA detection. *Science* **2002**, *297* (5586), 1536-1540.
23. McQuade, D. T.; Pullen, A. E.; Swager, T. M., Conjugated polymer-based chemical sensors. *Chem. Rev.* **2000**, *100* (7), 2537-2574.

24. Jiang, H.; Taranekekar, P.; Reynolds, J. R.; Schanze, K. S., Conjugated Polyelectrolytes: Synthesis, Photophysics, and Applications. *Angew. Chem., Int. Ed.* **2009**, *48* (24), 4300-4316.
25. Kim, H. N.; Guo, Z.; Zhu, W.; Yoon, J.; Tian, H., Recent progress on polymer-based fluorescent and colorimetric chemosensors. *Chem. Soc. Rev.* **2011**, *40* (1), 79-93.
26. Kim, F. S.-J.; Ren, G.-Q.; Jenekhe, S. A., One-Dimensional Nanostructures of π -Conjugated Molecular Systems: Assembly, Properties, and Applications from Photovoltaics, Sensors, and Nanophotonics to Nanoelectronics. *Chem. Mater.* **2011**, *23* (3), 682-732.
27. Nguyen, T.-Q.; Martel, R.; Avouris, P.; Bushey, M. L.; Brus, L.; Nuckolls, C., Molecular interactions in one-dimensional organic nanostructures. *J Am Chem Soc* **2004**, *126* (16), 5234-42.
28. Beljonne, D.; Pourtois, G.; Silva, C.; Hennebicq, E.; Herz, L. M.; Friend, R. H.; Scholes, G. D.; Setayesh, S.; Mullen, K.; Bredas, J. L., Interchain vs. intrachain energy transfer in acceptor-capped conjugated polymers. *Proc. Natl. Acad. Sci.* **2002**, *99* (17), 10982-10987.
29. Nguyen, T.-Q.; Wu, J.; Doan, V.; Schwartz, B. J.; Tolbert, S. H., Control of energy transfer in oriented conjugated polymer-mesoporous silica composites. *Science* **2000**, *288* (5466), 652-656.
30. Wang, C. F.; White, J. D.; Lim, T. L.; Hsu, J. H.; Yang, S. C.; Fann, W. S.; Peng, K. Y.; Chen, S. A., Illumination of exciton migration in rodlike luminescent conjugated polymers by single-molecule spectroscopy. *Phys. Rev. B: Condens. Matter Mater. Phys.* **2003**, *67* (3), 035202/1-035202/8.
31. Hennebicq, E.; Pourtois, G.; Scholes, G. D.; Herz, L. M.; Russell, D. M.; Silva, C.; Setayesh, S.; Grimsdale, A. C.; Muellen, K.; Bredas, J.-L.; Beljonne, D., Exciton Migration in Rigid-Rod Conjugated Polymers: An Improved Foerster Model. *J. Am. Chem. Soc.* **2005**, *127* (13), 4744-4762.
32. Van Averbeke, B.; Beljonne, D.; Hennebicq, E., Energy transport along conjugated polymer chains: through-space or through-bond? *Adv. Funct. Mater.* **2008**, *18* (3), 492-498.
33. Van Averbeke, B.; Beljonne, D., Conformational Effects on Excitation Transport along Conjugated Polymer Chains. *J. Phys. Chem. A* **2009**, *113* (12), 2677-2682.
34. Fan, C.; Wang, S.; Hong, J. W.; Bazan, G. C.; Plaxco, K. W.; Heeger, A. J., Beyond superquenching: Hyper-efficient energy transfer from conjugated polymers to gold nanoparticles. *Proc. Natl. Acad. Sci.* **2003**, *100* (11), 6297-6301.

35. Reineck, P.; Gomez, D.; Ng, S. H.; Karg, M.; Bell, T.; Mulvaney, P.; Bach, U., Distance and Wavelength Dependent Quenching of Molecular Fluorescence by Au@SiO₂ Core-Shell Nanoparticles. *ACS Nano* **2013**, 7 (8), 6636-6648.
36. Dulkeith, E.; Ringler, M.; Klar, T. A.; Feldmann, J.; Javier, A. M.; Parak, W. J., Gold Nanoparticles Quench Fluorescence by Phase Induced Radiative Rate Suppression. *Nano Lett.* **2005**, 5 (4), 585-589.
37. Polavarapu, L.; Mamidala, V.; Guan, Z.; Ji, W.; Xu, Q.-H., Huge enhancement of optical nonlinearities in coupled Au and Ag nanoparticles induced by conjugated polymers. *Appl. Phys. Lett.* **2012**, 100 (2), 023106/1-023106/3.
38. Rodriguez-Fernandez, J.; Pastoriza-Santos, I.; Perez-Juste, J.; Garcia de Abajo, F. J.; Liz-Marzan, L. M., The Effect of Silica Coating on the Optical Response of Sub-micrometer Gold Spheres. *J. Phys. Chem. C* **2007**, 111 (36), 13361-13366.
39. Tovmachenko, O. G.; Graf, C.; van den Heuvel, D. J.; van Blaaderen, A.; Gerritsen, H. C., Fluorescence enhancement by metal-core/silica-shell nanoparticles. *Adv. Mater.* **2006**, 18 (1), 91-95.
40. Enustun, B. V.; Turkevich, J., Coagulation of colloidal gold. *J. Am. Chem. Soc.* **1963**, 85 (21), 3317-28.
41. Kobayashi, Y.; Inose, H.; Nakagawa, T.; Gonda, K.; Takeda, M.; Ohuchi, N.; Kasuya, A., Control of shell thickness in silica-coating of Au nanoparticles and their X-ray imaging properties. *J. Colloid Interface Sci.* **2011**, 358 (2), 329-333.
42. Chavez, C. A.; Choi, J.; Nesterov, E. E., One-Step Simple Preparation of Catalytic Initiators for Catalyst-Transfer Kumada Polymerization: Synthesis of Defect-Free Polythiophenes. *Macromolecules* **2014**, 47 (2), 506-516.
43. He, M.; Zhao, L.; Wang, J.; Han, W.; Yang, Y.; Qiu, F.; Lin, Z., Self-Assembly of All-Conjugated Poly(3-alkylthiophene) Diblock Copolymer Nanostructures from Mixed Selective Solvents. *ACS Nano* **2010**, 4 (6), 3241-3247.
44. Xu, T.; Yan, M.; Hoefelmeyer, J. D.; Qiao, Q., Exciton migration and charge transfer in chemically linked P3HT-TiO₂ nanorod composite. *RSC Adv.* **2012**, 2 (3), 854-862.
45. Banerji, N.; Cowan, S.; Vauthey, E.; Heeger, A. J., Ultrafast Relaxation of the Poly(3-hexylthiophene) Emission Spectrum. *J. Phys. Chem. C* **2011**, 115 (19), 9726-9739.
46. Banerji, N.; Seifert, J.; Wang, M.; Vauthey, E.; Wudl, F.; Heeger, A. J., Ultrafast spectroscopic investigation of a fullerene poly(3-hexylthiophene) dyad. *Phys. Rev. B: Condens. Matter Mater. Phys.* **2011**, 84 (7, Pt. A), 075206/1-075206/14.

47. Xie, Y.; Li, Y.; Xiao, L.; Qiao, Q.; Dhakal, R.; Zhang, Z.; Gong, Q.; Galipeau, D.; Yan, X., Femtosecond Time-Resolved Fluorescence Study of P3HT/PCBM Blend Films. *J. Phys. Chem. C* **2010**, *114* (34), 14590-14600.

CHAPTER 5. EXPERIMENTAL SECTION

5.1 General information

All reactions were performed under an atmosphere of dry nitrogen. Melting points were determined in open capillaries and are uncorrected. Column chromatography was carried out on silica gel (Sorbent Technologies, 60 Å, 40-63 µm) slurry packed into glass columns. Tetrahydrofuran (THF), dichloromethane, ether, and toluene were dried by passing through activated alumina, and N, N-dimethylformamide (DMF) by passing through activated molecular sieves, using a PS-400 Solvent Purification System from Innovative Technology, Inc. The water content of the solvents was periodically controlled by Karl Fischer titration (using a DL32 coulometric titrator from Mettler Toledo). All other solvents were additionally purified and dried by standard techniques. Isopropylmagnesium chloride (2.0 M solution in THF) was purchased from Acros Organics, all other reagents and solvents were obtained from Aldrich and Alfa Aesar and used without further purification. Organometallic reagents were titrated with salicylaldehyde phenylhydrazone prior to use.¹ UV-visible spectra were recorded on Varian Cary 50 UV-Vis or agilent Cary 5000 UV-VIS-NIR Spectrometer. Fluorescence studies were carried out with a PTI QuantaMaster4/2006SE spectrofluorimeter. ¹H NMR spectra were recorded at 400 MHz, and ¹³C NMR – at 100 MHz, and are reported in ppm downfield from tetramethylsilane; ³¹P NMR spectra were obtained at 162 MHz and are reported in ppm relative to 80% aqueous H₃PO₄ as external standard.

5.2 Transient absorption optical setup

The transient absorption optical setup has been previously reported.²⁻³ Briefly, a titanium:sapphire laser amplifier generates 70 fs pulses centered at 800 nm, with a repetition rate of 10 kHz and a pulse power of 7 W. The beam passes through a beam splitter to generate the

pump and probe pulses. The latter passes through a nonlinear crystal, β -barium borate to generate 400 nm pulses through frequency doubling. The 400 nm and residual 800 nm pulses are focused into a quartz flow cell containing water to generate femtosecond white light that extends from 300 nm to 1100 nm. The pump beam passes through an optical parametric amplifier (OPA) to generate 380 nm pulses, which are then focused to a spatial overlap with probe beam into a 3 mm quartz cell containing the sample under stirring. A computer-controlled delay stage is used to insure the pump-probe temporal delay and multiple spectra are acquired for statistical analysis.

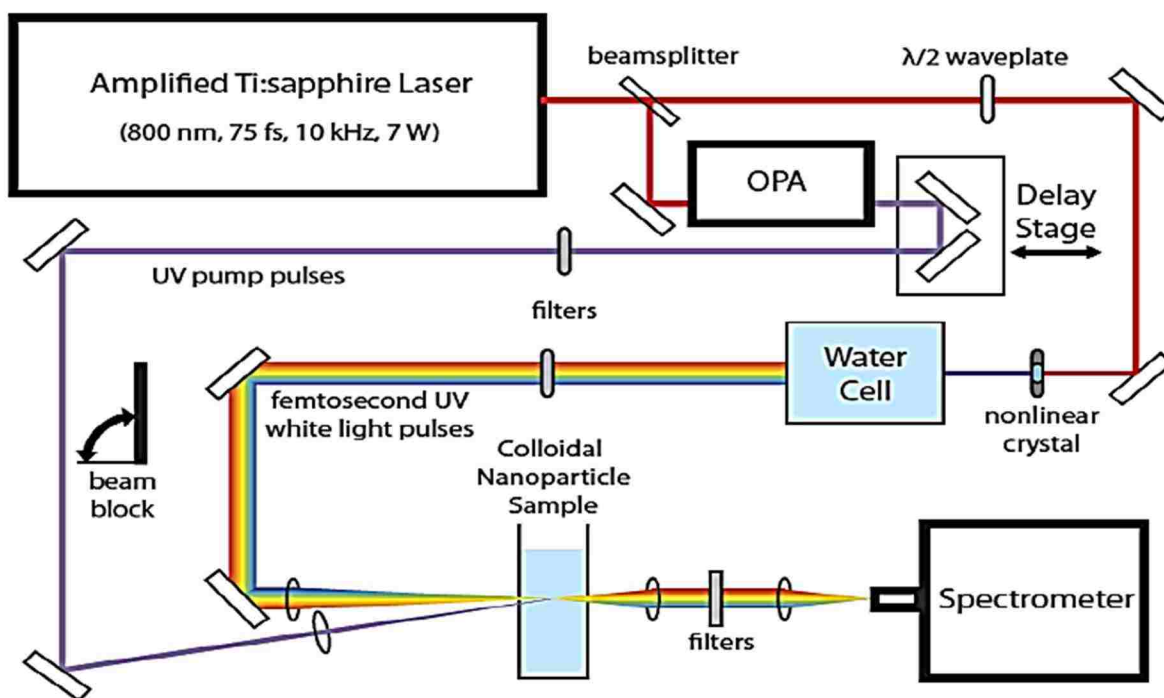


Figure 5.1: Schematic diagram of the ultrafast transient absorption setup.

5.3 Synthetic details

5.3.1 Synthesis of Silica nanoparticles⁴

In a three-necked flask equipped with a mechanical stirrer, 17.5 ml of Igepal-CO-520 in 225 ml of cyclohexane was added. The mixture was stirred for 15 minutes to homogenize. To this

mixture was added 5 ml of ammonium hydroxide (25 vol%). The mixture was again stirred for 20 minutes. To this mixture, a mixture of TEOS in ethanol solution (1ml of TEOS in 4 ml of ethanol) was added dropwise over 40 minutes. The resultant mixture solution was stirred overnight. Reaction was quenched by addition of ethanol and precipitate was centrifuged and washed 5 times sequentially with ethanol, water, ethanol, and toluene, to ensure the mixture is free from excess reactants.

5.3.2 Preparation of gold nanoparticles⁵

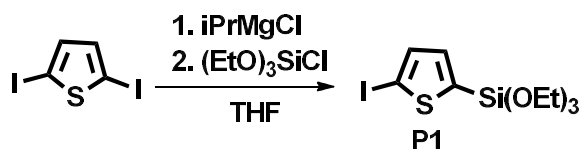
The synthesis of silica-coated gold nanoparticles was performed using the modified literature procedure.¹ An aqueous solution of sodium citrate (100 μ L of 0.34 M solution, 0.34 mmoles) was added to a solution of HAuCl₄ (0.2 ml of 5 mmol solution) (Aldrich) in 10 ml of degassed water with stirring at 80⁰-90⁰ C. Previously deaerated Milli-Q water (18 MOhm cm) was used, and nitrogen was bubbled during the entire process. Color changed to red which confirmed the formation of gold nanoparticles. Gold nanoparticles were then ultra-centrifuged at a rate of 5500 rpm and washed with water and ethanol and then again re-dispersed and centrifuged. This re-dispersion and centrifugation were done 4-5 times to remove excess reagents. Finally, the particles were redispersed in 10 ml ethanol and used in the next step.

5.3.3 Preparation of gold@silica nanoparticles.⁶

To a 500 ml, 3 neck flask equipped with mechanical stirrer was added 20 ml of water and 80 ml of ethanol. To this mixture was added 0.2 ml of gold sol solution prepared as described above. 0.1 ml of 3-(aminopropyl)trimethoxysilane and 5 ml of tetraethoxysilane (0.4 ml in 4.6 ml of ethanol, 1.79 mmol) (Aldrich). Add sodium hydroxide solution (100 ml of 0.1 M, 10 mmol) was added dropwise after 15 minutes and the resulting mixture was stirred overnight. Gold@silica nanoparticles were ultra-centrifuged at a rate of 5500 rpm and washed with water and ethanol and

then again re-dispersed and centrifuged. This re-dispersion and centrifugation were done 4-5 times to remove excess reagents. . Finally, the particles were redispersed in 10 ml toluene and used in the next step.

5.3.4 Synthesis of Triethoxy(5-iodothiophen-2-yl)silane (P1)



Scheme 5.1: Synthesis of Triethoxy(5-iodothiophen-2-yl)silane (P1)

Synthesis of precursor P1 (scheme 5.1) was done by a substitution reaction of chlorotriethoxysilane with Grignard reagent, prepared by treatment of 2,5-diiodothiophene with *i*-PrMgCl. A solution of *i*-PrMgCl (1ml of 2.0 M solution in THF, 3.0 mmol) was added dropwise to a stirred solution of 1g (3 mmol) of 2,5-diiodothiophene in 3ml of THF at 0°C. The reaction mixture was stirred for 1 hour, and then the temperature was lowered to -78°C. Chlorotriethoxysilane (1.75 ml, 9 mmol) was added dropwise. The resulting solution was precipitated into hexanes, the solids were filtered, and the filtrate was concentrated in vacuo, and subjected to Kugelrohr distillation (ca. 85 °C at 10 mTorr,) to afford P1 as a colorless oil (1.1 g, 50%). It was dissolved in 15 ml of toluene to make a 0.2 M stock solution which was kept at -30 °C in an inert atmosphere glovebox. ¹H- NMR (CDCl₃) δ 7.31 (d, *J* = 4 Hz, 1H), 7.13 (d, *J* = 4 Hz, 1H), 3.87 (q, *J* = 8 Hz, 6H), 1.24 (t, *J* = 8,9H) (figure B-1).

5.3.5 Synthesis of Bis[1,3-bis(diphenylphosphino)propane]nickel(0)

Bis[1,3-bis(diphenylphosphino)propane]nickel(0) (Ni(dppp)₂) was prepared following the literature procedure (figure B-2).⁶

5.3.6 Immobilization of precursor P1 on gold@silica or silica nanoparticles and conversion to Ni(II)- modified nanoparticles

Silica-coated gold nanoparticles (8 ml) prepared as described above were dispersed in 10 ml of toluene in an inert atmosphere (glove box) at room temperature. A solution of P1 precursor (10 ml of 3 mM solution in toluene) was added to the nanoparticles dispersion in 10 ml of toluene, and the resulting mixture was kept at 60 °C for one day. After completing surface immobilization of the precursor, the solution was centrifuged, and the toluene solution was decanted. The particles were redispersed in toluene, ultrasonicated for 10 min, centrifuged, and toluene was again removed by decantation. The procedure was repeated 3 more times to ensure complete removal of the unattached precursor P1.

The surface-modified nanoparticles were then transferred to a solution containing 88mg (0.1mmol) of Ni(dppp)₂ in 10 ml of toluene. The reaction mixture was stirred at 40⁰C for 2 days. The resulting solution was centrifuged, and the toluene solution was decanted under nitrogen. The procedure of adding toluene and subsequent decantation was repeated 3 more times to ensure complete removal of the unattached Ni(dppp)₂.

5.3.7 General preparation of gold@silica or silica nanoparticles core with conjugated polymer shell

The Ni(II) surface-modified nanoparticles were transferred to freshly prepared 10 mM solution of Grignard monomer in THF, which was prepared by the reaction of 0.1 ml (0.2 mmol) of 2 M solution of *i*-PrMgCl with 10 mmol of the either 2,5-dibromothiophene, or 1,4-diiodobenzene in 20 ml of THF. The resulting solution was stirred at room temperature for 24 h to allow for surface-initiated polymerization to proceed. An aliquot of reaction mixture was taken and quenched with methanol to give homopolymer-functionalized nanoparticles. The remaining portion was left for regeneration. The quenched nanoparticles were removed by centrifugation,

and washed thoroughly in sequence with fresh THF, toluene, methanol, chloroform and ultrasonicated each time gently and then re-suspended in 1,2-dichlorobenzene.

5.3.8 General preparation of block copolymer coated gold@silica or silica nanoparticles

The remaining un-quenched portion of homopolymer grafted nanoparticles was washed with toluene and centrifuged to remove excess of Grignard reagent and was redispersed in 5 ml of toluene for regeneration with Ni(dppp)₂. 44 mg (0.05 mmol) of Ni(dppp)₂ in 5 ml of toluene was added to the solution containing nanoparticles and heated to 40⁰ C for 2 days. Upon completion, the reaction was centrifuged and washed 5 times with toluene to remove excess of reagents. Finally, the nanoparticles were re-suspended in 5 ml of THF. Into this solution was added a solution of second Grignard monomer in THF, which was prepared by reaction of 0.1 ml (0.2 mmol) of 2 M solution of *i*-PrMgCl with 10 mmol of the either 1,4-diiodobenzene or 2,5-dibromothiophene in 15 ml of THF. The resulting solution was kept at room temperature for 24 h to allow for surface-initiated polymerization to proceed. The reaction was quenched with methanol. The quenched nanoparticles were removed by centrifugation, and washed sequentially with fresh THF, toluene, methanol, and chloroform and ultrasonicated each time gently and then re-suspended in 1,2-dichlorobenzene.

5.4 References

1. Love, B. E.; Jones, E. G., The use of salicylaldehyde phenylhydrazone as an indicator for the titration of organometallic reagents. *J. Org. Chem.* **1999**, *64* (10), 3755-3756.
2. Karam, T. E.; Smith, H. T.; Haber, L. H., Enhanced Photothermal Effects and Excited-State Dynamics of Plasmonic Size-Controlled Gold-Silver-Gold Core-Shell-Shell Nanoparticles. *J. Phys. Chem. C* **2015**, *119* (32), 18573-18580.
3. Karam, T. E.; Siraj, N.; Warner, I. M.; Haber, L. H., Anomalous Size-Dependent Excited-State Relaxation Dynamics of NanoGUMBOS. *J. Phys. Chem. C* **2015**, *119* (50), 28206-28213.

4. Rosu, C.; Selcuk, S.; Soto-Cantu, E.; Russo, P. S., Progress in silica polypeptide composite colloidal hybrids: from silica cores to fuzzy shells. *Colloid Polym. Sci.* **2014**, *292* (5), 1009-1040.
5. Kobayashi, Y.; Inose, H.; Nakagawa, T.; Gonda, K.; Takeda, M.; Ohuchi, N.; Kasuya, A., Control of shell thickness in silica-coating of Au nanoparticles and their X-ray imaging properties. *J. Colloid Interface Sci.* **2011**, *358* (2), 329-333.
6. Corain, B.; Bressan, M.; Rigo, P., Behavior of nickel (0) diphosphine complexes towards unsaturated organic compounds. *J. Organometal. Chem.* **1971**, *28* (1), 133-6.

APPENDIX A PERMISSIONS

A-1 PERMISSIONS

For Figure 1.1

4/15/2016 RightsLink® by Copyright Clearance Center



The screenshot shows the RightsLink interface. At the top left is the Copyright Clearance Center logo. In the center is the RightsLink logo. On the right are buttons for Home, Create Account, and Help, along with a Live Chat icon. Below the logos is the ACS Publications logo with the tagline "Most Trusted. Most Cited. Most Read." To the right of the ACS logo is a box with a LOGIN button and text: "If you're a copyright.com user, you can login to RightsLink using your copyright.com credentials. Already a RightsLink user or want to learn more?". Below the ACS logo is a list of metadata: Title: Advances in Molecular Design and Synthesis of Regioregular Polythiophenes; Author: Itaru Osaka, Richard D. McCullough; Publication: Accounts of Chemical Research; Publisher: American Chemical Society; Date: Sep 1, 2008; Copyright © 2008, American Chemical Society.

Title: Advances in Molecular Design and Synthesis of Regioregular Polythiophenes

Author: Itaru Osaka, Richard D. McCullough

Publication: Accounts of Chemical Research

Publisher: American Chemical Society

Date: Sep 1, 2008

Copyright © 2008, American Chemical Society

PERMISSION/LICENSE IS GRANTED FOR YOUR ORDER AT NO CHARGE

This type of permission/license, instead of the standard Terms & Conditions, is sent to you because no fee is being charged for your order. Please note the following:

- Permission is granted for your request in both print and electronic formats, and translations.
- If figures and/or tables were requested, they may be adapted or used in part.
- Please print this page for your records and send a copy of it to your publisher/graduate school.
- Appropriate credit for the requested material should be given as follows: "Reprinted (adapted) with permission from (COMPLETE REFERENCE CITATION). Copyright (YEAR) American Chemical Society." Insert appropriate information in place of the capitalized words.
- One-time permission is granted only for the use specified in your request. No additional uses are granted (such as derivative works or other editions). For any other uses, please submit a new request.

If credit is given to another source for the material you requested, permission must be obtained from that source.

BACK

CLOSE WINDOW

Copyright © 2016 Copyright Clearance Center, Inc. All Rights Reserved. [Privacy Statement](#), [Terms and Conditions](#). Comments? We would like to hear from you. E-mail us at: customer care@copyright.com

For Figure 1.2

4/17/2016 RightsLink® by Copyright Clearance Center

 **Copyright Clearance Center**
Most Trusted. Most Cited. Most Read.

RightsLink®

[Home](#) [Create Account](#) [Help](#)  **Live Chat**

 **ACS Publications**
Most Trusted. Most Cited. Most Read.

Title: One-Step Simple Preparation of Catalytic Initiators for Catalyst-Transfer Kumada Polymerization: Synthesis of Defect-Free Polythiophenes

Author: Carlos A. Chavez, Jinwoo Choi, Evgueni E. Nesterov

Publication: Macromolecules

Publisher: American Chemical Society

Date: Jan 1, 2014

Copyright © 2014, American Chemical Society

LOGIN

If you're a [copyright.com](#) user, you can login to RightsLink using your [copyright.com](#) credentials; Already a [RightsLink](#) user or want to [learn more?](#)

PERMISSION/LICENSE IS GRANTED FOR YOUR ORDER AT NO CHARGE

This type of permission/license, instead of the standard Terms & Conditions, is sent to you because no fee is being charged for your order. Please note the following:

- Permission is granted for your request in both print and electronic formats, and translations.
- If figures and/or tables were requested, they may be adapted or used in part.
- Please print this page for your records and send a copy of it to your publisher/graduate school.
- Appropriate credit for the requested material should be given as follows: "Reprinted (adapted) with permission from (COMPLETE REFERENCE CITATION). Copyright (YEAR) American Chemical Society." Insert appropriate information in place of the capitalized words.
- One-time permission is granted only for the use specified in your request. No additional uses are granted (such as derivative works or other editions). For any other uses, please submit a new request.

If credit is given to another source for the material you requested, permission must be obtained from that source.


[BACK](#)


[CLOSE WINDOW](#)


Copyright © 2015 [Copyright Clearance Center, Inc.](#) All Rights Reserved. [Privacy statement](#), [Terms and Conditions](#). Comments? We would like to hear from you, E-mail us at customerscare@copyright.com


For Figure 1.6

5/6/2016 RightsLink® by Copyright Clearance Center

 **Copyright Clearance Center**

 **RightsLink**

[Home](#) [Create Account](#) [Help](#)  **Live Chat**

 **ACS Publications** Most Trusted. Most Cited. Most Read.

Title: Chain-Growth Polymerization of Unusual Anion-Radical Monomers Based on Naphthalene Diimide: A New Route to Well-Defined n-Type Conjugated Copolymers

Author: Volodymyr Senkovskyy, Roman Tkachov, Hartmut Komber, et al.

Publication: Journal of the American Chemical Society

Publisher: American Chemical Society

Date: Dec 1, 2011

Copyright © 2011, American Chemical Society

[LOGIN](#)

If you're a **copyright.com** user, you can login to RightsLink using your copyright.com credentials. Already a **RightsLink** user or want to [learn more?](#)

PERMISSION/LICENSE IS GRANTED FOR YOUR ORDER AT NO CHARGE

This type of permission/license, instead of the standard Terms & Conditions, is sent to you because no fee is being charged for your order. Please note the following:

- Permission is granted for your request in both print and electronic formats, and translations.
- If figures and/or tables were requested, they may be adapted or used in part.
- Please print this page for your records and send a copy of it to your publisher/graduate school.
- Appropriate credit for the requested material should be given as follows: "Reprinted (adapted) with permission from (COMPLETE REFERENCE CITATION). Copyright (YEAR) American Chemical Society." Insert appropriate information in place of the capitalized words.
- One-time permission is granted only for the use specified in your request. No additional uses are granted (such as derivative works or other editions). For any other uses, please submit a new request.


If credit is given to another source for the material you requested, permission must be obtained from that source.

[BACK](#) [CLOSE WINDOW](#)


Copyright © 2016 Copyright Clearance Center, Inc. All Rights Reserved. [Privacy statement](#), [Terms and Conditions](#), [Comments?](#) We would like to hear from you. E-mail us at customerservice@copyright.com


For Figure 1.7

4/18/2016 RightsLink® by Copyright Clearance Center

 **Copyright Clearance Center**
MinThrued. Most Cited. Most Used.

RightsLink

[Home](#) [Create Account](#) [Help](#)  **Live Chat**

 **ACS Publications** **Title:** Grafting of Poly(3-hexylthiophene) from Poly(4-bromostyrene) Films by Kumada Catalyst-Transfer Polycondensation: Revealing of the Composite Films Structure

Author: Natalya Khanduyeva, Volodymyr Senkovskyy, Tetyana Beryozkina, et al

Publication: Macromolecules

Publisher: American Chemical Society

Date: Oct 1, 2008

Copyright © 2008, American Chemical Society

LOGIN

If you're a [copyright.com](#) user, you can login to RightsLink using your [copyright.com](#) credentials. Already a [RightsLink](#) user or want to [learn more?](#)

PERMISSION/LICENSE IS GRANTED FOR YOUR ORDER AT NO CHARGE

This type of permission/license, instead of the standard Terms & Conditions, is sent to you because no fee is being charged for your order. Please note the following:

- Permission is granted for your request in both print and electronic formats, and translations.
- If figures and/or tables were requested, they may be adapted or used in part.
- Please print this page for your records and send a copy of it to your publisher/graduate school.
- Appropriate credit for the requested material should be given as follows: "Reprinted (adapted) with permission from (COMPLETE REFERENCE CITATION). Copyright (YEAR) American Chemical Society." Insert appropriate information in place of the capitalized words.
- One-time permission is granted only for the use specified in your request. No additional uses are granted (such as derivative works or other editions). For any other uses, please submit a new request.

If credit is given to another source for the material you requested, permission must be obtained from that source.


BACK


CLOSE WINDOW


Copyright © 2016 Copyright Clearance Center, Inc. All Rights Reserved. [Privacy statement](#), [Terms and Conditions](#). Comments? We would like to hear from you. E-mail us at customerservice@copyright.com


For Figure 1.8

4/17/2016 RightsLink® by Copyright Clearance Center

 **Copyright Clearance Center**

 **RightsLink®**

[Home](#) [Create Account](#) [Help](#)  **Live Chat**

 **ACS Publications** Most Trusted. Most Cited. Most Read.

Title: "Hairy" Poly(3-hexylthiophene) Particles Prepared via Surface-Initiated Kumada Catalyst-Transfer Polycondensation

Author: Volodymyr Senkovskyy, Roman Tkachov, Tetyana Beryozkina, et al

Publication: Journal of the American Chemical Society

Publisher: American Chemical Society

Date: Nov 1, 2009

Copyright © 2009, American Chemical Society

LOGIN

If you're a [copyright.com](#) user, you can login to RightsLink using your copyright.com credentials. Already a [RightsLink](#) user or want to [learn more?](#)

PERMISSION/LICENSE IS GRANTED FOR YOUR ORDER AT NO CHARGE

This type of permission/license, instead of the standard Terms & Conditions, is sent to you because no fee is being charged for your order. Please note the following:

- Permission is granted for your request in both print and electronic formats, and translations.
- If figures and/or tables were requested, they may be adapted or used in part.
- Please print this page for your records and send a copy of it to your publisher/graduate school.
- Appropriate credit for the requested material should be given as follows: "Reprinted (adapted) with permission from (COMPLETE REFERENCE CITATION). Copyright (YEAR) American Chemical Society." Insert appropriate information in place of the capitalized words.
- One-time permission is granted only for the use specified in your request. No additional uses are granted (such as derivative works or other editions). For any other uses, please submit a new request.

If credit is given to another source for the material you requested, permission must be obtained from that source.


[BACK](#)


[CLOSE WINDOW](#)


Copyright © 2016 [Copyright Clearance Center, Inc.](#) All Rights Reserved. [Privacy statement](#), [Terms and Conditions](#), [Comments?](#) We would like to hear from you. E-mail us at customerscare@copyright.com


For Figure 1.9

4/18/2016 RightsLink® by Copyright Clearance Center

 **Copyright Clearance Center**

 **RightsLink**

[Home](#) [Create Account](#) [Help](#)  **Live Chat**

 **ACS Publications**
Most Trusted. Most Cited. Most Read.

Title: Surface-Confined Nickel Mediated Cross-Coupling Reactions: Characterization of Initiator Environment in Kumada Catalyst-Transfer Polycondensation

Author: S. Kyle Sontag, Gareth R. Sheppard, Nathan M. Usselman, et al

Publication: Langmuir

Publisher: American Chemical Society

Date: Oct 1, 2011

Copyright © 2011, American Chemical Society

LOGIN

If you're a [copyright.com](#) user, you can login to RightsLink using your [copyright.com](#) credentials. Already a [RightsLink](#) user or want to [learn more?](#)

PERMISSION/LICENSE IS GRANTED FOR YOUR ORDER AT NO CHARGE

This type of permission/license, instead of the standard Terms & Conditions, is sent to you because no fee is being charged for your order. Please note the following:

- Permission is granted for your request in both print and electronic formats, and translations.
- If figures and/or tables were requested, they may be adapted or used in part.
- Please print this page for your records and send a copy of it to your publisher/graduate school.
- Appropriate credit for the requested material should be given as follows: "Reprinted (adapted) with permission from (COMPLETE REFERENCE CITATION). Copyright (YEAR) American Chemical Society." Insert appropriate information in place of the capitalized words.
- One-time permission is granted only for the use specified in your request. No additional uses are granted (such as derivative works or other editions). For any other uses, please submit a new request.

If credit is given to another source for the material you requested, permission must be obtained from that source.

[BACK](#)

[CLOSE WINDOW](#)

Copyright © 2016 [Copyright Clearance Center, Inc.](#) All Rights Reserved. [Privacy statement](#), [Terms and Conditions](#). Comments? We would like to hear from you. E-mail us at customerscare@copyright.com

For figure 1.10

5/6/2016

RightsLink® by Copyright Clearance Center



RightsLink®

Home

Account Info

Help



Title: Surface-initiated Kumada catalyst-transfer polycondensation of poly(9,9-dioctylfluorene) from organosilica particles: chain-confinement promoted β -phase formation

Author: Roman Tkachov, Volodymyr Senkovskyy, Marta Horecha, Ulrich Oertel, Manfred Stamm, Anton Kiriy

Publication: Chemical Communications (Cambridge)

Publisher: Royal Society of Chemistry

Date: Dec 23, 2009

Copyright © 2009, Royal Society of Chemistry

Logged in as:
Sourav Chatterjee

LOGOUT

Order Completed

Thank you for your order.

This Agreement between Sourav Chatterjee ("You") and Royal Society of Chemistry ("Royal Society of Chemistry") consists of your license details and the terms and conditions provided by Royal Society of Chemistry and Copyright Clearance Center.

Your confirmation email will contain your order number for future reference.

[Get the printable license.](#)

License Number	3853170470184
License date	May 05, 2016
Licensed Content Publisher	Royal Society of Chemistry
Licensed Content Publication	Chemical Communications (Cambridge)
Licensed Content Title	Surface-initiated Kumada catalyst-transfer polycondensation of poly(9,9-dioctylfluorene) from organosilica particles: chain-confinement promoted β -phase formation
Licensed Content Author	Roman Tkachov, Volodymyr Senkovskyy, Marta Horecha, Ulrich Oertel, Manfred Stamm, Anton Kiriy
Licensed Content Date	Dec 23, 2009
Licensed Content Volume	46
Licensed Content Issue	9
Type of Use	Thesis/Dissertation
Requestor type	non-commercial (non-profit)
Portion	figures/tables/images
Number of figures/tables/images	1
Distribution quantity	100
Format	print and electronic
Will you be translating?	no

For figure 1.11

5/8/2016 Rightslink® by Copyright Clearance Center

  [Home](#) [Create Account](#) [Help](#)  Live Chat

 **Title:** Surface-Initiated Synthesis of Conjugated Microporous Polymers: Chain-Growth Kumada Catalyst-Transfer Polycondensation at Work

Author: Volodymyr Senkovskyy, Irena Senkovska, Anton Kiriy

Publication: ACS Macro Letters

Publisher: American Chemical Society

Date: Apr 1, 2012

Copyright © 2012, American Chemical Society

[LOGIN](#)

If you're a [copyright.com](#) user, you can login to RightsLink using your [copyright.com](#) credentials. Already a [RightsLink](#) user or want to [learn more?](#)

PERMISSION/LICENSE IS GRANTED FOR YOUR ORDER AT NO CHARGE

This type of permission/license, instead of the standard Terms & Conditions, is sent to you because no fee is being charged for your order. Please note the following:

- Permission is granted for your request in both print and electronic formats, and translations.
- If figures and/or tables were requested, they may be adapted or used in part.
- Please print this page for your records and send a copy of it to your publisher/graduate school.
- Appropriate credit for the requested material should be given as follows: "Reprinted (adapted) with permission from (COMPLETE REFERENCE CITATION). Copyright (YEAR) American Chemical Society." Insert appropriate information in place of the capitalized words.
- One-time permission is granted only for the use specified in your request. No additional uses are granted (such as derivative works or other editions). For any other uses, please submit a new request.

If credit is given to another source for the material you requested, permission must be obtained from that source.

[BACK](#)

[CLOSE WINDOW](#)

Copyright © 2015 [Copyright Clearance Center, Inc.](#) All Rights Reserved. [Privacy statement](#), [Terms and Conditions](#).
Comments? We would like to hear from you, E-mail us at customerservice@copyright.com

For Figure 1.13

4/18/2016 RightsLink® by Copyright Clearance Center

 **Copyright Clearance Center**

 **RightsLink®**

[Home](#) [Create Account](#) [Help](#)  **Live Chat**

 **ACS Publications**
Most Trusted. Most Cited. Most Read.

Title: Conjugated Polyelectrolyte-Grafted Silica Microspheres
Author: Katsu Ogawa, Sireesha Chemburu, Gabriel P. Lopez, et al
Publication: Langmuir
Publisher: American Chemical Society
Date: Apr 1, 2007
Copyright © 2007, American Chemical Society

[LOGIN](#)
If you're a [copyright.com](#) user, you can login to RightsLink using your copyright.com credentials. Already a RightsLink user or want to [learn more?](#)

PERMISSION/LICENSE IS GRANTED FOR YOUR ORDER AT NO CHARGE

This type of permission/license, instead of the standard Terms & Conditions, is sent to you because no fee is being charged for your order. Please note the following:

- Permission is granted for your request in both print and electronic formats, and translations.
- If figures and/or tables were requested, they may be adapted or used in part.
- Please print this page for your records and send a copy of it to your publisher/graduate school.
- Appropriate credit for the requested material should be given as follows: "Reprinted (adapted) with permission from (COMPLETE REFERENCE CITATION). Copyright (YEAR) American Chemical Society." Insert appropriate information in place of the capitalized words.
- One-time permission is granted only for the use specified in your request. No additional uses are granted (such as derivative works or other editions). For any other uses, please submit a new request.

If credit is given to another source for the material you requested, permission must be obtained from that source.

[BACK](#)

[CLOSE WINDOW](#)

Copyright © 2016 [Copyright Clearance Center, Inc.](#) All Rights Reserved. [Privacy statement](#), [Terms and Conditions](#).
Comments? We would like to hear from you. E-mail us at customer-care@copyright.com

For figure 1.14

4/17/2016 RightsLink® by Copyright Clearance Center

 **Copyright Clearance Center**

 **RightsLink®**

[Home](#) [Create Account](#) [Help](#)  **Live Chat**

 **ACS Publications**
Most Trusted. Most Cited. Most Read.

Title: Disubstituted Polyacetylene Brushes Grown via Surface-Directed Tungsten-Catalyzed Polymerization

Author: Sarav B. Jhaveri, Kenneth R. Carter

Publication: Langmuir

Publisher: American Chemical Society

Date: Jul 1, 2007

Copyright © 2007, American Chemical Society

LOGIN

If you're a [copyright.com](#) user, you can login to RightsLink using your [copyright.com](#) credentials. Already a RightsLink user or want to [learn more?](#)

PERMISSION/LICENSE IS GRANTED FOR YOUR ORDER AT NO CHARGE

This type of permission/license, instead of the standard Terms & Conditions, is sent to you because no fee is being charged for your order. Please note the following:

- Permission is granted for your request in both print and electronic formats, and translations.
- If figures and/or tables were requested, they may be adapted or used in part.
- Please print this page for your records and send a copy of it to your publisher/graduate school.
- Appropriate credit for the requested material should be given as follows: "Reprinted (adapted) with permission from (COMPLETE REFERENCE CITATION). Copyright (YEAR) American Chemical Society." Insert appropriate information in place of the capitalized words.
- One-time permission is granted only for the use specified in your request. No additional uses are granted (such as derivative works or other editions). For any other uses, please submit a new request.

If credit is given to another source for the material you requested, permission must be obtained from that source.

[BACK](#)

[CLOSE WINDOW](#)

Copyright © 2016 [Copyright Clearance Center, Inc.](#) All Rights Reserved. [Privacy statement](#), [Terms and Conditions](#). Comments? We would like to hear from you. E-mail us at customerservice@copyright.com

APPENDIX B
NUCLEAR MAGNETIC RESONANCE DATA

A-2.

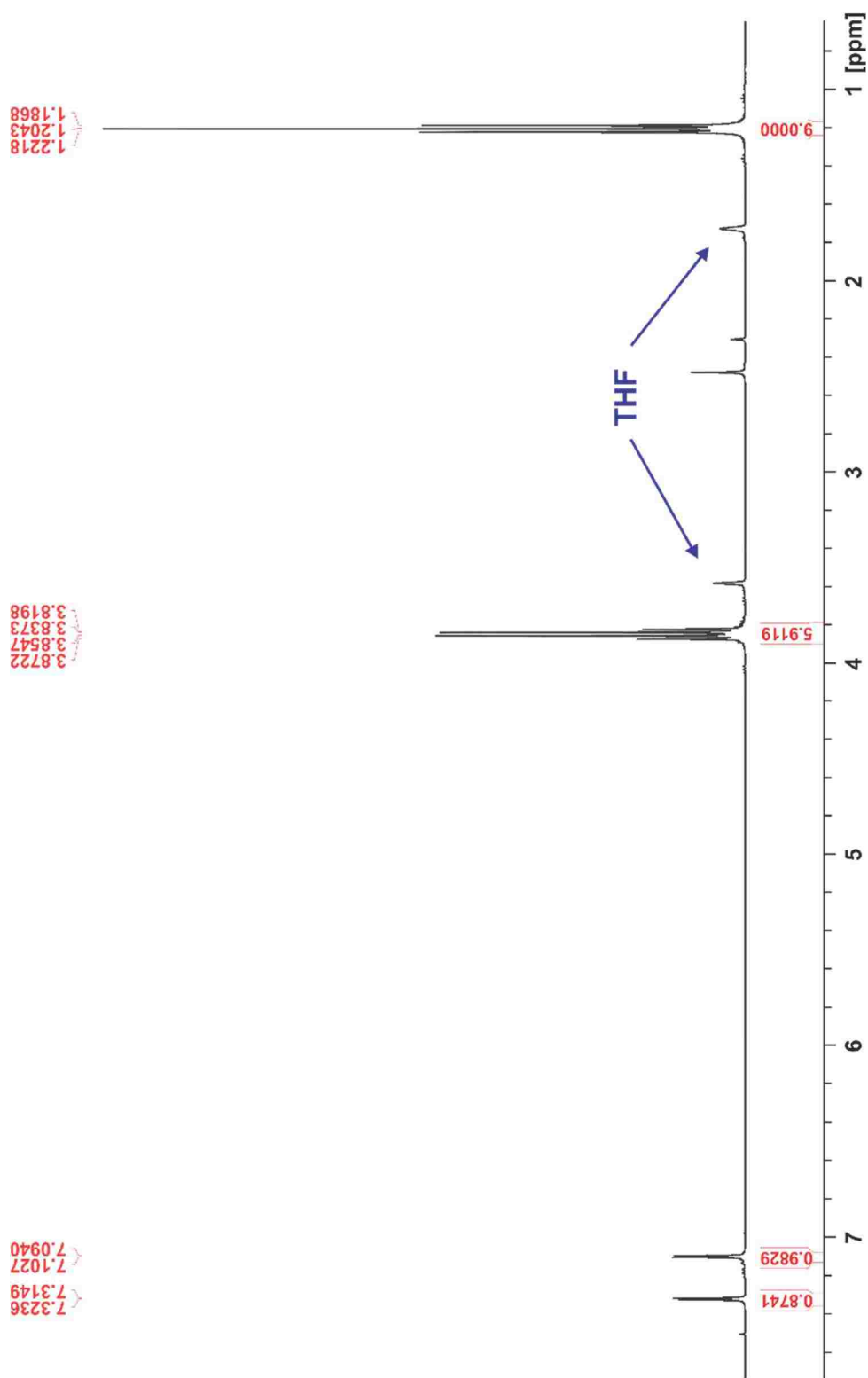


Figure B-1. ¹H NMR spectrum (400 MHz, THF-D₈) of 2-triethoxysilyl-5-iodothiophene **2**.

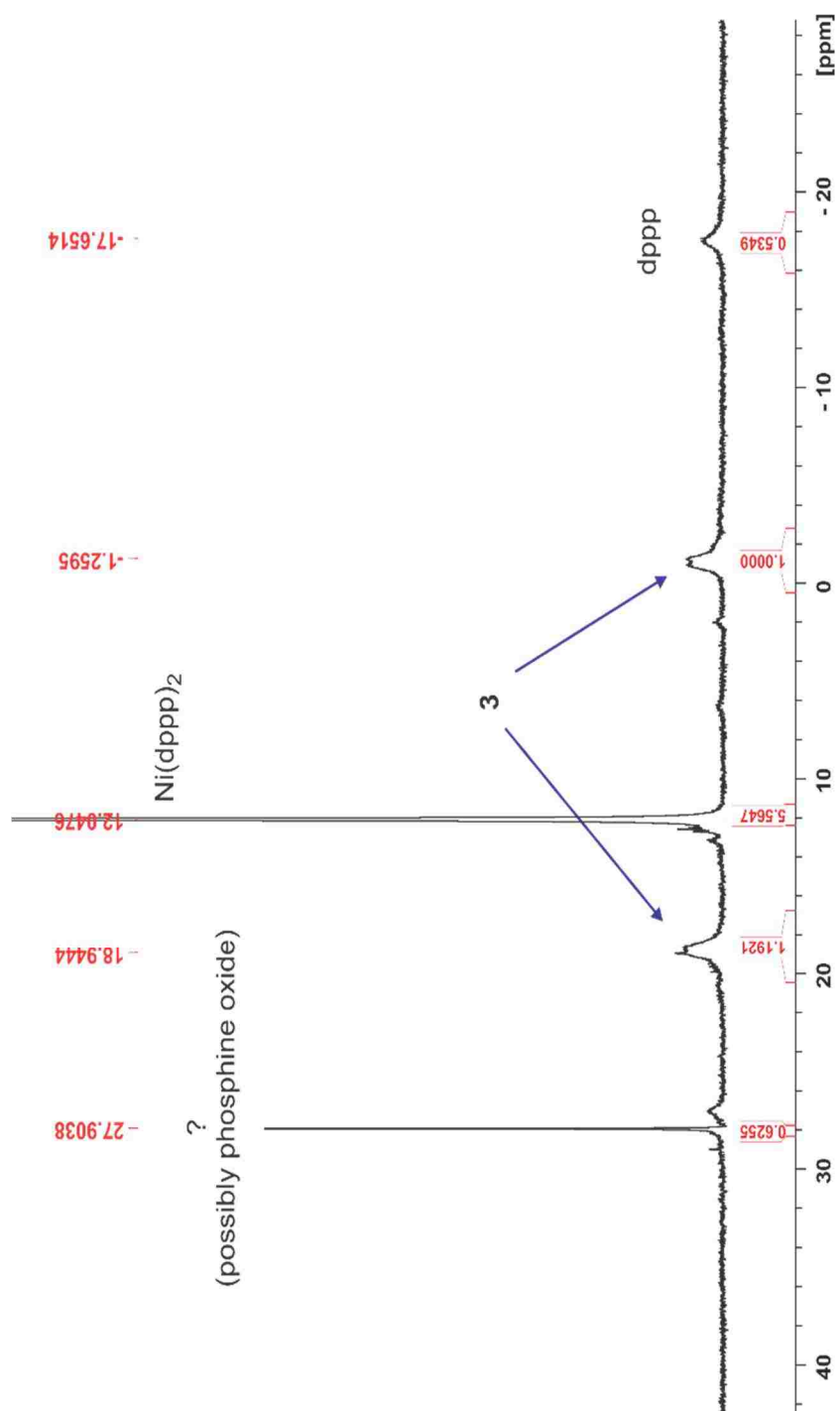


Figure B-2. ^{31}P NMR spectrum of the reaction between compound **2** and 2 equivalents of $\text{Ni}(\text{dppp})_2$ to form $\text{Ni}(\text{II})$ catalytic initiator **3**. The reaction was carried out for 24 h in toluene at 45 °C, followed by removing toluene by evaporating *in vacuo* and redissolving the residue in THF to acquire the NMR spectrum.

VITA

Sourav Chatterjee was born in 1980 in Siliguri, West Bengal, India. After graduating from high school, he enrolled at the University of Delhi in Delhi, India as a Chemistry Honours major. He completed his Bachelors as well as Masters from University of Delhi. He began his research career in the lab of Dr. R.B. Mathur at National physical laboratory located on NPL, Delhi. It is at this national lab that he studied synthesis and characterization of carbon nanotubes hybrid materials used for energy applications and published a peer reviewed paper which is cited more than 150 times till now. In May of 2007, he graduated with a Bachelor and Master of Science in Chemistry. He then moved to Lowell, Massachusetts to attend University of Massachusetts at lowell for his Master study in Chemistry and joined research lab of late professor Daniel J. Sandman. He published two peer reviewed journal before moving to Baton Rouge. He joined Louisiana State University for his doctoral studies under the guidance of Professor Evgueni E. Nesterov. His research and contributions at LSU include development of new approaches towards the preparation of hybrid inorganic core /organic shell nanoparticles and semiconducting polymer thin films and to study their photo-physical properties in solid as well as in solution. Sourav is a candidate for the Doctor of Philosophy in Polymer Chemistry, which will be awarded in August 2016 with a dissertation entitled, "Hybrid inorganic core- conjugated polymer shell nanoparticles prepared by surface-initiated polymerization".